This is to certify that the
dissertation entitled

STRUCTURAL AND CATALYTIC DETERMINANTS OF INTRACELLULAR CYCLOOXYGENASE PROTEIN DEGRADATION

presented by

URI R. MBONYE

has been accepted towards fulfillment
of the requirements for the

Doctoral degree in Biochemistry

William L. Smith
Major Professor's Signature

04/27/07
Date

MSU is an affirmative-action, equal-opportunity employer

STRUCTURAL AND CATALYTIC DETERMINANTS OF INTRACELLULAR CYCLOOXYGENASE PROTEIN DEGRADATION

By

Uri R. Mbonye

A DISSERTATION

Submitted to
Michigan State Universtiy
in partial fulfillment of the requirements
for the degree of

DOCTOR OF PHILOSOPHY

Department of Biochemistry and Molecular Biology

2007

ABSTRACT

STRUCTURAL AND CATALYTIC DETERMINANTS OF INTRACELLULAR CYCLOOXYGENASE PROTEIN DEGRADATION

By

Uri R. Mbonye

Cyclooxygenases (COX-1 and COX-2) are ER-resident, membrane-bound glycoproteins that catalyze the committed step in the synthesis of biologically active lipid hormones called prostanoids. COX-1 is constitutively expressed in many mammalian cells, whereas COX-2 is usually expressed inducibly and transiently. In murine NIH/3T3 fibroblasts, COX-2 protein is degraded by a proteasome-dependent process with a half-life ($t_{1/2}$) of about 2 h whereas COX-1 is reasonably stable ($t_{1/2}$> 12 h). The mature forms of the COX isoforms are very similar in structure except that COX-2 has a unique 19-amino acid (19-aa) segment of unknown function located just near the C-terminus. Here, we provide evidence that the major role of the 19-aa cassette is to mediate entry of COX-2 into the ER-associated degradation (ERAD) system that transports ER proteins to the cytoplasm for degradation by the 26S proteasome. COX-1 expressed heterologously in HEK293 cells is quite stable ($t_{1/2}$> 24 h) while COX-2 expressed heterologously is degraded with a $t_{1/2}$ of ~5 h and its degradation is blocked by proteasome inhibitors. A deletion mutant of COX-2 lacking 18 residues of the 19-aa cassette retains native COX-2 enzymatic activity and subcellular localization but, unlike native COX-2, is stable in HEK293 cells ($t_{1/2}$> 24 h). Conversely, inserting the COX-2 cassette near the C-terminus of COX-1 yields a mutant *ins*594-612 COX-1 that is unstable ($t_{1/2}$ ~ 3 h). A mannosidase inhibitor that can block entry of ER proteins into the ER-associated degradation system,

retards the degradation of COX-2 and *ins*594-612 COX-1. Scanning mutagenesis of the 19-aa cassette has revealed that Asn-594, an *N*-glycosylation site at the beginning of the 19-aa cassette, is required, albeit insufficient to enable ERAD entry of COX-2 and *ins*594-612 COX-1. The remaining 16 amino acids of the 19-aa cassette are not only essential for COX-2 degradation but are also required for the enzyme to become glycosylated at Asn-594. Structural and biochemical analysis of the region immediately upstream of Asn-594 has revealed an 8-residue α-helical region that appears to impede Asn-594 glycosylation. We propose that a structural conformational change of the α-helical structure mediated by the C-terminal 16-residue sequence of the 19-aa cassette is needed for Asn-594 glycosylation. We show that the helical region upstream of Asn-594 and the 19-aa cassette actually constitute a C-terminal 27 instability element (27 IE) that dictates the intracellular stability of COX-2 by regulating glycosylation at Asn-594. We have also identified a second distinct mechanism of COX-2 protein turnover that is induced by arachidonic acid (AA), a major cylooxygenase (COX) fatty acid substrate. AA-dependent degradation of COX-2 is blocked by COX inhibitors, is not affected by inhibitors of proteasomal or lysosomal degradation, and occurs independently of the C-terminal 19-aa cassette of the enzyme. A COX-inactive point mutant of COX-2 (G533A COX-2) is resistant to AA-induced degradation even though it undergoes substrate-independent degradation at the same rate as native COX-2. Loss of COX-2 specific activity and prostanoid product formation is also observed in COX-2 expressing cells treated with AA. We propose that substrate-dependent inactivation of COX-2 causes structural damage to the enzyme that subsequently leads to its degradation.

To Baba, my Mom, and the loving memory of my grandfather Reuben Rwabusizoni

ACKNOWLEDGMENTS

I would like to express my utmost gratitude to my advisor Dr. Bill Smith for his wonderful mentorship. He has done an excellent job of guiding me through a very challenging and thought-provoking thesis project. I have relied on his remarkable guidance and intellectual and technical expertise to be able to successfully complete my graduate career. I also sincerely acknowledge my advisory committee for providing me with very helpful advice and constantly ensuring that my thesis research is on the right track.

I extend my appreciation to members of our lab, both present and past, for all the collaboration, advice, technical help, and friendship that I have received throughout my graduate career. Much thanks goes to Dr. Rana Sidhu for teaching me how to use the PyMOL software for protein structure analysis. He has also been a very cool and approachable guy that I have constantly turned to for suggestions and help on wide-ranging issues. Much thanks also goes to: Dr. Chong Yuan for teaching me, among other things, the very useful technique of overlap-extension PCR; Dr. Masayuki Wada and Jill Rieke for collaborative research related to examining the biological function of the COX-2 C-terminal 19-amino acid cassette; Drs. Cindy DeLong and Inseok Song for helpful discussions and teaching me how to perform TLC assays; and Drs. Jiayan Liu, Yeon-Joo Kang, and Christine Harman for intellectually stimulating discussions. Thank you all for providing me with a conducive and friendly atmosphere to pursue my thesis research.

Finally, I take this opportunity to also thank my family for their constant love and support.

TABLE OF CONTENTS

LIST OF TABLES

LIST OF FIGURES

ABBREVIATIONS

2-AG ether	2-arachidonyl glycerol ether
3'-UTR	3'-untranslated region
19-aa	C-terminal 19-amino acid cassette of COX-2
AA	arachidonic acid
BFA	brefeldin A
CHX	cycloheximide
COX	cyclooxygenase
$cPLA_2\alpha$	cytosolic phospholipase $A_2\alpha$
DHLA	dihomo-γ-linolenic acid
EDA	eicosadienoic acid
Endo H	endoglycosidase H
EPA	eicosapentaenoic acid
Epox	epoxomicin
ER	endoplasmic reticulum
ERAD	ER-associated degradation
ER Man I	ER α-1,2 mannosidase I
FB	flurbiprofen
FBS	fetal bovine serum
GI	glucosidase I
GII	glucosidase II
Glc	glucose
GlcNAc	N-acetyl glucosamine
hu	human
IFN-γ	interferon-γ
KIF	kifunensine
LA	linoleic acid
Leup	leupeptin
LPS	bacterial lipopolysaccharide
Man	mannose
mu	murine
NSAID	non-steroidal anti-inflammatory drug
OA	oleic acid
OST	oligosaccharyltransferase
ov	ovine
PBS	phosphate buffered saline
POX	peroxidase
$sPLA_2$	secretory phospholipase A_2
tet	tetracycline
TLC	thin layer chromatography
UGGT	UDP-glucose glucosyltransferase
UPSTRM8	the 8 amino acid segment immediately upstream of Asn-594 in COX-2

CHAPTER I

LITERATURE REVIEW

Introduction

Prostanoids, namely prostaglandins, prostacyclin and thromboxanes, are potent lipid signaling molecules that are synthesized in most mammalian tissues. These lipid hormones belong to the family of twenty carbon fatty acid derivatives that are collectively known as eicosanoids. Prostanoids act locally in an autocrine or paracrine manner through transmembrane G-protein coupled receptors to elicit a wide range of physiological and pathological responses (1-7). The major fatty acid precursor for prostanoids is widely believed to be arachidonic acid (AA), a twenty carbon fatty acid that is a metabolite of the dietary essential fatty acid linoleic acid. Once synthesized *de novo* AA is preferentially esterified to the *sn*-2 position of glycerophospholipids in lipid bilayers of cell membranes during phospholipid remodeling (Fig. 1) (8). The release of free AA from membrane phospholipids by phospholipase A_2 is tightly regulated and represents the initial and first rate-limiting step of prostanoid synthesis (8-10). A second key point of control of prostanoid synthesis is the subsequent step involving the conversion of free AA to prostaglandin H_2 (PGH_2) by prostaglandin endoperoxide H_2 synthase (PGHS) also known as cyclooxygenase (COX). This step is also rate-limiting for prostanoid formation and is considered to be the committed step in the pathway (1,3). Cell specific prostanoid synthases then catalyze the isomerization or reduction of PGH_2 to form various bioactive prostanoids (Fig. 2).

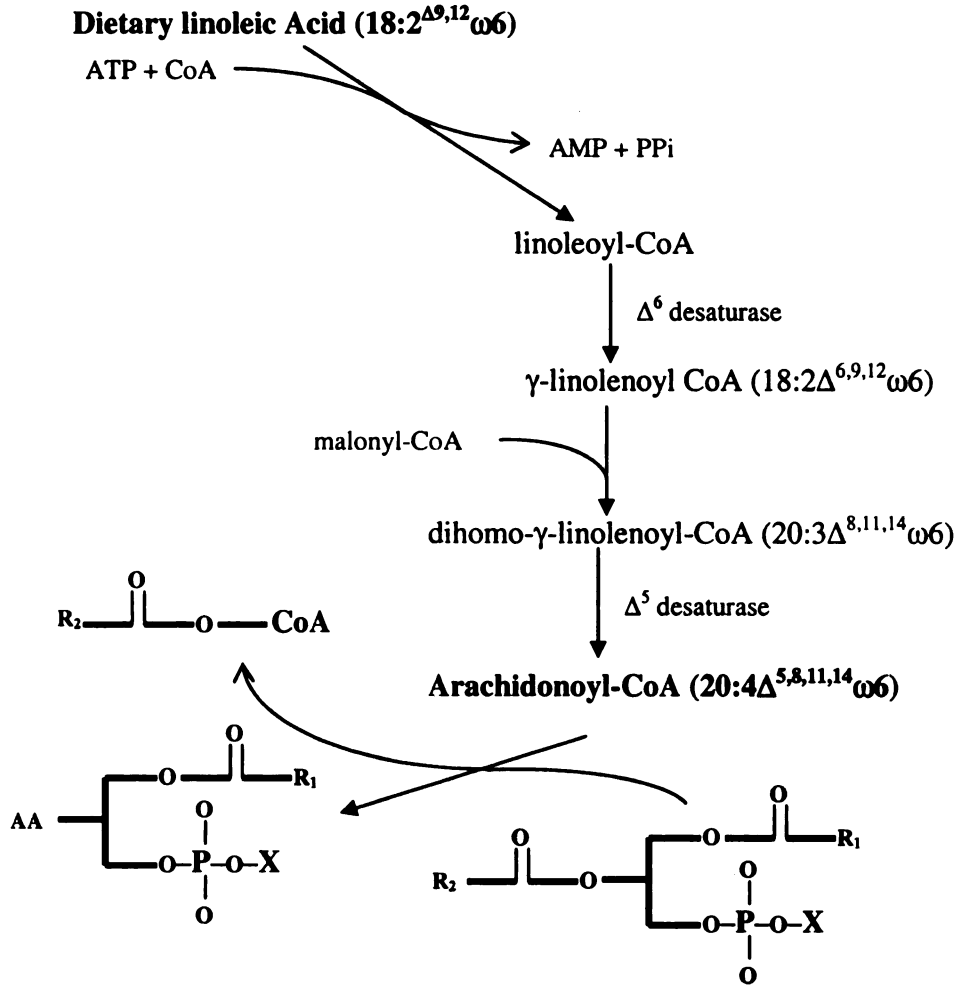

Figure 1. Synthesis and incorporation of AA into membrane glycerophospholipids. All mammalian cells except erythrocytes synthesize AA from the essential fatty acid linoleic acid (LA). As shown in the above scheme, AA synthesis from LA involves formation of two additional double bonds (Δ5 and Δ8) and two-carbon chain elongation. Once synthesized, AA is specifically incorporated into the *sn*-2 position of glycerophospholipids by acyltransferase during phospholipid remodeling.

There are two known isoforms of cyclooxygenase: COX-1 and COX-2. Both are membrane-bound heme-containing glycoproteins that possess two sequential catalytic activities: a cyclooxygenase activity that bis-oxygenates AA to form the hydroperoxide prostaglandin G_2 (PGG_2) and a peroxidase activity that reduces the 15-hydroperoxyl

group of PGG_2 to form PGH_2 (Fig. 2) (1,3,7). COX-1 and COX-2 are structural and functional homodimers and are known to associate monotopically with the luminal faces of the endoplasmic reticulum (ER) membrane and the nuclear envelope (11-17). Their membrane association is such that the opening of the cyclooxygenase active site is in the lipid bilayer to allow the uptake of mobilized free AA. Despite being monotopically associated with the membrane these isoenzymes are considered to be integral membrane proteins because they can only be removed from the membrane with detergent and not with chaotropic salts (15). Thus, by associating with one leaflet of the lipid bilayer, the COXs constitute a unique class of integral membrane binding proteins.

COX-1 and -2 are encoded by different genes; nonetheless, they share ~60% identity in primary structure. Both isoforms have a cleavable N-terminal signal peptide sequence, an epidermal growth factor-like domain, a membrane binding domain, and a globular catalytic domain. At the C-termini of COX-1 and -2 are KDEL-like motifs that have been shown to be important for retention of the enzymes in the ER (18,19). Adjacent to the ER retention signal of COX-2 is a 19-amino acid insertion that is lacking in COX-1 (Fig. 3). This C-terminal insertion also confers COX-2 with an additional consensus site for *N*-glycosylation. The biological role of this COX-2 C-terminal insertion will be explored in detail in Chapters II and III.

Although COX-1 and COX-2 are structural and functional isoforms, they have different expression patterns and biological functions. COX-1 is constitutively expressed in resting cells of most tissues (1,20). In contrast, COX-2 expression is usually absent in resting cells and can be induced in fibroblast, epithelial, endothelial, macrophage, and smooth muscle cells in response to growth factors, cytokines, mitogenic, and pro-

inflammatory stimuli (1,20-24). Induced COX-2 expression is usually observed to be transient (21-24). It is possible that the differential expression profiles of COX-1 and -2 may contribute to their contrasting biological roles. In general, prostanoids generated as a result of COX-1 activity are believed to play housekeeping roles (25) while those generated by COX-2 are not only important physiologically but have also been implicated in various pathophysiological processes such as inflammation (26), pain (27), fever (28), angiogenesis (29), and tumorigenesis (30). The COXs are the best known cellular target for non-steroidal anti inflammatory drugs (NSAIDs) such as aspirin, ibuprofen, indomethacin, and flurbiprofen (1).

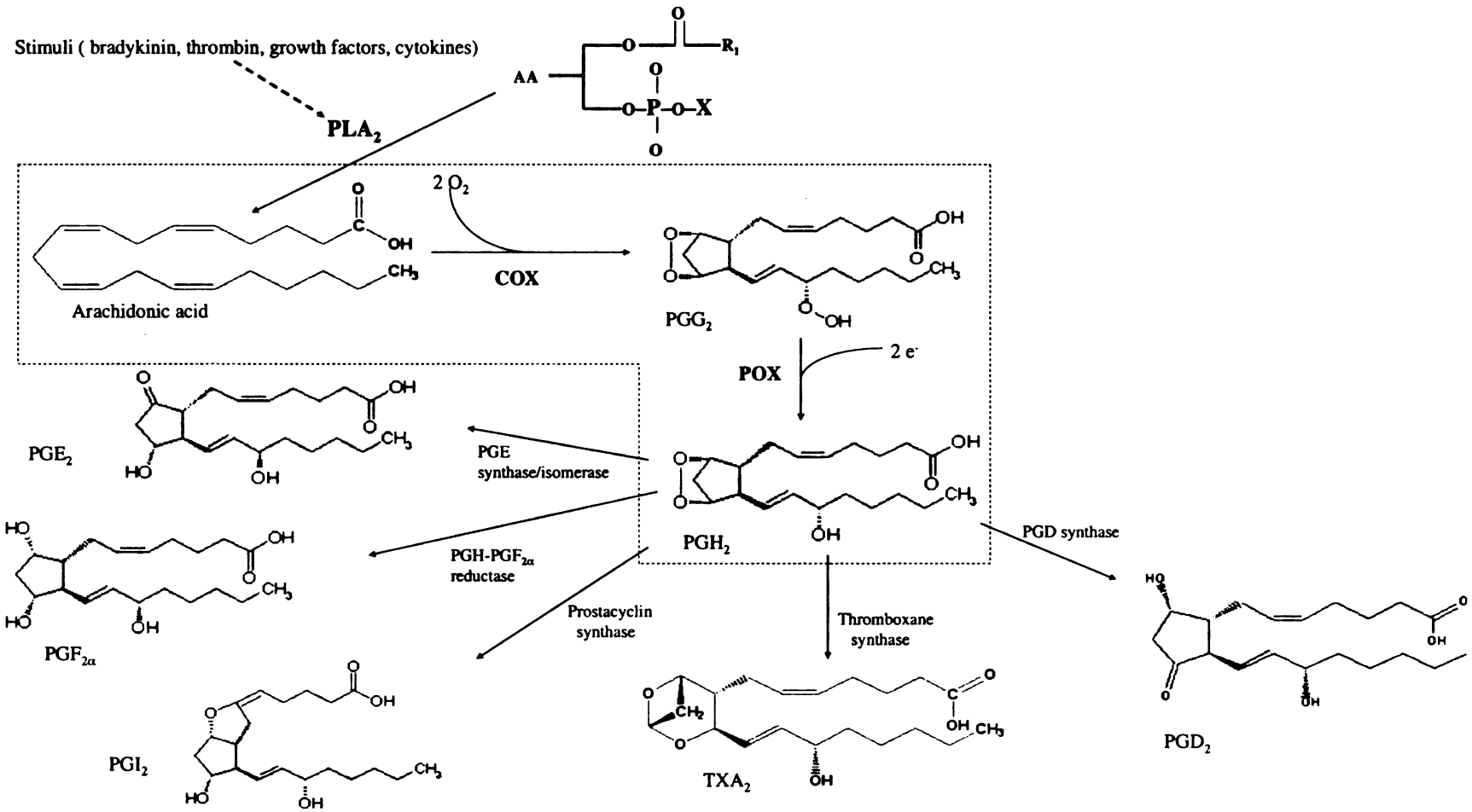

Figure 2. Stimulus-induced synthesis of bioactive prostanoids. The first rate limiting step of prostanoid formation is the stimulus-dependent mobilization of AA from membrane phospholipids by phospholipase A_2 (PLA_2). Free AA is converted to PGH_2 in a two-step reaction (boxed) catalyzed by the cyclooxygenase (COX) and peroxidase (POX) activities of COX-1 and -2. PGH_2 is a direct precursor for various prostanoids and their generation is stimulus- and cell-type specific. NSAIDS inhibit the COX activities of COX-1 and COX-2.

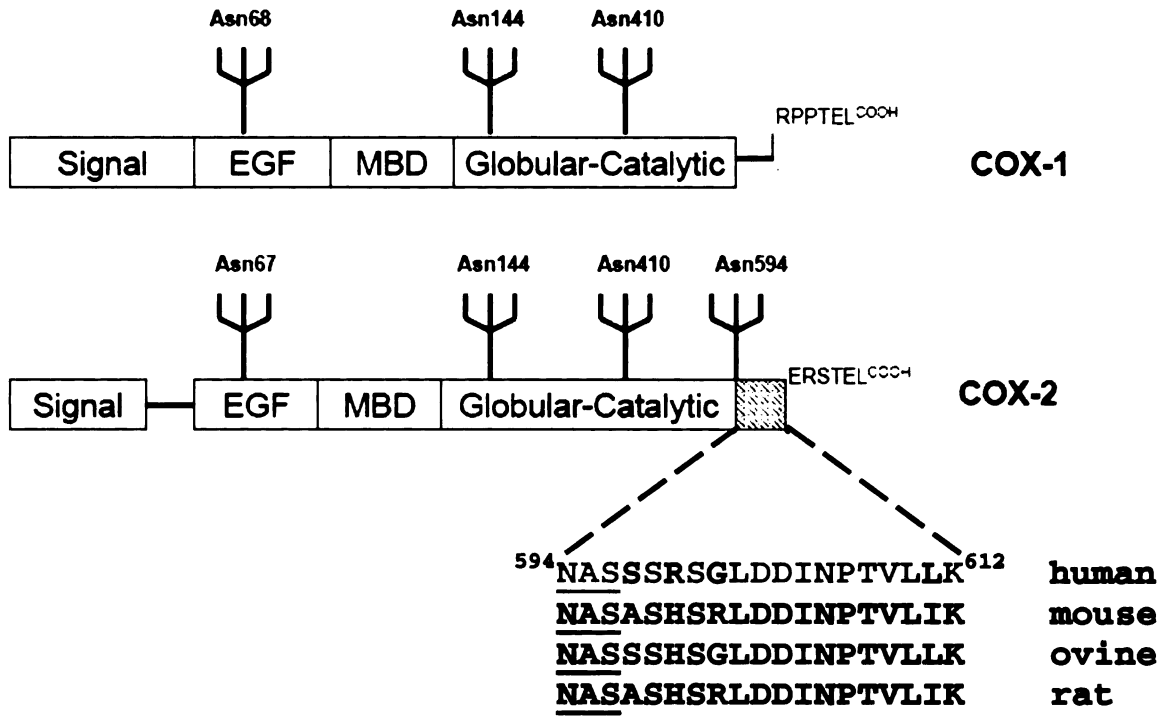

Figure 3. Domain alignment of COX-1 and COX-2 highlighting major differences in their primary structures. The cleavable ER signal sequence of COX-2 is shorter (18 residues) than that of COX-1 (25 residues). COX-1 is found to be glycosylated at three sites whereas COX-2 has four functional *N*-glycosylation sites. The last glycosylation site of COX-2 (Asn-594) is variably glycosylated and is part of a unique C-terminal 19-amino acid insertion (19-aa). Numbering for COX-1 begins with the Met at the translation start site. Numbering for COX-2 parallels the COX-1 numbering in which the start of the mature, processed COX-2 protein has the same number as the start of the mature, processed COX-1 (12). The Asn-594 glycosylation site is underlined, and 19-aa residues that are conserved in humans, mouse, sheep, and rat have been colored green. Images in this dissertation are presented in color.

Mobilization of Endogenous AA for Prostanoid Synthesis

Membrane glycerophospholipids can be deacylated at the *sn*-2 position by phospholipase A_2 (PLA_2) enzymes leading to the production of free polyunsaturated fatty acids, usually AA (31), and lysophospholipids. The mobilization of AA from the cell membrane for prostanoid synthesis depends on stimuli that will activate catalysis and/or

induce the expression of the PLA_2s involved. Therefore, AA liberation from the membrane is rate limiting for prostanoid metabolism. There is overwhelming evidence to indicate that of the nearly 22 mammalian PLA_2 enzymes that have been cloned and characterized, cytosolic $PLA_2\alpha$ ($cPLA_2\alpha$) and certain members of the family of secretory PLA_2s ($sPLA_2$) are largely responsible for the mobilization of AA for prostanoid metabolism (32-34). Of these two categories of Ca^{2+}-dependent PLA_2s, a consensus is emerging that $cPLA_2\alpha$ is critical for stimulus-dependent liberation of AA from membrane phospholipids.

$cPLA_2\alpha$ is expressed constitutively in most mammalian cell types (35). The expression of $cPLA_2\alpha$ can be elevated by various stimuli such as growth factors, cytokines and proinflammatory agonists (36-40). It is tightly regulated by multiple signaling pathways that control intracellular Ca^{2+} concentration and the phosphorylation state of the enzyme. Under the appropriate stimuli that will raise the intracellular cytosolic Ca^{2+} concentration to micromolar levels (eg. bradykinin and thrombin) (35,41-43), $cPLA_2\alpha$ will bind Ca^{2+} at its N-terminal C2 domain and, consequently, translocate to the ER membrane and nuclear envelope (44-46). It is thought that if the Ca^{2+} flux is low and transient, phosphorylation of the C-terminal catalytic domain of $cPLA_2\alpha$ by mitogen activated protein kinases (MAPKs) may increase the affinity of the Ca^{2+}-bound lipase for membrane binding (10,47). Ca^{2+}-dependent membrane association enables $cPLA_2\alpha$ to preferentially cleave AA from the *sn*-2 position of phospholipid substrates. That $cPLA_2\alpha$ is the phospholipase that is essential for mobilizing free AA from cellular membranes for eicosanoid metabolism is unequivocally demonstrated by studies using genetically deficient $cPLA_2\alpha$ mice. These mice are generally reported to be healthy and fertile (48-

50). However, they are resistant to pathologies that require the actions of prostanoids and other eicosanoids generated from the agonist-induced mobilization of AA (48,49,51-57). These models include collagen-induced rheumatoid arthritis, bleomycin-induced lung fibrosis, brain ischemia reperfusion injury, acute respiratory distress syndrome, autoimmune diabetes, multiple sclerosis, and intestinal polyposis (48,49,51-57).

$sPLA_2$s, particularly those belonging to Groups IIA, V, and X are thought to complement $cPLA_2\alpha$ activity by augmenting the release of cellular AA under certain pathophysiological settings such as those of an inflammatory response where the stimulus is robust and prolonged (58-60). Since $sPLA_2$s are usually expressed extracellularly it is reasonable to expect that these lipases would have a significant role in transcellular prostanoid biosynthesis. $sPLA_2$s require micromolar to millimolar concentrations of Ca^{2+} for catalytic activity and will indiscriminately hydrolyze cell surface phospholipids at the *sn*-2 position (10,61). Recent evidence has shown that prior to their secretion $sPLA_2$s could also act on intracellular membranes to mobilize endogenous AA (33,34). The expression of $sPLA_2$s, which is usually low in unstimulated immune effector cells (ie. macrophages, neutrophils, and mast cells) and in tissues of normal healthy individuals, is induced by proinflammatory stimuli such as IL-1β, TNFα, interferon-γ, phorbol ester, and bacterial lipopolysaccharide (62-66). Abnormally high levels of $sPLA_2$-IIA can be detected in synovial fluid of patients with rheumatoid arthritis (67,68) or in plasma of patients experiencing systemic inflammation (69-71). Not surprisingly, the marked elevation of $sPLA_2$-IIA during an inflammatory response is often accompanied by an induction of COX-2 expression and elevation of prostaglandins (10,72). The possible functional coupling between $sPLA_2$-IIA and COX-2 to generate prostaglandins in

inflammatory cells such as macrophages and mast cells appears to absolutely require $cPLA_2\alpha$ activity (34,73,74). These observations have implied that the activation of $cPLA_2\alpha$ precedes the mobilization of AA by $sPLA_2$-IIA for COX-2-mediated eicosanoid formation. However, the mechanistic basis for this crosstalk between $cPLA_2\alpha$ and $sPLA_2$-IIA is not understood.

Coupling between Cyclooxygenases and PLA_2s

Free AA that is mobilized by $cPLA_2\alpha$ and $sPLA_2$ is acted upon by cyclooxygenases to form the intermediate PGH_2 that is a substrate for terminal prostanoid synthases. It is still not clear whether there is preferential coupling between cyclooxygenases and the PLA_2s. Several research groups have reported that there exists two distinct phases of prostaglandin synthesis that are to a significant extent dictated by the stimulus involved in activating PLA_2, the endogenous levels of free AA, and the temporal expression of COX-2 (75-77). The immediate phase usually occurs within minutes after stimulation with bradykinin or calcium ionophore (A23187) and is characterized by a rapid and transient increase in cytoplasmic Ca^{2+} concentration (76). Since COX-1 is constitutively expressed, it is reasonable to expect that during the immediate phase of prostaglandin and thromboxane synthesis $cPLA_2\alpha$ is functionally coupled to COX-1. The delayed phase of prostaglandin synthesis which is induced by proinflammatory stimuli such as IL-1β occurs over several hours of cell stimulation and is largely mediated by inducible COX-2 activity (76). The delayed phase also appears to be dependent on $cPLA_2\alpha$ activity even though this phase is not concomitant with the cytoplasmic elevation of Ca^{2+} (36,78,79).

It is well known that COX-1 and COX-2 are differentially sensitive to the levels of endogenous AA. During the immediate phase the levels of liberated AA reach a level that is sufficiently high enough to be utilized by COX-1 (76,77). However, the burst of AA release during the immediate phase is transient and as cells progress into the delayed phase AA release becomes limiting for prostaglandin synthesis. That COX-2 has been shown to be preferentially capable of utilizing AA at low concentrations (1,76,77) would reasonably explain why this COX isoform is the predominant cyclooxygenase during the delayed phase. It has been suggested that differences in the enzymatic properties of COX-1 and COX-2 may account for their segregated utilization of AA in cells that coexpress both enzymes (1).

Functional Coupling Between Cyclooxygenases and Terminal Prostanoid Synthases

Cyclooxygenases are thought to exhibit distinct functional coupling with the downstream prostanoid synthases, which include prostaglandin E_2, prostaglandin D_2, prostaglandin $F_{2\alpha}$, prostacyclin, and thromboxane synthases. It is well established that in platelet cells, which do not express COX-2, thromboxane A_2 (TXA_2) is synthesized due to functional coupling between COX-1 and thromboxane synthase (TxAS), both of which are constitutively expressed (80). Platelet-synthesized TXA_2 acts in an autocrine fashion to induce platelet aggregation and in a paracrine fashion to contract vascular smooth muscle cells (81). The beneficial effect of low dose aspirin in reducing the risk of myocardial infarction and other cardiovascular diseases is due to the suppression of platelet TXA_2 synthesis. Stimulation of macrophage cells with Ca^{2+} ionophore leads to formation of TXA_2 during the immediate phase (82). In this case, constitutively

expressed COX-1 is functionally linked to TxAS. Eliciting the delayed phase in macrophage cells by stimulation with bacterial lipopolysaccharide (LPS) can also result in TXA_2 synthesis due to coupling between inducible COX-2 and TxAS (82).

The anti-thrombotic and vasodilatory activities of prostacylin (PGI_2) (83) counteract the effects of TXA_2 to achieve a balance that is crucial for maintaining vascular homeostasis. Vascular endothelial cells synthesize prostacyclin under normal physiological conditions (84) and during stress (85,86). Very low basal levels of PGI_2 can be detected in resting endothelial cells attributable to COX-1/PGI synthase coupling (87). In these cells mechanical stimuli, such as shear stress, and inflammatory stimuli, such as LPS or TNFα, result in coordinate induction of COX-2 expression and a dramatic rise in the levels of PGI_2 (85-87). That COX-2 is functionally coupled to PGI synthase in vascular endothelial cells provides an explanation for the negative side effects of anti-inflammatory COX-2 selective inhibitors on the cardiovascular system. Recent clinical trials have shown that these inhibitors are associated with an increased risk of myocardial infarction and stroke (88,89). Vascular smooth muscle cells, which express high basal levels of PGI synthase (90), are reported to generate PGI_2 under stress and/or inflammatory conditions (91). In LPS- or TNFα- stimulated macrophage cells, COX-2-derived PGI_2 is thought to be important for the resolution of the inflammatory response through suppression of the synthesis of proinflammatory cytokines (92).

PGD synthase (PGDS) catalyzes the isomerization of the endoperoxide PGH_2 to form PGD_2. Notably, PGD_2 is produced in brain where it is involved in sleep induction and regulation of pain (93,94). PGD_2 is also synthesized by mast cells in response to allergens and is believed to mediate allergic and inflammatory responses (95-97). The

chemical dehydration of PGD_2 yields 15-deoxy-$\Delta^{12,14}$-PGJ_2 which is thought to be the endogenous ligand for the nuclear receptor PPARγ (98-100). Acting via PPARγ this cyclopentenone prostaglandin has been shown to have anti-inflammatory activity and is thought to be formed during the resolution phase to counter the proinflammatory effects of other prostaglandins, including PGD_2 (100-103). Two distinct forms of PGDS exist: lipocalin-type PGDS (L-PGDS), a secreted protein that is highly expressed in the central nervous system (CNS), and hematopoietic PGDS (H-PGDS) expressed in mast cells, megakaryocytes, and macrophage cells (104). In a model of systemic inflammation, PGD_2 synthesis in the CNS by L-PGDS is dependent on COX-2 activity (105). In mast cells, the generation of PGD_2 upon challenge with IgE/antigen or A23187 is COX-1 dependent (40,82). However, stimulating mast cells with cytokines in the presence of IgE/antigen not only induces COX-2 expression but also results in a six-fold increase in PGD_2 synthesis (106).

Prostaglandin E_2 (PGE_2) is the major prostanoid that has been implicated in the pathophysiology of inflammation, pain, and fever. Genetic inactivation of COX-2 or selective inhibition of the enzyme suppresses inflammation, pain, and fever concomitant with a marked decrease in PGE_2 generation (107-109). This observation is consistent with the idea that PGE_2 synthesis under these pathophysiological conditions is mainly COX-2-derived. Three PGE synthase enzymes that catalyze the conversion of PGH_2 to PGE_2 have been identified. These are cytosolic PGE synthase (cPGES), and membrane-bound PGE synthases-1 and -2 (mPGES-1 and -2). cPGES is constitutively expressed in a wide variety of cell types (110) and its expression is usually not enhanced by proinflammatory stimuli. This enzyme has been shown to be capable of forming PGE_2

from COX-1-, but not COX-2-, derived PGH_2, particularly during the immediate Ca^{2+}-dependent phase of prostaglandin synthesis (110). Of the three PGE synthases, mPGES-1 is believed to be crucial for PGE_2 generation under various pathological conditions. mPGES-1 is coordinately induced with COX-2 in cells and tissues in which COX-2-derived PGE_2 is believed to exert physiological and/or pathological actions (109). Just like COX-2, mPGES-1 expression can be inhibited by anti-inflammatory glucocorticoids (111). Macrophage cells isolated from mPGES-1 null mice generate much smaller amounts of PGE_2 relative to wild type upon stimulation with LPS (112). Just like $cPLA_2\alpha$ and COX-2 deficient mice (51,113), mPGES-1 nulls have been reported to be resistant to collagen-induced arthritis (114), a model of chronic inflammation. Moreover, similar to COX-2-deficient mice (108), these mPGES-1 null mice have an impaired LPS-induced febrile response that is accompanied by a significant reduction of PGE_2 levels in the central nervous system (115). These observations suggest that functional coupling between $cPLA_2\alpha$, COX-2, and mPGES-1 is important for stimulus-induced PGE_2 formation under various stress or pathological conditions.

Regulation of Cyclooxygenase Gene Expression

Transcriptional Regulation

Although COX-1 and COX-2 exhibit a high degree of structural homology they are the products of two distinct genes that are regulated differently. COX-1 is constitutively expressed in most mammalian tissues (1,20). The COX-1 gene is approximately 22 kb in length, is located on chromosome 9, and is transcribed as a 2.8 kb mRNA (20). The COX-1 gene promoter is TATA-less, CAAT-less, GC-rich, and

contains multiple transcription start sites (116). These promoter features are usually characteristic of housekeeping genes that are constitutively expressed under basal conditions. The COX-1 promoter also contains three potential SP1 binding sites at -610, -111, and -89 relative to the ATG start codon. Reporter gene assays have demonstrated that the SP1 sites at -610 and -111 are functionally important in maintaining basal constitutive expression of COX-1 (117). Inducible COX-1 expression has been observed in a few cell types. For instance, differentiation of megakaryoblasts into megakaryocytes *in vitro* upon stimulation with phorbol ester (PMA) is usually accompanied by at least a 5-fold increase in COX-1 mRNA and protein (118,119). Megakaryocytes are the precursors of platelets which lack nuclei and constitutively express high basal levels of COX-1. Recently, it has been reported that the SP1 site at -111 works in conjunction with an intronic *cis*-acting AP-1 site to facilitate PMA-induced expression of COX-1 in megakaryoblasts (119). Inducible COX-1 is also observed in vascular endothelial cells that have been subjected to shear stress (86). Upon induction, COX-1 mRNA expression is usually prolonged in these cells. In contrast, induction of COX-2 mRNA by shear loading of endothelial cells is short-lived (86,120).

COX-2 was initially identified as a mitogen-responsive immediate early gene in fibroblast cells (121-124). Since then inducible COX-2 expression has been reported in a wide variety of cell types, including smooth muscle cells, macrophages, endothelial cells, synoviocytes, chondrocytes, pancreatic islet cells, and epithelial cells lining the airways, stomach and intestine. Importantly, induced COX-2 is reported to be short-lived in endothelial, smooth muscle, fibroblast, and epithelial cells (21-24). However, there are a few exceptions to the inducible and transient expression of COX-2; constitutive

expression of COX-2 has been reported in kidney, neuronal cells, and lung epithelial cells under physiological conditions (125-127). COX-2 expression is notably absent in erythrocytes, lymphocytes, and platelets. Various stimuli will induce COX-2 depending on the cell type. These stimuli include mitogens, inflammatory cytokines (IL-1β, IL-1α, TNFα, and interferon-γ), pro-inflammatory factors (eg. gram negative bacterial LPS), growth factors (FGF, PDGF, VEGF, and EGF), hormones (estrogen, luteinizing hormone, follicle stimulating hormone), oncogenes (v-Src and v-Ras), and mechanical stimuli such as fluid shear stress (1,20). Many of these COX-2-inducing stimuli will also activate the mobilization of AA from the cell membrane. More recently, it has been shown that some prostaglandins, particularly PGE_2, which would be formed during the immediate phase due to COX-1 activity, may activate their respective G protein coupled receptors to induce COX-2 in a cyclic AMP- and protein kinase A-dependent fashion (128).

The 8.3 kb COX-2 gene is located on chromosome 1 and is mainly transcribed as a 4.5 kb mRNA (20). The last exon of the COX-2 gene encodes the 3'-untranslated region (3'-UTR), which contains multiple copies of the 'AUUUA' RNA instability elements that have a crucial role in the post-transcriptional regulation of COX-2 (20,129). Unlike COX-1, the COX-2 promoter is replete with putative *cis*-acting regulatory elements suggesting tight and complex regulation of the gene by numerous signaling pathways. Of these *cis* elements, those that have been identified to have a regulatory role in COX-2 transcription include E-Box, cAMP response element (CRE), NFκB, AP-1, CAAT enhancer binding protein (C/EBP), SP1, serum response element (SRE), and peroxisome proliferator response element (PPRE) (1,20,130,131). Subtle differences exist

in the COX-2 promoter sequence between the human and mouse gene. For instance, the human gene has one CRE, one NFκB, and two C/EBP elements while the mouse gene has one C/EBP, two CRE, and two NFκB sites.

Depending on the cell type and the stimulus, distinct combinations of *cis*-regulatory elements will be utilized to activate COX-2 transcription. This is most evident during septic shock, a systemic inflammatory response of the host to infection by gram negative bacteria. The initial recognition of the LPS component of the bacterial cell wall by monocytes and macrophages that comprise the host innate immune system will lead to the activation of COX-2 gene transcription (130,132). LPS is recognized by toll-like receptor 4 (TLR4) resulting in signaling cascades that lead to the simultaneous activation of the NFκB, and the three MAP kinase (ERK, p38, and JNK) pathways (131,133). LPS-induced MAP kinase signaling activates C/EBP, CREB, and the AP-1 transcription factor complex (130,131,133). These activated trans-acting factors localize to the nucleus and bind the COX-2 promoter upon which they act in concert to stabilize the binding of coactivator complexes that are responsible for recruiting the basal transcriptional machinery (ie. RNA polymerase II and its associated factors) needed to initiate transcription.

COX-2 inducible gene expression can be strongly retarded by glucocorticoids. There is evidence indicating that these anti-inflammatory steroids may exert part of their inhibitory action by suppressing COX-2 transcription. However, it is not clear how glucocorticoids negatively regulate COX-2 transcription; moreover, the COX-2 promoter lacks a glucocorticoid response element suggesting that the regulation may be indirect. Several research groups have independently shown that dexamethasone, a glucocorticoid

analog, prevents the activation of NFκB and its subsequent nuclear localization by upregulating the expression of IkBα (134,135), an NFκB-interacting protein that sequesters the transcription factor in the cytosol. Therefore, it is highly likely that glucocorticoids may inhibit COX-2 transcription by interfering with the activation of NFκB.

The anti-inflammatory cyclopentenone prostaglandin 15-deoxy-$\Delta^{12,14}$-PGJ_2 (15-d PGJ_2), the dehydration product of PGD_2, is known to suppress COX-2 transcription (136,137). 15-d PGJ_2 binding to its nuclear receptor PPARγ inhibits PMA-mediated induction of COX-2 in human epithelial cells by preventing binding of the AP-1 trans-acting complex to the promoter and the subsequent recruitment of the CBP/p300 coactivator complex (138). Inhibition of AP-1 transactivation of COX-2 can be rescued by a PPAR response element decoy oligonucleotide suggesting that ligand-bound PPARγ may bind the PPRE site of the COX-2 promoter to repress transcription.

Post-transcriptional regulation

COX-2 mRNA has a very short half-life. This can be explained by the presence of multiple copies of the AUUUA motif within the 3'-UTR of COX-2 mRNA that are known to direct mRNA decay (20,129). Deletion of these *cis*-acting decay motifs from the 3'-UTR of COX-2 stabilizes the transcript (20,22). Unlike COX-2, COX-1 mRNA is very stable and its 3'-UTR lacks these AU-rich elements (AREs) (22). The mechanism by which AREs promote mRNA degradation in mammalian cells is not clearly understood. There is general agreement that AREs promote deadenylation of the polyA tail which precedes 5' to 3' or 3' to 5' exonuclease cleavage of the message (139-142). Most

recently, Stoecklin *et al.* have reported that ARE-mediated deadenylation leads to decapping of the 5' 7-methyl guanosine cap causing the message to be degraded 5'to 3' by the exonuclease Xrn1 (142).

Although numerous ARE binding proteins have been shown to interact with COX-2 AREs, the ARE binding protein(s) responsible for initiating ARE-mediated decay of COX-2 mRNA is yet to be identified. The activation of the p38 MAPK pathway by pro-inflammatory stimuli has been implicated in stabilizing COX-2 mRNA (143). Stabilization of the COX-2 transcript by p38 MAPK signaling is inhibited by the glucocorticoid dexamethasone and is believed to require a 123-nucleotide region within the 3'-UTR and immediately downstream of the termination codon that has six ARE copies (144). It is not clear what ARE binding proteins become activated by p38 MAPK signaling to effect ARE-dependent COX-2 stabilization. However, various ARE binding proteins such as CUGBP2 and HuR have been shown to bind the COX-2 3'-UTR and stabilize the transcript. HuR-mediated COX-2 transcript stabilization has been reported in colon cancer cells where COX-2 is aberrantly over-expressed (145). In contrast, CUGBP2-mediated COX-2 transcript stabilization is observed in epithelial cells undergoing apoptosis due to radiation exposure (146,147). In these cells, CUGBP2 has also been shown to have the paradoxical role of inhibiting translation of the COX-2 transcript. This is believed to be the mechanism by which radiation-induced expression of CUGBP2 in epithelial cells inhibits COX-2-mediated formation of PGE_2 that is known to have anti-apoptotic and mitogenic activities.

The translational silencing of COX-1 has been reported to occur in megakaryocytes. During the PMA-induced differentiation of the megakaryocytic cell line

MEG-01 COX-1 mRNA is upregulated within a day of PMA treatment while an increase in COX-1 protein is not observed for several days (118). Duquette and Laneuville have reported a correlation between the occupancy of a putative 20-nucleotide *cis* element within the COX-1 3'-UTR by a protein complex and the inhibition of COX-1 protein synthesis (118). This complex of COX-1 mRNA binding proteins is yet to be characterized.

Cyclooxygenase protein turnover

It is well established that the distinct profiles of expression of COX-1 and COX-2 observed in some mammalian cells could at least be partly attributed to differences in regulation of the isoforms at the transcriptional and post-transcriptional levels. Although it is not clear whether these enzymes are also regulated differently at the post-translational level by proteolysis, their distinct patterns of expression suggest that this may be the case. Certainly, rapid turnover of COX-2 in tissues where the enzyme is transiently expressed may serve a significant physiological role in regulating the levels of prostanoids whose synthesis is attributed to this COX isoform. Consistent with this idea Rockwell and co-workers have reported observing the accumulation of COX-2 in its native form and as polyubiquitin conjugates in HT4 neuronal-like cells treated with inhibitors or disruptors of proteasomal degradation (148,149). In contrast, COX-1 protein levels were unaffected by this treatment. These experimental results suggest that COX-2 may be selectively regulated by the ubiquitin-proteasome pathway, which has been implicated in the proteolysis of intracellular proteins with short half-lives. My thesis will

attempt to identify and effectively address the molecular basis for the selective regulation of COX-2 by proteolytic degradation.

Cyclooxygenase Protein Structure and Subcellular Compartmentation

Cyclooxygenases are membrane-bound, heme-containing glycoproteins that are resident in the ER lumen and the contiguous lumen of the nuclear envelope (11-17). They are believed to exist and function as homodimers with each monomeric subunit possessing cyclooxygenase and peroxidase active sites (11,17,150). X-ray crystal structures of mature COX-1 and COX-2 from several mammalian species have already been determined. Their three dimensional structures exhibit a high degree of homology which would be expected since both enzymes are ~60% identical in primary structure.

The maturation of COX-1 and COX-2 in the ER lumen involves cleavage of the N-terminal ER targeting signal sequence, *N*-glycosylation at multiple sites, disulfide bond formation, heme incorporation, membrane insertion, and dimerization. These co-translational and post-translational modifications yield COX-1 and COX-2 mature glycoproteins with monomeric masses of ~70 and ~72-74 kDa, respectively (151). There are three major folding domains in mature COX-1 and -2: an epidermal growth factor (EGF) domain, a membrane binding domain (MBD), and a globular catalytic domain (Figs. 3 and 4). The EGF domain forms a significant portion of the dimer interface; however, it is not clear whether it is critical for homodimerization. It has been proposed that the EGF domain may have an important role in enabling the monotopic insertion of the maturing cyclooxygenase into the membrane (152). The MBD is the only membrane anchor for cyclooxygenases that has been identified thus far. It is made up of four

consecutive amphipathic α-helices that surround the opening of the cyclooxygenase active site (Figs. 4 and 5). Hydrophobic and aromatic side chains protrude downwards from these amphipathic helices and become inserted into one leaflet of the lipid bilayer. Hydropathy analysis of the MBD of both isoforms indicates that the COX-1 MBD is significantly more hydrophobic than that of COX-2 (16). Nonetheless, in both cases the MBD-mediated monotopic insertion creates an unusually tight membrane association that cannot even be disrupted with a high salt wash (15,16). Therefore, the cyclooxygenases constitute a unique class of monotopic integral membrane binding proteins.

The cyclooxygenase catalytic domain is globular and is mostly comprised of α-helical secondary structure. The cyclooxygenase (COX) active site is an ~25 Å long hydrophobic channel that begins at the MBD and extends upwards into the protein hydrophobic core. In order to be utilized as substrate, unesterified AA has to enter the COX active site through the mouth formed by the MBD. The productive conformation of AA at the COX active site is such that its ω end extends into the hydrophobic core while the Δ carboxyl end is stabilized at the mouth of the active site through electrostatic interactions with the guanidium group of Arg-120 (153,154). The peroxidase (POX) active site is solvent-exposed and contains a ferric-protoporphyrin IX heme group that is bonded to the proximal histidine, His-388 (Fig. 5b). Both COX isoforms can be purified as apo-enzymes indicating that the ferric heme is reversibly bound to the POX site. Although the POX and COX active sites are spatially distinct they are functionally interdependent. The COX oxygenation reaction requires activation by POX activity (155,156). In turn, PGG_2 formed at the COX active site diffuses to the POX active site where it is reduced to form PGH_2.

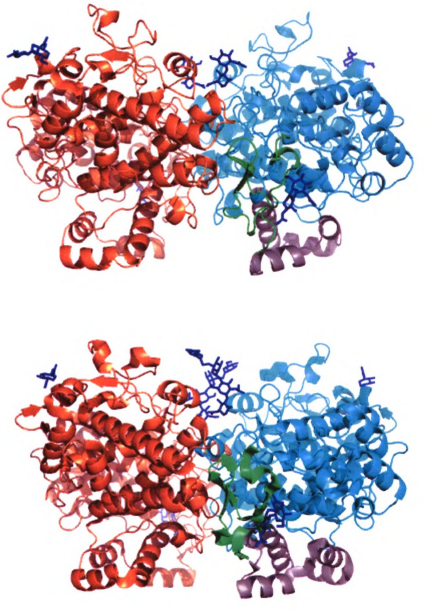

Figure 4. Ribbons diagrams of the three dimensional structures of ovine COX-1 (top) and murine COX-2 (bottom). The COX-1 and COX-2 structures are virtually superimposable. One monomer of each enzyme is colored orange; the other monomer is colored to show the N-terminal epidermal growth factor-like domain (green) at the dimer interface, the four amphipathic helices that make up the membrane binding domain (gray), and the globular catalytic domain (cyan). *N*-linked oligosaccharide groups (blue) are also shown.

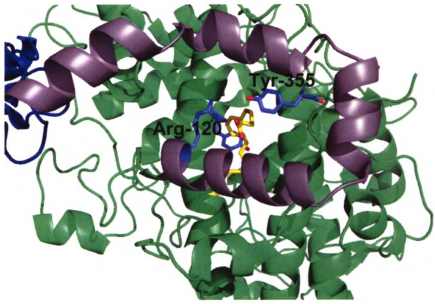

Figure 5a. A view from the membrane plane showing the opening into the cyclooxygenase active site of ovine COX-1 created by the membrane binding domain (gray). The carboxylate group of bound AA (yellow) forms a salt bridge with the guadinium group of Arg-120 thereby stabilizing the substrate at the active site. Shown in the background is the catalytic residue Tyr-385 which is suitably positioned to abstract the 13*pro*S hydrogen of AA.

Subtle differences exist between the primary structures of COX-1 and COX-2. The N-terminal signal sequence of COX-1 is longer (25 residues) and more hydrophobic than that of COX-2 (18 residues) (Fig. 3). After cleavage of the signal sequence the N-terminal most residue in both enzymes is usually an alanine. For convenience in structural comparisons between the isoforms the sequence of mature COX-2 is numbered such that it parallels the COX-1 numbering in which the start of the mature, processed COX-2 protein has the same number as the start of the mature, processed COX-1 (12). COX-2 numbering parallels that of COX-1 up to the C-terminus, where a 19-amino acid insertion occurs in COX-2 six residues in from the C-terminal end. This C-terminal

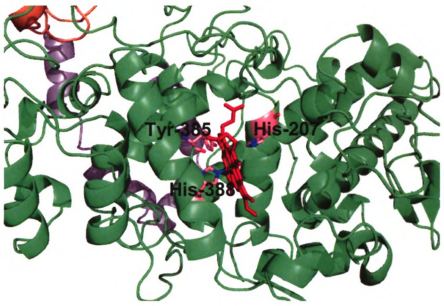

Figure 5b. A view from the top showing the peroxidase active site of ovine COX-1. Proximal His-388 coordinates the heme prosthetic group (red) at the active site by bonding to the ferric heme. Mutagenesis studies have shown that both His-388 and distal His-207 are important for POX catalysis. Although the role of distal His-207 in POX catalysis has not been lucidly defined, it's proposed to be important for deprotonation of the hydroperoxide substrate and reprotonation of the alkyloxide ion intermediate to form an alcohol (151). Tyr-385 and the membrane binding domain (gray) are shown to indicate the position of the COX active site relative to the POX active site.

insertion imparts COX-2 with a consensus *N*-glycosylation site at Asn-594 (Fig. 3) that has no counterpart in COX-1. As a result COX-1 is found to be *N*-glycosylated at three sites, while COX-2 is glycosylated at its first three *N*-glycosylation sites and variably glycosylated at Asn-594 (151).

It has been hypothesized that the C-terminal COX-2 insertion may serve as a signal to regulate protein turnover or the subcellular compartmentation of COX-2 (1,152). In view of the short-lived expression of COX-2 protein in cellular contexts

where COX-1 is constitutive (21-24), it is possible that the insertion could mediate the selective and rapid degradation of COX-2. The C-terminus of COX-2 has not been successfully resolved in its entirety by X-ray crystallography analysis. The last resolved residue in the highest resolution murine COX-2 crystal structure attained thus far (the human COX-2 structure is not available in the PDB even though it has already been solved) is Ser-596 (157), the final amino acid in the Asn-594 *N*-glycosylation consensus sequence at the beginning of the insertion. This *N*-glycosylation site is part of a two-turn helix (TKTATINAS) that is linked to an upstream helix by a long 15-residue loop that includes 11 resolved residues (KGCPFTSFNVQ) and an unresolved 4-residue sequence (DPQP) (Fig. 6). Asn-594 is not glycosylated in the murine structure presumably because the amide group of its side chain is pointed upwards towards the upstream helix that is at a distance of ~4.5 Å. This space is barely sufficient to accommodate an *N*-glycan group. Moreover, a disulfide bridge between Cys-569 of the upstream helix and Cys-575 of the loop may further hinder Asn-594 glycosylation. Therefore, in order for Asn-594 to be glycosylated a local conformational change would have to occur, probably involving breakage of the disulfide bond and movement of the long and inherently flexible intervening loop.

The inability to resolve the remaining 16 amino acids of the C-terminal 19-amino acid insert in COX-2 crystal structures may be an indication that this portion is largely disordered and lacks any degree of secondary structure. The hydroxyl side chain of Ser-596 is solvent-exposed and is situated close to the surface of the membrane (157). The KDEL-like C-terminal ER retention signal of COX-2 also has to be solvent-exposed and near the membrane in order to be bound by membrane proteins involved in ER retention

(18,19). Therefore, the unresolved portion of the COX-2 insert may occur on the surface of the protein close to the membrane surface. My thesis project has tested the hypothesis that the biological role of the C-terminal 19-amino acid insertion is to selectively regulate COX-2 protein turnover. I have also attempted to decipher the molecular mechanism by which the COX-2 insertion may initiate and promote protein degradation. My findings are presented and discussed in detail in Chapters II and III.

6A.

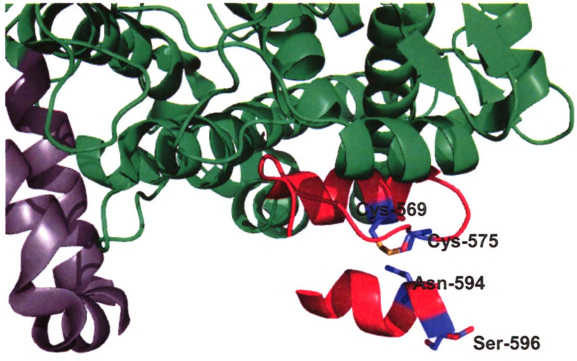

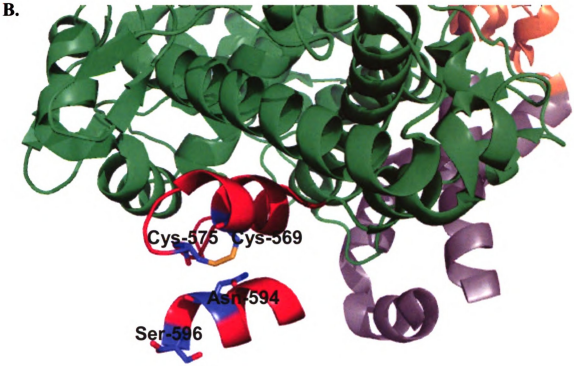

Figure 6. Ribbon diagrams showing two views (A and B) of the C-terminal structure of murine COX-2. The last resolved residue in this structure is Ser-596 which is the final amino acid of the Asn-594 consensus glycosylation site. Not surprisingly, Asn-594 is not glycosylated most likely because its amide side chain is pointed away from the surface and in the direction of a nearby helix. Both helices are separated by a long 15-residue loop; the last four residues of this loop are not resolved in the structure. A disulfide bond is formed between the thiols of Cys-569 and Cys-575 which may prevent glycosylation of Asn-594. Futhermore, the distance between Asn-594 and Cys-569 is too small to accommodate an N-glycan group. For Asn-594 to become glycosylated the disulfide bond may have to be reduced to increase the flexibility of the loop. The catalytic domain is colored green and the MBD is colored gray.

Cyclooxygenase Catalysis, Substrate Specificity, and Suicide Inactivation

The committed step in the prostanoid synthesis pathway, catalyzed by COX-1 and COX-2, is actually a two-reaction step that involves: a) the incorporation of two molecules of O_2 to AA (5,8,11,14-eicosatetraenoic acid) to form the hydroperoxy endoperoxide PGG_2, and b) the two electron reduction of PGG_2 to form the hydroxy endoperoxide PGH_2(1,3). The endoperoxide bridge of PGH_2 is then acted upon by distinct terminal prostanoid synthases to form different prostanoids. The proposed catalytic mechanism of the cyclooxygenases is shown in Fig. 7 (156,158). Both the peroxidase (POX) and cyclooxygenase (COX) reactions are dependent on the ferric-protoporphyrin IX (Fe^{3+}-IX) heme prosthetic group which is coordinated at the active site by proximal His-388. The POX activity is required to initiate the COX activity. Cyclooxygenase catalysis commences at the POX active site where an initiator hydroperoxide that is yet to be identified oxidizes the heme group by removal of two electrons yielding an oxyferryl heme radical intermediate called compound I. Neutralization of this radical intermediate requires an electron provided by a neighboring tyrosine residue (Tyr-385) in an intramolecular reaction that leads to the formation of intermediate II comprising an oxyferryl heme and a tyrosyl radical. Thereafter, the reactive tyrosyl radical initiates COX catalysis by abstracting the 13-pro*S* hydrogen from AA at the COX active site yielding a radical at the 13-carbon (C-13). The AA radical undergoes an isomerization that eventually transfers the radical to C-11. Subsequently, an endoperoxide bridge is formed between C-9 and C-11 after reaction with one molecule of O_2. As this happens, a second molecule of O_2 is added to the C-15 position forming the hydroperoxyl PGG_2.

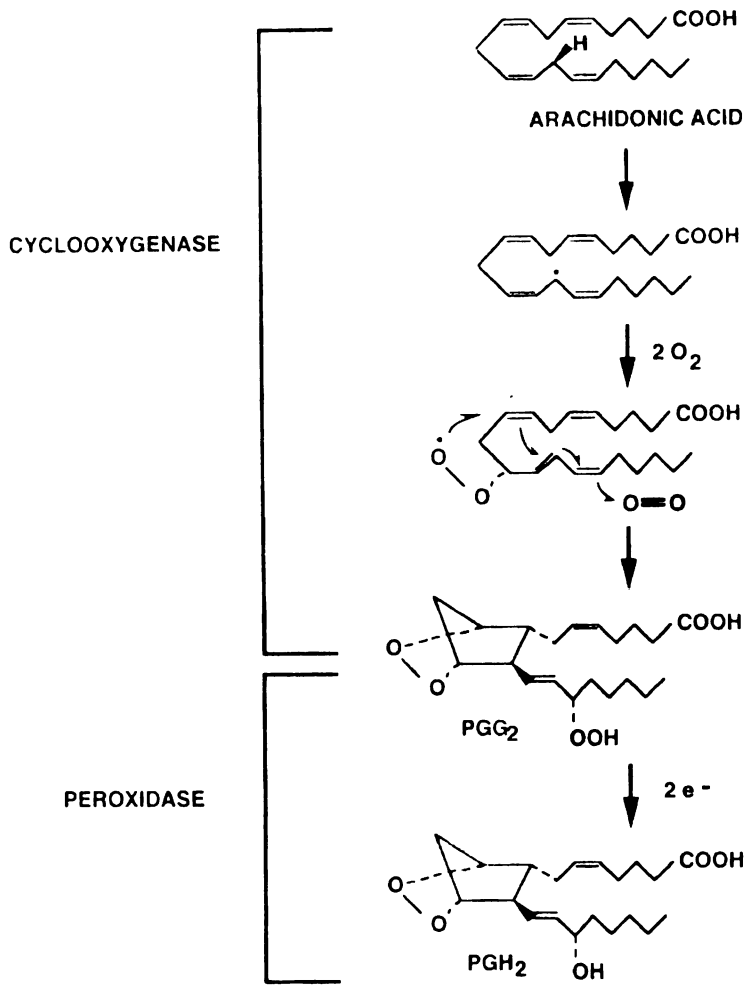

Figure 7a. Mechanism for bis-oxygenation of AA and subsequent reduction of PGG_2 to form PGH_2. Reproduced with permission from Ref. 156.

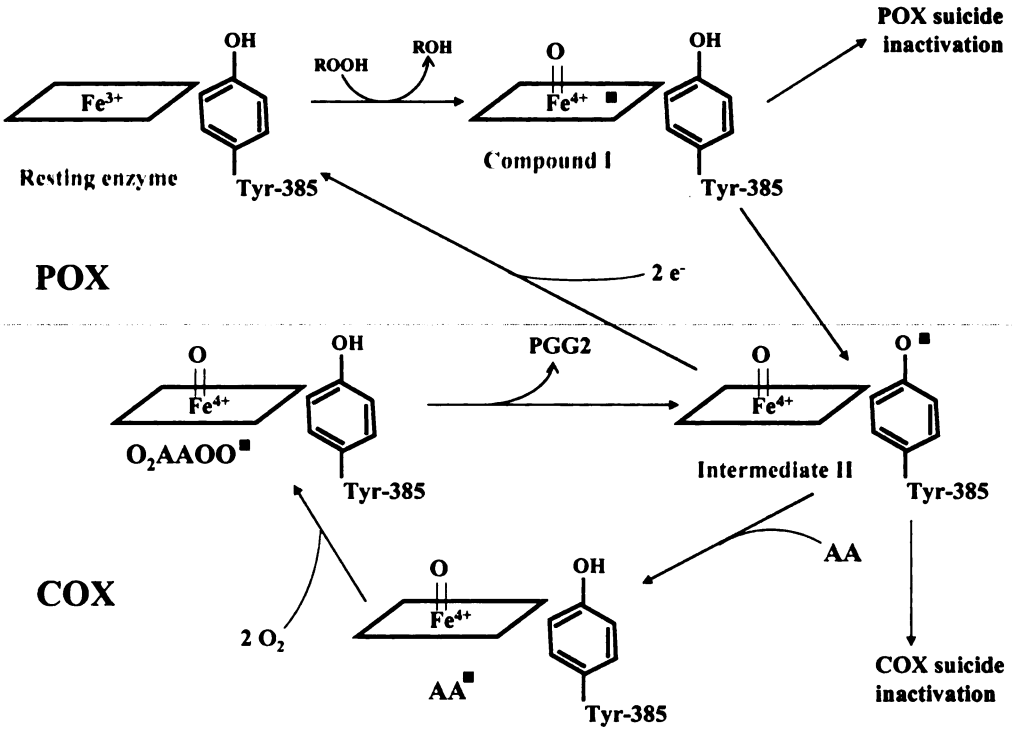

Figure 7b. Proposed catalytic mechanism of the COX isoforms. Cyclooxygenase catalysis is initiated by hydroperoxide which oxidizes the ferric heme to form compound I. This enzyme intermediate undergoes an intramolecular rearrangement of electrons resulting in a shift of the radical from the heme to Tyr-385. Both radical intermediates are very reactive and may cause modifications in the protein that lead to suicide inactivation. The reactive tyrosyl radical at Tyr-385 will abstract the 13*pro*S hydrogen of AA as shown in Fig. 7a leaving a radical at C-13. This initiates bis-oxygenation of AA to form PGG_2 which is subsequently reduced at the POX site to form PGH_2. The reduction of PGG_2 is coupled with formation of compound I and the initiation of a second catalytic cycle.

There is no direct channel connecting the COX and POX active sites through which PGG_2 can diffuse. It has been proposed that PGG_2 must exit the COX site by first diffusing through the opening in the MBD and then traveling around the protein surface in order to reach the POX site (156). The two electron reduction of PGG_2 at the POX site has the dual role of forming PGH_2 and regenerating compound I for procession through

another catalytic cycle. The kinetic constants for the COX activity of COX-1 and -2 are very similar. When AA is utilized as substrate, both enzymes have similar COX specific activities (~25-30 μmol/min of substrate per mg of enzyme) and the K_m of the purified or microsomal (membrane-bound) forms of these enzymes is ~ 5 μM (1).

The catalytic activities of the cyclooxygenase isoforms are distinctly regulated. This became initially apparent when Reddy and Herschman demonstrated that stimulus-induced prostaglandin synthesis in mitogen-stimulated 3T3 fibroblasts could almost entirely be attributed to inducible COX-2 activity, even though COX-1 is constitutively expressed at detectable levels in these cells (77). A year later, it was reported that the COX activities of COX-1 and COX-2 are initiated by different levels of hydroperoxide (155). Using varying amounts of the hydroperoxide scavenger, glutathione peroxidase, to regulate the levels of hydroperoxide in the reaction mixture needed to initiate COX activity, Kumalcz and Wang were able to show that both COX-1 and COX-2 COX activities could be stimulated by nanomolar concentrations of hydroperoxide, with the latter activity requiring 10-fold less hydroperoxide. Interestingly, they also noted that addition of COX-2 to a COX reaction mixture containing COX-1 did not significantly improve COX-1 activity at low hydroperoxide concentrations, suggesting that the amount of PGG_2 generated by COX-2 was not sufficient to initiate COX-1 COX activity. Therefore, it is conceivable that in cells coexpressing both isoforms COX-2 could be the functionally active isoform with COX-1 remaining in its latent or resting form at low intracellular hydroperoxide levels. That COX-1 is mostly active during the immediate phase of prostanoid synthesis would suggest the possibility of a peroxide flux that would be sufficiently high to activate COX-1 during this phase but insufficient to activate COX-

1 during the delayed phase. Alternatively, the inability of COX-1 to utilize AA at low concentrations as is observed during the delayed phase could also contribute to the temporal segregation of COX-1 and COX-2 activities.

Although the hydroperoxide responsible for initiating COX activity *in vivo* is not known, COX-1 and -2 can utilize a broad variety of hydroperoxides as substrates. In addition to PGG_2, COX-1 and -2 can reduce hydrogen peroxide, *t*-butyl hydroperoxide, ethyl hydroperoxide, 15-hydroperoxy eicosatetraenoic acid (15-HPETE), and cumene hydroperoxide (156). Despite their broad substrate specificity, the COXs tend to prefer secondary alkyl hydroperoxides such as 15-HPETE and PGG_2 (156,159,160) and (Liu and Smith, unpublished results). With respect to COX activity, AA, the physiological substrate of both COX isoforms, is the most preferred substrate as determined by kinetic measurements of oxygenation efficiency (156,161). Unlike COX-1, COX-2 can also oxygenate a variety other substrates *in vitro* albeit not as efficiently as AA (156). These substrates include, 2-arachidonyl glycerol (2-AG), an ester derivative of AA, anandamide, an amide derivative of AA, eicosapentaenoic acid (EPA), and dihomo-γ-linolenic acid (DHLA). COX-2 is able to selectively utilize 2-AG and anandamide as substrates because it has an active site side pocket extension that creates a larger active site compared to that of COX-1 that can accommodate these arachidonyl derivatives (3). This side pocket extension has been exploited by the pharmaceutical industry to design selective COX-2 NSAIDs.

The POX and COX activities of the COXs are well known to undergo self inactivation after an unknown number of rounds of catalytic turnover. POX and COX self inactivation is irreversible and is also mechanism-based since it is induced by POX or

COX substrate, and proceeds from heme and tyrosyl radical intermediates formed during the POX and COX reactions, respectively (3,156). However, the specific structural changes in the holoenzyme that lead to suicide inactivation remain unknown. Mevkh *et al.* noted that COX self inactivation is accompanied by dramatic changes in protein structure as is manifested by the increased susceptibility of the inactive enzyme to trypsin cleavage and the increased number of exposed histidine residues subject to chemical covalent modification (162,163). POX and COX suicide inactivation have only been observed *in vitro* and it is still not clear whether the COXs can undergo self-inactivation *in vivo*. Suicide inactivation could indeed serve as an additional control mechanism for regulating prostanoid synthesis *in vivo*. In this regard it would be interesting to investigate whether the inactive forms of COX-1 and -2 are more susceptible to degradation compared to the native forms. It is well established that misfolded or structurally damaged proteins present in the ER can be targeted for degradation by a process known as ER-associated degradation (164-166). It is possible that COX-2 might selectively undergo suicide inactivation at endogenous hydroperoxide or AA levels that would be insufficient to inactivate COX-1. If indeed the inactive protein gets degraded, this could explain the short-lived nature of COX-2. Chapter IV of my thesis explores inactivation-induced COX-2 protein turnover as a potential mechanism for regulating COX-2 protein levels *in vivo*.

Proteolytic Degradation of Intracellular Proteins

Lysosomal hydrolysis and ubiquitin-proteasome degradation are the two major pathways for the degradation of intracellular proteins. Lysosomal protein degradation is a

non-selective process that is catalyzed by cysteine hydrolases called cathepsins which function optimally at the low acidic pH of the lysosome (167). In addition to digesting exogenous proteins that have been internalized through phagocytosis or receptor-mediated endocytosis, lysosomes are also known to engulf and indiscriminately degrade cytosolic and organelle proteins in bulk (168,169). This process, known as autophagy, is usually activated for the clearance of cytosolic protein aggregates and damaged organelles (168). Autophagy is also induced by cell starvation and can be inhibited by the mTOR (mammalian target of rapamycin)/phosphatidylinositol-3 kinase signaling pathway (170).

The selective degradation of intracellular proteins is largely non-lysosomal and appears to be mediated mainly by the ubiquitin-proteasome pathway. The 26S proteasome is a ~2 MDa cytosolic and nuclear multi-protein complex that catalyzes the selective degradation of three classes of protein substrates: a) normal short-lived proteins; b) structurally defective proteins; and c) misfolded proteins (171). The 26S proteasome consists of a barrel shaped, channel-like 20S proteolytic core that is capped on each end with a 19S ATPase subunit (172). The proteolytic core comprises three known catalytic activities, namely trypsin-like, chymotrypsin-like, and peptidyl-glutamyl activities (173).

For most proteasome substrates the prerequisite for degradation is polyubiquitination, a process that involves the sequential attachment of molecules of the highly conserved 76-amino acid ubiquitin to the ε-amino group of one or more internal lysine residues of the protein to form a long polymer of ubiquitin (174). Conjugation of the protein substrate with a polyubiquitin tag is catalyzed by three different enzymes (Fig. 8) (174,175). Firstly, the carboxyl end of ubiquitin is conjugated to a thiol group at the

active site of a ubiquiting activating enzyme (E1) in an ATP-dependent manner. Formation of the thioester linkage will activate ubiquitin for transfer to an active site cysteine residue of ubiquitin conjugating enzyme (E2). Finally, ubiquitin protein ligase (E3) will specifically recognize the protein substrate and aid in the transfer of the ubiquitin moiety to the amide side chain of an exposed lysine residue. The successive addition of ubiquitin molecules to one another will occur in a similar three-step reaction where the carboxyl end of one ubiquitin molecule is conjugated to a specific lysine (Lys-48) of the previously conjugated ubiquitin. The 19S subunit of the 26S proteasome will specifically recognize the polyubiquitin tag on the substrate (174,175). Thereafter, the polyubiquitin tag will be removed by deubiquitinating enzymes associated with the proteasome (176). Meanwhile, the 19S subunit will employ its ATP-dependent chaperone-like activity to unfold the protein and deliver it through the narrow pore of the 20S core for proteolytic cleavage (177). Some normally short-lived proteins like ornithine decarboxylase and cyclin D1 are known to undergo ubiquitin-independent proteasome degradation (178,179). These proteins become targeted for proteasome destruction upon conjugation with the molecule antizyme which has been shown to facilitate recognition of the substrate by the 19S subunit (180,181).

Proteolytic Degradation of Endoplasmic Reticulum-associated Proteins

It has long been known that most substrates for the 26S proteasome complex are present in the nucleus and cytosol. However, evidence has been accumulating within the last decade to show that the 26S proteasome has a pivotal role in ER quality control involving the elimination of misfolded, structurally damaged, and unassembled proteins that are

generated in the ER (164-166,182-186). During the synthesis of membrane and secretory proteins in the ER, these proteins undergo various co-translational modifications, such as *N*-glycosylation and disulfide bond formation, that facilitate proper folding. The ER possesses a surveillance or quality control system that ensures that newly synthesized proteins are properly folded, *N*-glycosylated, and correctly assembled prior to exiting into the secretory pathway (186). Since the native state of a protein is considered to possess its lowest free energy (187), the surveillance system may selectively identify proteins with non-native structure based on their lower thermodynamic stabilities. Non-native proteins will be retained in the ER until they have achieved their native state. Otherwise, those proteins that are irreversibly defective will be unfolded and exported to the cytosol where they are degraded by the 26S proteasome. The pathway for the proteasomal degradation of ER-associated proteins has been termed ER-associated degradation (ERAD) (164-166,182-186).

It has been recently proposed that the topology of the ERAD substrate relative to the ER membrane and the subcellular location of its misfolded or defective lesion will determine the manner by which the protein is selected and targeted for cytosolic proteasomal degradation (188-190). ERAD glycoprotein substrates that are wholly luminal or that are membrane-bound with substantially large luminal domains will be selected for degradation in the ER lumen (189,190). The key mediators of substrate selection in the ER lumen include the ER-resident molecular chaperone Hsp70 heavy chain binding protein (BiP), the ER-resident lectin binding chaperone calnexin and its homologue calreticulin, and ER-resident oxidoreductases such as ERp57 and protein

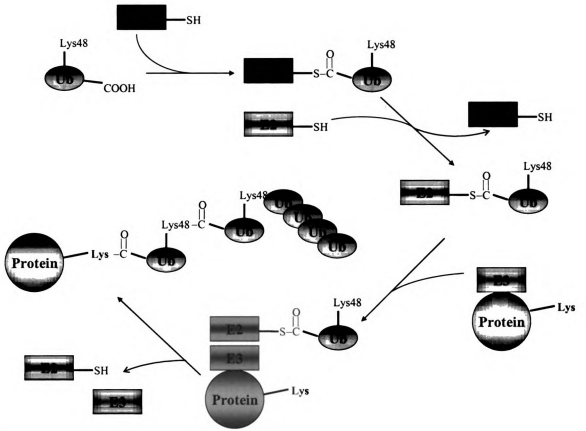

Figure 8. Mechanism for the polyubiquitination of proteins prior to their degradation by the 26S proteasome. Ubiquitin is activated for conjugation by E1 in an ATP-dependent manner. Activated ubiquitin is then transferred to the ubiquitin conjugating enyzme E2. After selecting the protein substrate, E3 ligase in conjunction with E2 will catalyze ubiquitin transfer to an exposed lysine residue on the protein. Polyubiquitination results due to the successive addition of ubiquitin molecules to one another where the carboxyl end of one ubiquitin molecule is conjugated to a specific lysine (Lys-48) of the previously conjugated ubiquitin.

disulfide isomerase (PDI) (164-166,183,186,190). Mueller *et al.* have recently demonstrated that SEL1L, a mammalian homologue of the yeast Hrd1p/Hrd3p E3 ligase complex component Hrd3p is essential of the cytomegalovirus-mediated removal of MHC class I heavy chains from the ER lumen (191). Their observations suggest that SEL1L may be a component of the ER luminal surveillance system and would therefore

have an important role in the recognition of luminal ERAD glycoprotein substrates. The putative role of SEL1L in glycoprotein ERAD is consistent with its topology and that of its yeast homologue Hrd3p; both are ER membrane proteins with relatively large luminal domains (191). ER-resident chaperones will retain improperly folded glycoproteins in the ER and assist them to fold properly. If the glycoprotein cannot be folded into its native conformation, or if its native structure has been disrupted, it becomes selected for ERAD (Fig. 9). The process is thought to begin with the recognition of exposed hydrophobic sequences on the glycoprotein by BiP and other molecular chaperones. These hydrophobic sequences are more likely to be exposed if the protein is unfolded, misfolded, or if its native structure has been compromised. By binding to these hydrophobic regions BiP prevents the aggregation of the misfolded protein in the ER (192). A specific *N*-linked glycan on the surface of the misfolded protein is processed to an oligosaccharide containing two molecules of N-acetyl glucosamine, nine mannoses, and one glucose molecule ($Glc_1Man_9GlcNAc_2$) by glucosidase I and glucosidase II. This monoglucosylated oligosaccharide is specifically recognized by the membrane-bound lectin calnexin and its soluble ER luminal homologue calreticulin. Upon binding, these lectins in conjuction with BiP and the oxidoreductase ERp57 will assist in the productive folding of the glycoprotein (193-195). If the protein becomes properly folded, cleavage of the terminal glucose of the *N*-linked oligosaccharide by glucosidase II will release the bound calnexin or calreticulin. If the protein is not properly folded, $Man_9GlcNAc_2$ will be reglucosylated by UDP-glucose glycosyltransferase (UGGT) so that the improperly folded protein is reentered into the calnexin/calreticulin cycle. UGGT is a folding sensor that will preferentially glucosylate ER proteins that have solvent-exposed hydrophobic

sequences (196,197). Repeated alterations of deglucosylation and reglucosylation will retain the glycoprotein in the calnexin/calreticulin cycle. If the glycoprotein spends significant time in this folding cycle, it will be considered to be terminally defective. In this case, the α1,2-linked terminal mannose residue of the *N*-linked oligosaccharide is irreversibly cleaved by ER α1,2 mannosidase I to form $Man_8GlcNAc_2$ (198-200). A Man_8-binding lectin such as ER-degradation mannosidase I-like protein (EDEM) or Yos9p will bind $Man_8GlcNAc_2$ and facilitate the delivery of the terminally defective glycoprotein to the export machinery on the ER membrane (201-205). At this juncture, the ERAD substrate will have been unfolded by the combined action of PDI, which breaks disulfide bonds, and other chaperones in order to be exported as an extended polypeptide chain (206-209).

The molecular mechanism for the vectorial export or retrotranslocation of the ERAD glycoprotein substrate across the ER membrane is yet to be clarified. The export process requires energy and there is some evidence to indicate that the Sec61 translocon, which is involved in ER protein import, may also be involved in protein export (206,210-213). The recent X-ray crystal structure of the archeal SecY complex (214), a homolog of the eukaryotic Sec61 translocon, shows that the protein-conducting channel can only allow the passage of a molecule with a maximum diameter of 10-12 Å (215). This pore size of the translocon is barely large enough to permit the retrotranslocation of ER polypeptides with their bulky *N*-glycan groups intact. However, there is evidence to suggest that the Sec61 protein-conducting channel may be very flexible (216). Indeed, while mediating cotranslational protein translocation the translocon pore size has been measured to be about 40-60 Å in diameter (217). Recently, a mammalian ER multi-

spanning membrane protein called Derlin-1 was identified that shows weak resemblance to the Der1p, a yeast transmembrane protein required for the degradation of yeast ERAD luminal substrates. Derlin-1 is proposed to be the putative retrotranslocation channel in mammalian cells based on several studies showing its requirement for ERAD and its ability to simultaneously associate with luminal ERAD substrates and accessory cytosolic components such as the p97(Cdc48)/Ufd1/Npl4 complex that have been shown to facilitate export or removal of the ERAD substrates from the ER (164,218-221). After the identification of Derlin-1 two additional mammalian orthologues of Der1p, Derlin-2 and Derlin-3, were later identified during a microarray screen for ER-stress inducible genes (222). Derlin-2 and Derlin-3 exhibit ~75% homology and are ~30% identical to Derlin-1 (222). In the same study overexpression of Derlins-2 or -3 facilitated the degradation of a misfolded mutant of the glycoprotein α1-antitrypsin (222).

While the mechanism of ERAD is yet to be clearly defined in mammalian cells, it has been extensively studied in yeast *S. cerevisiae*. Screening yeast genetic mutants that are defective in ERAD, has enabled the functional components involved to be easily characterized. By conducting homology database searches it was then possible to identify homologs or functional equivalents of these yeast ERAD components in mammalian cells. In both yeast and mammals the vectorial transport of the luminal ERAD substrate across the putative export channel is ATP-dependent and is believed to be facilitated by a cytosolic ATPase complex p97(Cdc48 in yeast)/Ufd1/Npl4 that specifically recognizes and binds polyubiquitin chains (164,220,223). As the substrate appears in the cytosol it is polyubiquitinated by a series of membrane-bound ubiquitin conjugating enzymes such as Ubc6p (UBC6) and Ubc7p (UBC7), and membrane-bound E3 ubiquitin ligases, that

include Doa10, Hrd1p (HRD), and gp78 (164,188,189,221,224,225). The mammalian putative export channel Derlin-1 can form membrane complexes with Hrd1p (226). p97/Ufd1/Npl4 is recruited to the membrane by interacting with Derlin-1 through an accessory protein VIMP (p97-interacting membrane protein) (219). Recently, this ATPase complex has also been shown to interact with the E3 ligases gp78 (227) and Hrd1p (228) which may also contribute to its recruitment to the membrane. Membrane-associated p97/Ufd1/Npl4 will bind the nascent polyubiquitin chain on the protein and employ its ATPase activity to pull the polypeptide out of the ER (229). As the glycoprotein substrate appears on the cytosolic side of the membrane it is deglycosylated by peptide:N-glycanase (230,231). The deglycosylated substrate is then delivered to the 26S proteasome for degradation.

ER membrane proteins with defective lesions on their cytoplasmic or membrane binding domains will be degraded by an ERAD pathway that is distinct from the one described above (188,190). Degradation of these substrates does not appear to involve recognition by the ER luminal surveillance system and is independent of their *N*-glycosylation status. Thus, the targeting of ER luminal proteins for proteasomal degradation has been designated ERAD-L to distinguish this ERAD pathway from ERAD-C and ERAD-M which degrade ER membrane proteins with defective cytosolic or transmembrane portions, respectively (188).

A few mammalian ER membrane-associated proteins are known to be regulated by ERAD under physiological conditions. These include, HMG-CoA reductase, hepatic microsomal cytochrome p450 CYP3A4, and inositol 1,4,5-triphosphate (IP_3) receptor (232-234). Even though all three membrane proteins have luminal portions, they are

likely to be degraded by an ERAD pathway other than ERAD-L since their turnover does not appear to require the ER luminal quality control system. IP_3 receptors, which form channels that control Ca^{2+} release from the ER, are degraded in response to steady state elevated intracellular levels of IP_3 (234). ERAD of IP_3 receptors has been shown to be mediated by Ubc7 and p97/Ufd1/Npl4 (234,235). HMG-CoA reductase is a tightly regulated enzyme that catalyzes the rate-limiting step in cholesterol biosynthesis involving the conversion of 3-hydroxy-3-methylglutaryl CoA to mevalonate. It is a multi-spanning ER membrane protein with a large cytosolic catalytic domain. Mevalonate or sterols induce proteasomal degradation of HMG-CoA reductase by stimulating the binding of the membrane protein Insig-1 or Insig-2 to the membrane domain of the reductase (236,237). Formation of the reductase-insig complex probably disrupts the native structure of the enzyme because it is immediately polyubiquitinated by gp78 and degraded by the proteasome (237-239). CYP3A4 undergoes substrate-induced suicide inactivation, a process that irreversibly damages the active site heme prosthetic group and makes the protein a substrate for ERAD (233).

Just like the cytochrome p450 CYP3A4, it is possible that COX-2 may undergo irreversible substrate-induced suicide inactivation *in vivo* leading to its clearance from the cell by ERAD. However, since COX-2 is an ER-resident luminal glycoprotein, its degradation would likely proceed through ERAD-L.

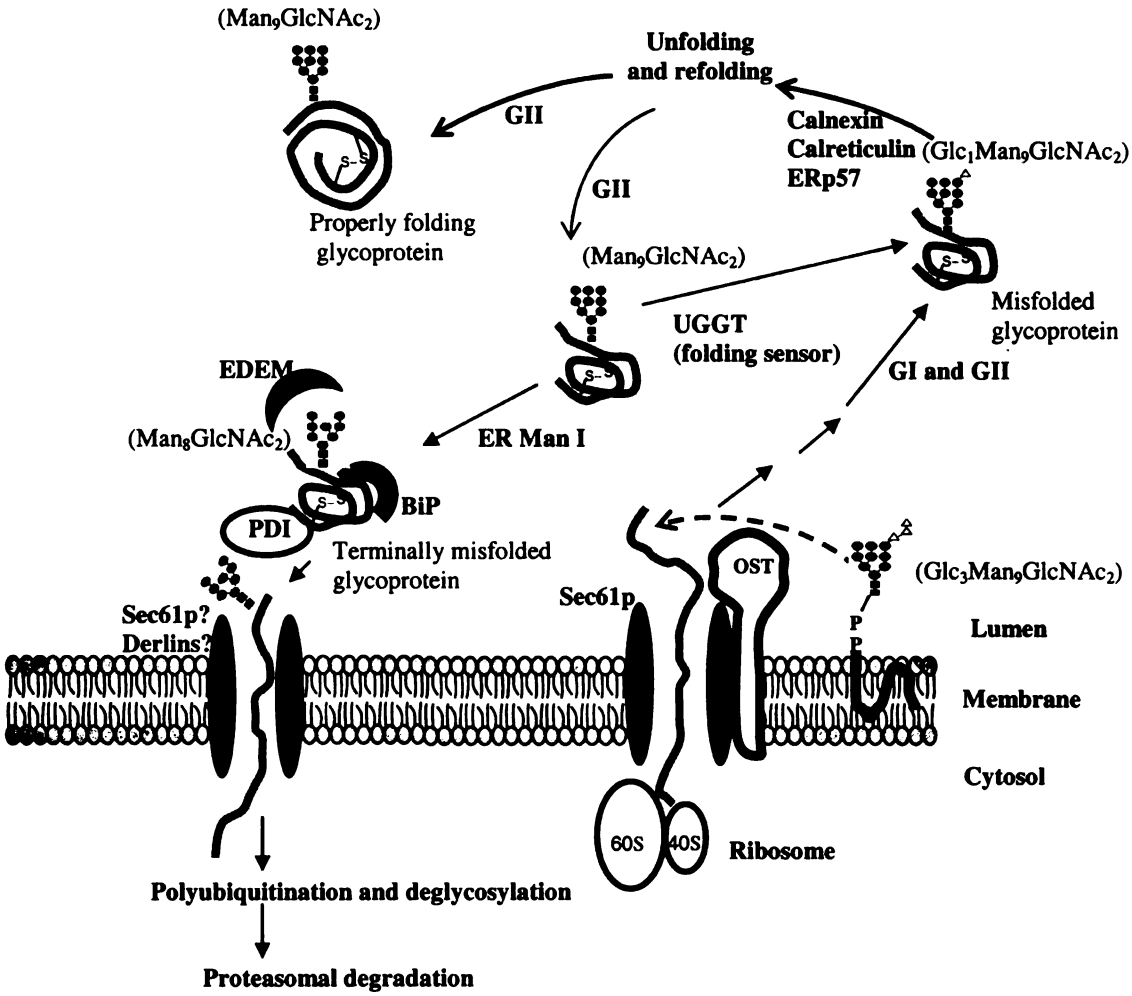

Figure 9a. Role of the calnexin/calreticulin cycle in ER quality control. *N*-glycosylation usually takes place co-translationally as the elongating polypeptide is translocated into the ER through the Sec61 translocon. Oligosaccharyltransferase (OST) transfers an intact $Glc_3Man_9GlcNAc_2$ from membrane-associated dolichyl pyrophosphate to an Asn-X-Ser/Thr site on the polypeptide (where X is any amino acid except proline). As ER-resident molecular chaperones such as BiP assist the Asn (*N*)-linked glycoprotein to properly fold, glucosidases I and II (GI and GII) cleave off the two terminal glucose residues. If the glycoprotein is not properly folded it will be brought into the calnexin/calreticulin cycle via the binding of calnexin/calreticulin to the monoglucosylated *N*-glycan group of the protein. The heterodimer complex of calnexin/calreticulin and ERp57 will unfold and refold the protein. The properly folding glycoprotein will be released from the calnexin/calreticulin cycle by GII cleavage of the remaining glucose residue. If the glycoprotein is not properly folded it will be maintained in the cycle by the UGGT which reglucosylates the $Man_9GlcNAc_2$ moiety. Misfolded glycoproteins that remain in the cycle for too long are eventually released through the action of α1,2 ER mannosidase I (ER Man I) which cleaves off the α1,2-linked mannose to form $Man_8GlcNAc_2$. This initiates ERAD of the terminally misfolded glycoprotein. The protein is unfolded with the help of BiP and PDI and exported out of the ER into the cytoplasm for proteasomal degradation.

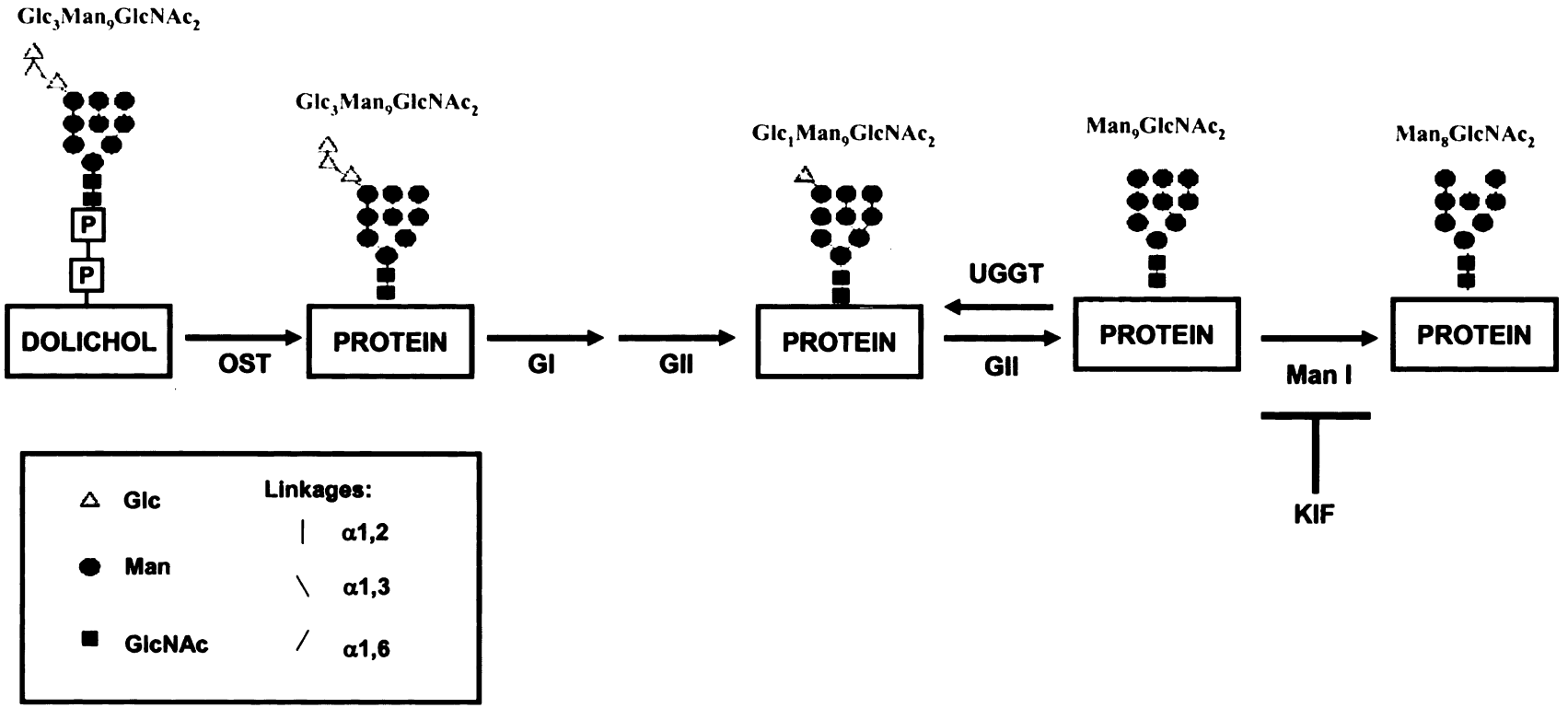

Figure 9b. Processing of *N*-linked oligosaccharides in the ER lumen during proten quality control. The oligosaccharide substrate for *N*-linked protein glycosylation is assembled onto dolichyl pyrophosphate at the membrane of the ER as $Glc_3Man_9GlcNAc_2$. After transfer of the oligosaccharide onto the protein by oligosaccharytransferase (OST), it is processed to a monoglucosylated form ($Glc_1Man_9GlcNAc_2$) by the activities of glucosidases I and II (GI and GII). This enables the glycoprotein to be entered into the calnexin/calreticulin cycle. Removal of the terminal glucose residue by GII releases the glycoprotein from the calnexin/calreticulin cycle. Re-glucosylation by UDP-glucose glucosyltransferase (UGGT) maintains the protein in the cycle. If the glycoprotein is terminally misfolded, ER mannosidase I (Man I) cleaves the terminal α1,2 linked terminal mannose residue. This step which is inhibited by kifunensine (KIF) is thought to be the committed step that initiates ERAD of the defective glycoprotein.

Table 1. Participants of glycoprotein ERAD-L in yeast and mammalian cells

	Yeast	Mammals	Role	References
Luminal				
	Kar2p	BiP	prevents aggregation of ERAD substrates	206,207
	Cne1p	Calnexin/ Calreticulin/ERp57	glycoprotein folding	193-195
	UGGT	UGGT	detects misfolded proteins and maintains them in the calnexin/calreticulin cycle	196,197
	α1,2 Man I	α1,2 Man I	initiates ERAD by irreversibly releasing terminally misfolded glycoproteins from the calnexin/calreticulin cycle	198-200
	PDI	PDI	unfolds the terminally misfolded glycoprotein in preparation for export to cytosol	209,210
	Htm1p	EDEMs (EDEM 1,2, and 3)	escorts the ERAD substrate to the export/retrotranslocation channel	203-205
	Yos9p	OS-9?	similar function as Htm1p/EDEM	201,202
Membrane				
	Hrd3p	SEL1L	role not clear; both have a large luminal domain that may be involved in selective recognition of ERAD substrates	188,191
	Sec61p	Sec61p	retrotranslocation	206, 210-213
	Der1p	Derlins (Derlin 1, 2, and 3)	retrotranslocation	218,219, 222
	Ubc6p and Ubc7p	UBC6 and UBC7	E2 ubuquitin conjugating enzymes	164,189
	Hrd1p	gp78 and HRD	E3 ubiquitin ligase	164,188, 189,224, 225
	Doa10	??	E3 ubiquitin ligase	164,188, 189
	Cue1p	??	anchors Ubc7p to the membrane	189
	??	VIMP	recruits p97 to the membrane	219
Cytosolic				
	Cdc48	p97	facilitates retrotranlocation	164,188, 218-221
	Ufd1	Ufd1	Cdc48/p97 cofactor	223
	Npl4	Npl4	Cdc48/p97 cofactor	223
	Png1	peptide:N-glycanase	deglycosylates ERAD substrates prior to their proteolytic cleavage	230,231

CHAPTER II

THE 19 AMINO ACID CASSETTE OF CYCLOOXYGENASE-2 MEDIATES ENTRY OF THE PROTEIN INTO THE ER-ASSOCIATED DEGRADATION SYSTEM

Summary

Cyclooxygenase (COX) isoforms catalyze the committed step in prostaglandin biosynthesis. The primary structures of COX-1 and COX-2 are very similar except that COX-2 has a 19-amino acid (19-aa) segment of unknown function located just inside its C-terminus. Here we provide evidence that the major role of the 19-aa cassette is to mediate entry of COX-2 into the ER-associated degradation system that transports ER proteins to the cytoplasm. COX-1 is constitutively expressed in many cells, whereas COX-2 is expressed inducibly and transiently. In murine NIH/3T3 fibroblasts COX-2 protein is degraded by a proteasome-dependent process with a half-life ($t_{1/2}$) of about 2 h whereas COX-1 is reasonably stable ($t_{1/2}$> 12 h). Similarly, COX-1 expressed heterologously in HEK293 cells is quite stable ($t_{1/2}$ >24 h) while COX-2 expressed heterologously is degraded with a $t_{1/2}$ of ~5 h and its degradation is blocked by proteasome inhibitors. A deletion mutant of COX-2 was prepared lacking 18 residues of the 19-aa cassette. This mutant retains native COX-2 enzymatic activity but, unlike native COX-2, is stable in HEK293 cells ($t_{1/2}$> 24 h). Conversely, inserting the COX-2 cassette near the C-terminus of COX-1 yields a mutant *ins*594-612 COX-1 that is unstable ($t_{1/2}$ ~3 h). Mutation of Asn-594, an *N*-glycosylation site at the beginning of the 19-aa cassette, stabilizes both COX-2 and *ins*594-612 COX-1; nonetheless, COX mutants that have the Asn-594 consensus glycosylation site but lack the remainder of the 19-aa cassette (ie.

*del*597-612 COX-2 and *ins*594-596 COX-1) are stable. Thus, although the Asn-594 glycosylation site is necessary for COX-2 degradation, at least part of the remainder of the 19-aa insert is also required. Finally, kifunensine, a mannosidase inhibitor that can block entry of ER proteins into the ER-associated degradation system, retards COX-2 degradation.

Introduction

Prostanoids are an important class of lipid mediators that are synthesized in almost all mammalian tissues. Prostanoids act in an autocrine and paracrine fashion through G protein-coupled receptors to elicit a variety of physiological and pathological responses (1). The committed step in the prostanoid synthesis pathway is catalyzed by the cyclooxygenase isozymes, COX-1 and COX-2 (1,3,7,17). Within a species, COX-1 and COX-2 exhibit ~60% amino acid sequence identity. Both isoforms are membrane-bound, ER-resident, heme-containing glycoproteins that function as homodimers (1,3,7,17,150). Structural and biochemical studies have shown that COX-1 and COX-2 are unusual integral membrane proteins that associate monotopically with the luminal face of the ER membrane and the contiguous inner membrane of the nuclear envelope (11,12,15,16,151).

Despite their close similarities in structure, catalytic function, and subcellular localization, COX-1 and COX-2 differ remarkably in their profiles of expression. COX-1 is constitutively expressed in resting cells of many tissues in the absence of COX-2 (1,20). Inducible expression of COX-2, which is usually short-lived, occurs in fibroblast, epithelial, endothelial, macrophage, and smooth muscle cells in response to growth

factors, cytokines, and proinflammatory stimuli and expression is usually transient (1,20-24). Differences in the patterns of expression of COX-1 and COX-2 genes have been quite clearly delineated in serum-stimulated NIH/3T3 fibroblasts (22,124,240). COX-1 mRNA and protein levels remain unchanged before and after serum stimulation of quiescent NIH/3T3 cells. In contrast, COX-2 mRNA and protein are barely detectable prior to stimulation, become significantly up-regulated shortly after stimulation and then rapidly decline to basal levels. It is well established that the different profiles of COX-1 and COX-2 expression as observed in serum-stimulated NIH/3T3 fibroblasts are partly attributable to differences in regulation of the isoforms at the transcriptional and post-transcriptional levels (1,20,240,241). It is still not clear the degree to which COX-1 and COX-2 may also be regulated differently at the post translational level. However, rapid degradation of COX-2 protein may serve a significant physiological role in regulating the levels of prostanoids whose syntheses occur via this isoform. Previous studies have indicated that COX-2 can be ubiquitinated and degraded by the 26S proteasome in the cytoplasm (148,149,242), suggesting that COX-2 degradation can involve exit from the ER via ER-associated degradation (ERAD) system(s) followed by proteolysis by the proteasome (165,183,206,243,244).

In the present study, we establish that COX-2 protein is preferentially and rapidly degraded in NIH/3T3 and HEK293 cells under conditions in which COX-1 is very stable. We also confirm that even though COX-2 is an ER-resident enzyme its degradation is proteasome-dependent. In investigating the molecular basis for the different rates of COX-1 and COX-2 degradation, we found that the 19-amino acid segment unique to COX-2 (Asn594-Lys612) and located six residues in from the carboxyl terminal end

targets the protein for rapid degradation through the ER-associated degradation (ERAD) pathway (s) (164-166).

Experimental Procedures

Materials. Dulbecco's modified Eagle medium (DMEM), fetal bovine serum (FBS), ponasterone A, tetracycline, and goat serum were from Invitrogen/Gibco. Bovine calf serum was from Hyclone. Cycloheximide, puromycin, and bacterial lipopolysaccharide (LPS) were obtained from Sigma-Aldrich. Kifunensine, MG132, epoxomicin, E64, and leupeptin were purchased from Calbiochem. Endoglycosidase H (Endo H) was purchased from Roche. Unlabeled arachidonic acid was purchased from Cayman Chemicals, while radioactive ^{14}C-arachidonic acid and ^{14}C-eicosapentaenoic acid were from American Radiolabeled Chemicals.

Construction of Plasmids for Transfection. Recombinant ovine (ov) COX-1 cDNA and human (hu) COX-2 cDNA were subcloned into pIND (Invitrogen) and pcDNA5/FRT/TO (Invitrogen), respectively. pIND is ecdysone-inducible while pcDNA5/FRT/TO is tetracycline- inducible. After subcloning, the Quick-Change™ site-directed mutagenesis kit (Stratagene) was used to create the following C-terminal mutants: N594A huCOX-2, *del*595-612 huCOX-2, *del*597-612 huCOX-2, and *ins*594-596 ovCOX-1. The COX-1 insertion mutants, *ins*594-612 ovCOX-1, *ins*594-612(N594A) ovCOX-1, and *ins*594-612 ovCOX-1 were created from the cDNA template for native ovCOX-1 by overlap extension PCR then subcloned into pIND using *Hind*III restriction sites. Correct cDNA orientation and mutations were confirmed by sequencing. The primers and the PCR conditions used to design the above mutants are shown in the 'Appendix' section.

Cell Culture and Transfection. NIH/3T3 fibroblasts at early passage (<6 passages) were cultured in DMEM supplemented with 10% bovine calf serum and 100 u/ml penicillin/streptomycin. To induce COX-2 expression, the cells were first made quiescent by serum starvation for 48 h in DMEM containing 0.2% bovine calf serum and thereafter treated with DMEM supplemented with 20% FBS for 4 h.

RAW 264.7 macrophage-like cells were cultured in DMEM supplemented with 10% FBS and 100 u/ml penicillin/streptomycin. To stimulate COX-2 expression, the cells were challenged with 200 ng/ml LPS.

HEK293-derived cell lines stably expressing native or mutant COX constructs were generated using either the tetracycline-inducible and ecdysone-inducible mammalian expression systems (Invitrogen) according to the manufacturer's protocol. Constructs that were expressed under the control of a tetracycline-inducible promoter were native huCOX-2, *del*595-612 huCOX-2, N594A huCOX-2, and *del*597-612 huCOX-2; those expressed under the control of the ecdysone-inducible promoter were native ovCOX-1, *ins*594-612 ovCOX-1, *ins*594-612(N594A) ovCOX-1, and *ins*594-596 ovCOX-1. Stably transfected HEK293 cells were cultured in DMEM supplemented with 10% FBS, 100 u/ml penicillin/streptomycin, and the appropriate pharmacological selective reagents. Inducible expression was achieved by a 24 h serum starvation in serum-free medium followed by treatment with 10 μg/ml tetracycline or 10 μM ponasterone A (ecdysone analog) for the appropriate times in normal culture medium.

Protein Degradation and Drug Treatments. A cycloheximide (CHX) decay experiment was performed to measure the protein stabilities of COX-1 and COX-2 in serum-treated NIH/3T3 cells. Briefly, quiescent cells were serum-stimulated for 4 h then

incubated for different times with 50 μM CHX in DMEM supplemented with 10% FBS. The protein degradation experiment was performed in the absence or presence of MG132 (20 μM and 50 μM), epoxomicin (3 μM and 5 μM), 25 μM leupeptin, and 25 μM E64.

HEK293 cells inducibly expressing wild-type or mutant cyclooxygenase constructs were grown to 80% confluency, serum-starved for 24 h, and then treated with 10 μg/ml tetracycline or 10 μM ponasterone A in complete culture medium to induce expression. Afterwards, the cells were incubated for various times with 50 μM puromycin to block translation in the absence or presence of 20 μM MG132, 25 μM KIF, or 50 μM KIF.

Enyzmatic Deglycosylation. For complete deglycosylation, HEK293 whole cell lysates were denatured by boiling in NuPAGE SDS sample loading buffer (Invitrogen) and then treated for at least 12 h with endoglycosidase H (Endo H) at a concentration of 0.4 mU/μl.

Western Transfer Blotting. After the appropriate treatments, NIH/3T3, RAW 264.7, and HEK293 cells were scraped into ice-cold PBS (phosphate-buffered saline), pH 7.4 containing 5 mM EDTA and a cocktail of protease inhibitors (Roche) and lysed by sonication. RIPA lysis buffer (10 mM Tris, pH 7.2, 150 mM NaCl, 5mM EDTA, 0.1% SDS, 1.0% Triton X-100, 1% deoxycholate) containing a protease inhibitor cocktail (Roche Applied Science) was also used for cell lysis. Protein concentrations were determined using the BCA protein assay kit (Pierce). The NuPAGE system (Invitrogen) was used to resolve the proteins in the whole cell lysates on a 7% tris-acetate polyacrylamide gel. After transfer to a nitrocellulose membrane, immunoblotting was performed with the appropriate primary antibody. Horseradish peroxidase-conjugated

anti-rabbit or anti-mouse IgG antibodies (Bio-Rad) were used as secondary antibodies. Immunodetection was performed using the Western Lighting Chemiluminescent kit (Amersham Biosciences) followed by exposure to X-ray film. Densitometry analysis was performed using ImageQuant TL software (Amersham Biosciences).

Antibodies Specific for COX-1 or COX-2. A previously generated (13), peptide-specific, polyclonal primary antibody for murine (mu) COX-2 against the epitope Ser598-Lys612 was used in the current study to detect muCOX-2 by immunoblotting. A polyclonal antibody raised against whole recombinant ovCOX-1 was used to detect muCOX-1. Peptide-specific, polyclonal primary antibodies for ovCOX-1 and huCOX-2 were synthesized by Covance Research Products against the following epitopes: Leu272-Gln283 of ovCOX-1 and Pro583-Asn594 of huCOX-2.

Immunocytofluorescence. Stably transfected HEK293 cells were grown on poly L-lysine-coated cover slips and induced with either 10 μg/ml tetracycline or 10 μM ponasterone A for the appropriate times. After fixation in 3.7% formaldehyde and permeabilization with 0.2% Triton X-100, the cover slips were blocked in 0.1% Triton-X-100 solution supplemented with 10% goat serum. Thereafter, the cover slips were incubated with the appropriate primary antibody against either ovCOX-1 or huCOX-2, extensively washed with PBS, and incubated with Alexa Fluor 488 fluorophore-conjugated secondary antibody (Invitrogen). After three additional extensive washes with PBS the cover slips were dried and mounted onto glass slides using Prolong antifade kit (Invitrogen). Microscopy was conducted on a Zeiss Atto Arc® 2 HBO 100W fluorescence microscope at a magnification of 200X.

Results

Rapid, Proteasome-dependent Degradation of COX-2. COX-1 is expressed constitutively in murine NIH/3T3 fibroblasts, whereas COX-2 is expressed inducibly and transiently(22,124,240). This raises the possibility that the protein stabilities of the COX isoforms are different with COX-2 being more susceptible to degradation. A cycloheximide (CHX) decay experiment in NIH/3T3 cells was performed to compare the stabilities of COX-1 and COX-2 (Figs. 10*a* and *b*). COX-2 was degraded with a short half-life ($t_{1/2}$) of ~2 h while COX-1 was more stable and did not appear to undergo degradation during the experiment ($t_{1/2}$ >12 h).

Although COX-2 expression is typically transient, a few tissues and cell types are reported to express COX-2 in a prolonged and/or constitutive manner (125,127,242,245,246). It is possible that COX-2 protein is stable under these conditions. To address this, we examined COX-2 protein degradation in LPS-stimulated murine RAW264.7 macrophage cells where COX-2 protein expression continues to increase up to 24 h after LPS treatment. COX-2 was also degraded rapidly ($t_{1/2}$~2 h) in LPS-challenged RAW 264.7 cells (data not shown) indicating that increased COX-2 stability is not responsible for prolonged expression of the enzyme at least in this cell type.

We performed experiments with several classes of protease inhibitors to determine the pathway responsible for the selective degradation of COX-2 in NIH/3T3 cells. The selective 26S proteasome inhibitors, epoxomicin and MG132 (Figs. 10*c* and *d*), significantly slowed COX-2 protein degradation at 4 and 8 h after CHX treatment

10A.

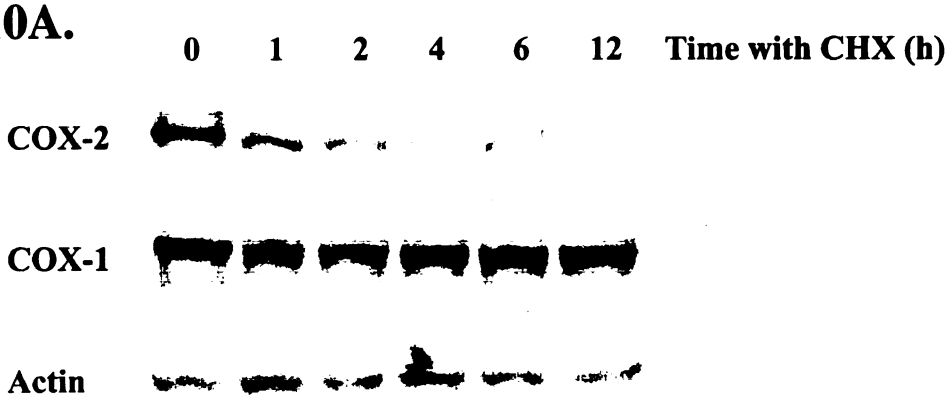
0 1 2 4 6 12 Time with CHX (h)
COX-2
COX-1
Actin

B.

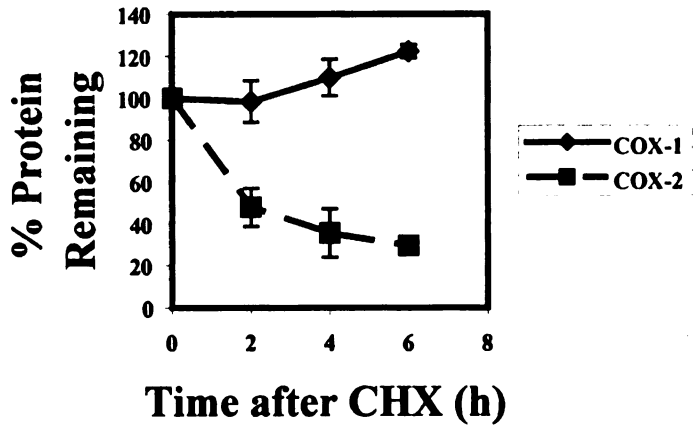
% Protein Remaining
140
120
100
80
60
40
20
0
0 2 4 6 8
Time after CHX (h)
COX-1
COX-2

C.

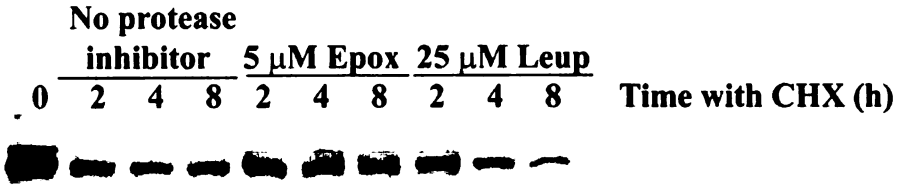
No protease inhibitor
5 μM Epox
25 μM Leup
0 2 4 8 2 4 8 2 4 8
Time with CHX (h)

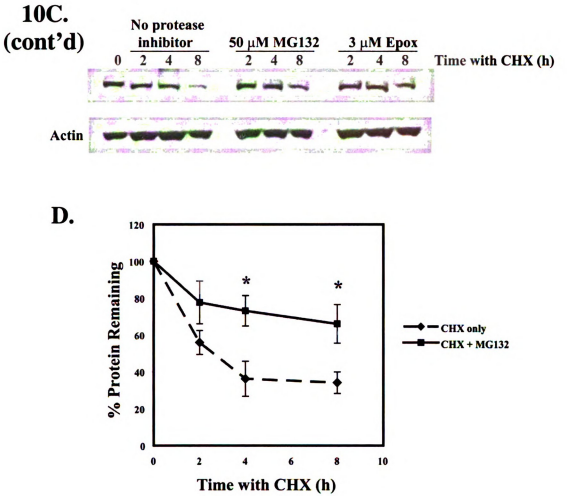

Figure 10. Cyclooxygenase protein degradation in serum-treated NIH/3T3 cells. *A*, Quiescent 3T3 cells were stimulated with 20% FBS for 4 h to induce COX-2 expression. Cycloheximide (CHX; 50 μM final concentration) was added to the medium and the cells were incubated for the indicated times. Cell lysates were then prepared and analyzed by Western blotting for COX-1, COX-2 and actin as described in the Methods section. *B*, Densitometry was performed to quantify the levels of COX-1 and COX-2 which were normalized to those of actin. Error bars denote +/- SE of the mean for three independent experiments. *C*, COX-2 expression was induced in murine NIH/3T3 cells and 50 μM CHX added to the medium as described in *A*. The cells were then treated for the indicated times with or without 3 μM or 5 μM epoxomicin (Epox), 25 μM leupeptin (Leup) or 50 μM MG132. COX-2 protein levels were examined by Western blotting and densitometry. *D*, Quantitative analysis of the effect of 20 μM MG132 on COX-2 protein stability in 3T3 cells. Densitometry values for each time point were from six independent experiments performed as described above and represent the mean +/- SE. Asterisks denote that a p value < 0.05 based on a Student's paired *t*-Test.

while two different cysteine protease inhibitors of lysosomal degradation, leupeptin (Fig. 10*c*) and E64 (data not shown), did not. At the 2-h time point in six independent experiments with 20 μM MG132, there was a trend but not a statistically significant inhibition (Fig. 10*d*). Accordingly, it is not clear whether a protease other than the 26S proteasome can also be involved in COX-2 degradation.

It should be noted that both 26S proteasome inhibitors prevented the degradation of the two alternatively glycosylated (ie. 72 and 74 kDa) forms of COX-2 (Figs. 10*c* and *d*). Overall, our findings and those of others (148,149,242) indicate that COX-2 can be degraded in the cytosol by the 26S proteasome. Because COX-2 is located on the luminal surface of the ER (13,15,16), our results imply that its degradation must involve transport across the ER membrane to the cytosol.

The Unique C-terminal 19-amino Acid Segment is Involved in COX-2 Degradation. Despite the high degree of structural similarity between the COX isoforms, COX-2 is distinct from COX-1 in possessing a unique 19-amino acid (19-aa) cassette that is located six residues in from the carboxyl-terminal end (Fig. 11*a*). The N-terminal most residue of the 19-aa insert is Asn-594, which is one of four functional *N*-glycosylation sites of COX-2. COX-1 has the other three *N*-glycosylation sites in common with COX-2 We used site-directed mutagenesis to test the hypothesis that the unique C-terminal 19-aa of COX-2 affects its degradation. HEK293 cells, which do not have detectable levels of COX-1 or COX-2, were used to stably and inducibly express native or C-terminal mutant versions of the cyclooxygenase enzymes (Fig. 11*b*). Native human (hu) COX-2 inducibly expressed in HEK293 cells was degraded with a $t_{1/2}$ of ~5 h while native ovine (ov)

11A.

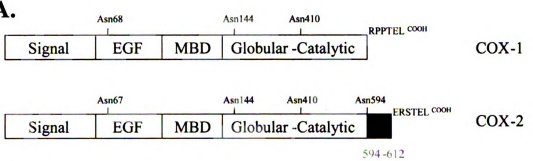

B.

^{580}FSVPDPELIKTVTI**NASSSRSGLDDINPTVLLK**ERSTEL^{618}	native huCOX-2
^{580}FSVPDPELIKTVTIN----------ERSTEL^{600}	*del*595-612 huCOX-2
^{580}FSVPDPELIKTVTI**AASSSRSGLDDINPTVLLK**ERSTEL^{618}	N594A huCOX-2
^{580}FSVPDPELIKTVTI**NAS**----------ERSTEL^{602}	*del*597-612 huCOX-2
^{580}FHVPDPRQEDRPGVE----------RPPTEL^{600}	native ovCOX-1
^{580}FHVPDPRQEDRPGV**NASSSRSGLDDINPTVLLK**ERPPTEL^{619}	*ins*594-612 ovCOX-1
^{580}FHVPDPRQEDRPGV**AASSSRSGLDDINPTVLLK**ERPPTEL^{619}	*ins*594-612(N594A) ovCOX-1
^{580}FHVPDPRQEDRPGV**NAS**----------RPPTEL^{603}	*ins*594-596 ovCOX-1

C.

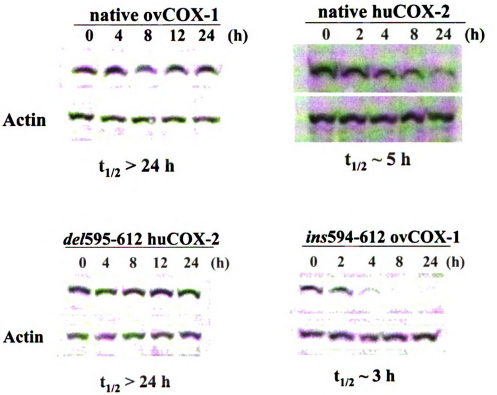

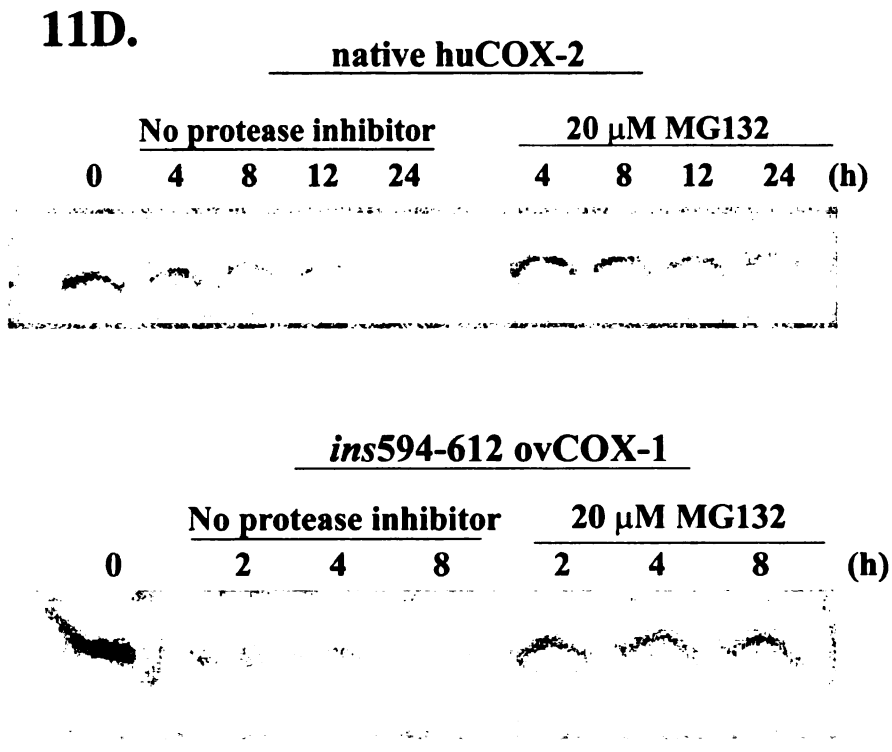

Fig. 11. Stability of heterologously expressed native and C-terminal cyclooxygenase mutants in HEK293 cells. *A*, Alignment of major folding domains of COX-1 and COX-2 showing consensus N-glycosylation sites and the relative position of the unique 19-amino acid (19-aa) insert located near the C-terminus of COX-2. Numbering for COX-1 begins with the Met at the translation start site. Numbering for COX-2 parallels the COX-1 numbering in which the start of the mature, processed COX-2 protein has the same number as the start of the mature, processed COX-1(12). *B*, Amino acid sequences of the C-termini of cyclooxygenase constructs that were stably transfected into HEK293 cells. The underlined sequence is the consensus N-glycosylation site at the start of the unique COX-2 19-aa cassette. Proteins that were expressed under the control of a tetracycline-inducible promoter were native huCOX-2, *del*595-612 huCOX-2, N594A huCOX-2, and *del*597-612 huCOX-2; those expressed under the control of the ecdysone-inducible promoter were native ovCOX-1, *ins*594-612 ovCOX-1, *ins*594-612(N594A) ovCOX-1, and *ins*594-596 ovCOX-1. *C*, HEK293 cell lines stably and inducibly expressing the constructs shown in *B* were grown to ~80% confluency, subjected to serum starvation for 24 h, and then treated with the appropriate inducing agent (10 μg/ml tetracycline or 10 μM ponasterone A) for 24 h (native huCOX-2, *del*595-612 huCOX-2, and *ins*594-612 ovCOX-1) or 12 h (native ovCOX-1). Puromycin (50 μM) was then added to block translation and protein levels were analyzed at different times by Western blotting. Densitometry was performed as described in the legend to Fig. 1. The Western blotting results are representative of at least three separate experiments from which protein half-life measurements were made. *D*, Following serum-starvation and COX protein induction of HEK293 cells expressing huCOX-2 and *ins*594-612 ovCOX-1 as described in *C*, 50 μM puromycin was added to inhibit translation in the presence or absence of 20 μM MG132. At the indicated times, cells were lysed and subjected to Western blotting. The results shown for each protein are representative of two independent experiments.

COX-1 was not degraded at a detectable rate ($t_{1/2}$ >24 h) (Fig. 11*c*). A deletion mutant *del*595-612 huCOX-2 was prepared that lacks 18 amino acids of the 19-aa; additionally, Asn-594 cannot be glycosylated in this mutant as the consensus *N*-glycosylation is no longer present. This deletion mutant was stable with a $t_{1/2}$ comparable to that of native ovCOX-1 (>24 h) (Fig. 11*c*). Inserting 19-aa of huCOX-2 near the C-terminus of ovCOX-1 yielded a mutant *ins*594-612 ovCOX-1 that had a relatively short $t_{1/2}$ of ~3 h (Fig. 11*c*). Degradation of both native COX-2 and *ins*594-612 ovCOX-1 was retarded by treatment with the proteasome inhibitor MG132 (Fig. 11*d*). These observations suggest that the 19-aa segment of COX-2 is involved in the rapid degradation of this COX isoform, perhaps by targeting it for proteolysis by the 26S proteasome.

The native and mutant proteins used in the studies depicted in Fig. 11 and in subsequent figures are inducibly expressed in HEK293 cells with different time courses. To the extent possible, we performed protein degradation experiments with HEK293 cells expressing comparable amounts of COX protein to achieve a more direct comparison of half-lives.

The subcellular distribution of the native and mutant proteins heterologously expressed in HEK293 cells was determined by immunofluorescent staining. Both mutant enzymes exhibited a perinuclear and diffuse pattern characteristic of COX-1 and COX-2 (Fig. 12) (13,14,19); we also determined by Western blotting that *del*595-612 huCOX-2 and *ins*594-612 ovCOX-1 are present in a high speed, microsomal membrane fraction prepared from HEK293 cells (data not shown). Dr. Masayuki Wada measured and compared the K_m and V_{max} values of native murine (mu) COX-2 and *del*595-612 muCOX-2 for oxygenation of arachidonic acid (Fig 13*a*). He also analyzed the products

formed from [1-^{14}C] arachidonic acid and [1-^{14}C] eicosapentanoic acid by both enzymes (Fig. 13*b*). The kinetic constants and product distributions were the same for the native and mutant enzymes. The specific cyclooxygenase activity of purified *ins*594-612 ovCOX-1 was also comparable to that of the purified native ovCOX-1 (38.2 and 40 μmol/min/mg, respectively; Dr. Rana Sidhu, unpublished results).

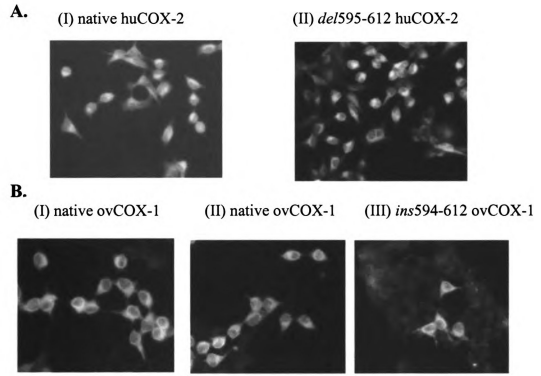

Fig. 12. Subcellular localization of native huCOX-2, *del*595-612 huCOX-2, native ovCOX-1 and *ins*594-612 ovCOX-1 in HEK293 cells. HEK293 cells stably expressing the various COX variants were grown on poly L-lysine-coated cover slips and induced with either 10 μg/ml tetracycline or 10 μM ponasterone A as described in the legend to Fig. 11. The cells were then fixed with formaldehyde, permeabilized with Triton X-100 and incubated with an appropriate primary antibody. *A*, For huCOX-2 *(I)* and *del*595-612 huCOX-2 *(II)* a rabbit anti-peptide antibody to residues 583-594 of huCOX-2 was used. *B*, For native ovCOX-1 *(I* and *II)* and *ins*594-612 ovCOX-1 *(III)* a rabbit anti-peptide antibody to residues 272-283 of ovCOX-1 was used for *(I)* while an antibody against whole ovCOX-1 was used for *(II)* and *(III)*. After washing with 1X PBS the cells were incubated with fluorophore-conjugated anti-rabbit IgG secondary antibody, washed with 1X PBS, mounted using an anti-fade reagent, and examined by fluorescence microscopy at a magnification of 200X.

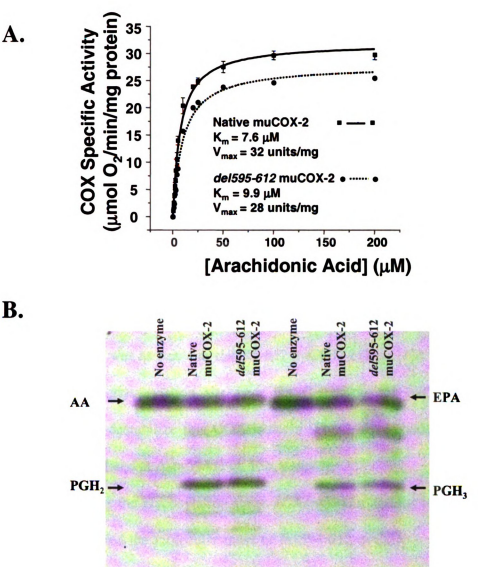

Figure 13. Kinetic properties of purified native muCOX-2 and *del*595-612 muCOX-2. *A*, Hexahistidine-tagged versions of muCOX-2 and *del*595-612 muCOX-2 were expressed in Sf21 insect cells and purified. Oxygen electrode assays were performed to compare the specific cyclooxygenase activities of the wild type and mutant enzyme. *B*, Similar amounts of purified hexahistidine-tagged muCOX-2 or *del*595-612 muCOX-2 (~23 mU) were incubated with 20 μM [1-^{14}C]arachidonic acid (AA) or [1-^{14}C]eicosapentaenoic acid (EPA) for 30 sec. The products were extracted, separated by thin-layer chromatography, and visualized by autoradiography. The radioactive band between EPA and PGH_3 has chromatographic properties of the PGH_3 degradation product 17-hydroxy-5,12,15-heptadecatrienoic acid. The experiments in *A* and *B* were carried out by Dr. Masayuki Wada.

Collectively, these results suggest that effects on substrate turnover or subcellular localization do not account for the large difference in the rates of degradation between the native and mutant enzymes.

Asn-594 Glycosylation Site is Necessary but not Sufficient to Effect COX-2 Degradation. A point mutation of the Asn-594 *N*-glycosylation site at the beginning of the 19-aa segment was sufficient to extend the $t_{1/2}$ of the mutated COX-2 (N594A huCOX-2) to >24 h (Fig. 14*a*). Consistent with this, *ins*594-612 ovCOX-1 was also stabilized by mutating the Asn-594 glycosylation site (Fig. 14*a*). However, a deletion mutant *del*597-612 huCOX-2 carrying the Asn-594 glycosylation site but lacking the rest of the 19-AA insert was as stable as *del*595-612 huCOX-2 (Fig. 14*b*). Similarly, insertion of a consensus *N*-glycosylation site near the C-terminus of ovCOX-1 (*ins*594-596 ovCOX-1) did not destabilize this COX isoform (Fig. 14*b*), although this mutant is at least partly glycosylated at Asn-594 (Fig. 15*a*, panel *I*).

In evaluating the glycosylation status of Asn-594 in various forms of COX-1 and COX-2, we compared the molecular mass of *ins*594-612 ovCOX-1 with that of *ins*594-612(N594A) ovCOX-1 and the mass of native huCOX-2 to N594A huCOX-2. The approximate mass of an *N*-linked oligosaccharide moiety is 2 kDa (151). Both native huCOX-2 and *ins*594-612 ovCOX-1 would be expected to have a total of four *N*-glycosylation sites (151,247). As anticipated, the electrophoretic mobility of *ins*594-612 ovCOX-1 was less than that of *ins*594-612(N594A) ovCOX-1 by a difference corresponding to about 2 kDa (Fig. 15*a*, panel *I*); moreover, deglycosylation of *ins*594-612 ovCOX-1 and *ins*594-612(N594A) ovCOX-1 by Endo H increased the mobilities of

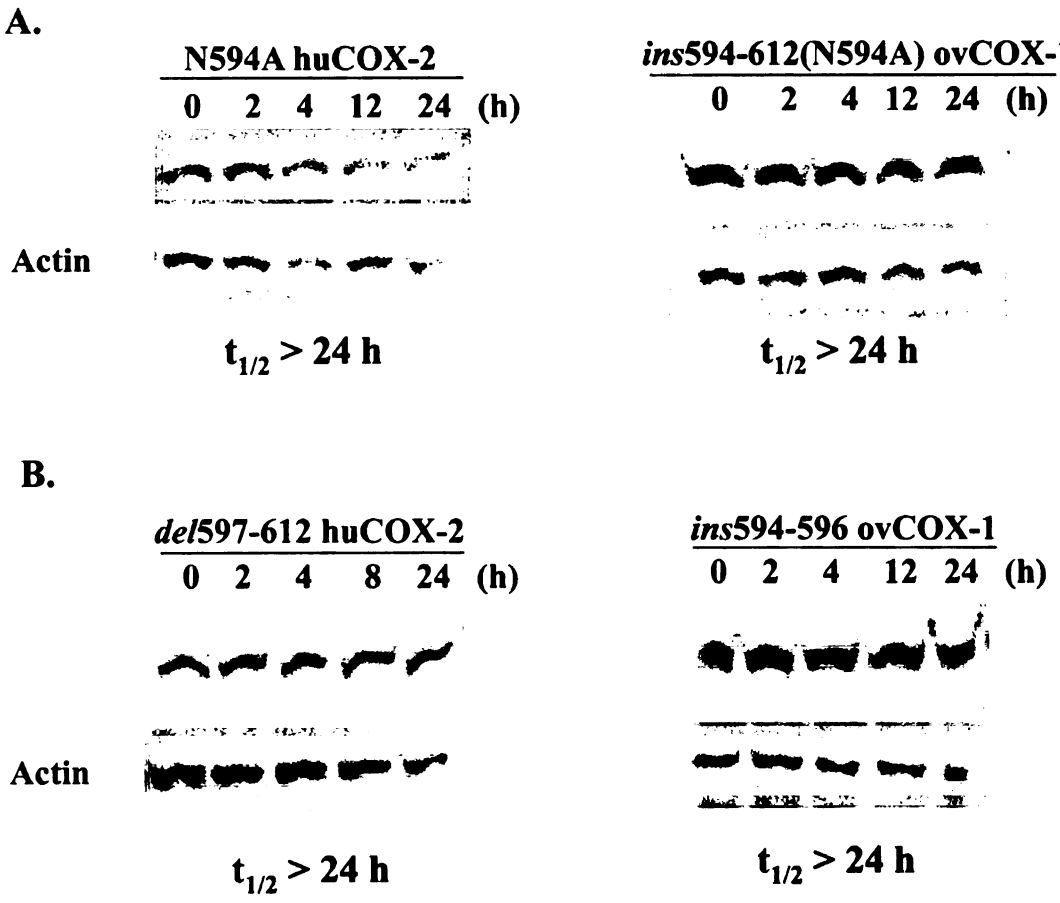

Figure 14. Stability of cyclooxygenase mutants in HEK293 cells having various modifications of the 19 amino acid cassette. *A* and *B*, Amino acid sequences of the C-termini of cyclooxygenase constructs that were stably transfected in HEK293 cells are shown in Fig. 11*B*. Proteins that were expressed under the control of the tetracycline-inducible promoter are N594A huCOX-2 and *del*597-612 huCOX-2; those expressed under the control of the ecdysone-inducible promoter were *ins*594-612(N594A) ovCOX-1 and *ins*594-596 ovCOX-1. Expression was induced for 12 h (N594A huCOX-2 and *del*597-612 huCOX-2) or 24 h (*ins*594-612(N594A) ovCOX-1 and *ins*594-596 ovCOX-1). Thereafter, the time course of degradation of the proteins was determined as described in the legend to Fig. 11. The results shown in *A* are representative of at least three independent experiments from which protein half-life measurements were made. The results shown in *B* are representative of two independent experiments.

both mutants such that they had apparently identical molecular masses (Fig. 15*a*, panel *II*). These results suggest that the difference in molecular mass between the two COX-1 insertion mutants results from glycosylation of Asn-594.

In contrast to the results obtained with the COX-1 mutants, we found no difference between the electrophoretic mobilities of native huCOX-2 and N594A huCOX-2 expressed in HEK293 cells (Fig. 15*b*, panel *I*). This is somewhat similar to what is seen with murine COX-2 expressed in *cos*-1 cells (151) where the major bands for native muCOX-2 and N594Q muCOX-2 have the same electrophoretic mobilities; however in the case of muCOX-2 expressed in *cos*-1 cells, a more slowly moving band was also observed. A second, less mobile band was observed with huCOX-2, but not N594A huCOX-2, when HEK293 cells were treated with KIF, an α1,2 ER mannosidase I inhibitor (Fig. 15*b*, panel II). Moreover, Endo H treatment led to deglycosylated forms of native COX-2 and N594A COX-2 that had the same molecular mass (Fig. 15*b*, panel *II*). In addition to causing the appearance of a second, alternatively glycosylated form of huCOX-2, KIF treatment of HEK293 cells expressing native huCOX-2 inhibits COX-2 degradation (Fig. 15*b*, panel *II*). Degradation of *ins*594-612 ovCOX-1 is also inhibited by KIF (Fig. 15*c*). This is a diagnostic feature of *N*-glycosylated proteins whose degradation involves transport to the cytoplasm by the ERAD system (199,200,248-251). These results are consistent with those obtained with 26S proteasome inhibitors in indicating that COX-2 degradation involves entry into the ERAD system prior to degradation by the 26S proteasome.

15A. (I)

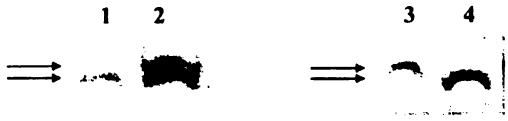

1. native ovCOX-1
2. *ins*594-596 ovCOX-1
3. *ins*594-612 ovCOX-1
4. *ins*594-612 (N594A) ovCOX-1

(II)

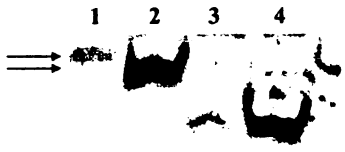

1. *ins*594-612 ovCOX-1
2. *ins*594-612(N594A) ovCOX-1
3. Endo H cleavage of 1
4. Endo H cleavage of 2

B. (I)

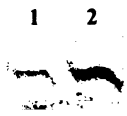

1. native huCOX-2
2. N594A huCOX-2

(II)

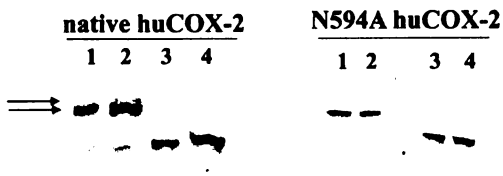

1. tet-induced
2. tet-induced + 12 h KIF
3. Endo H cleavage of 1
4. Endo H cleavage of 2

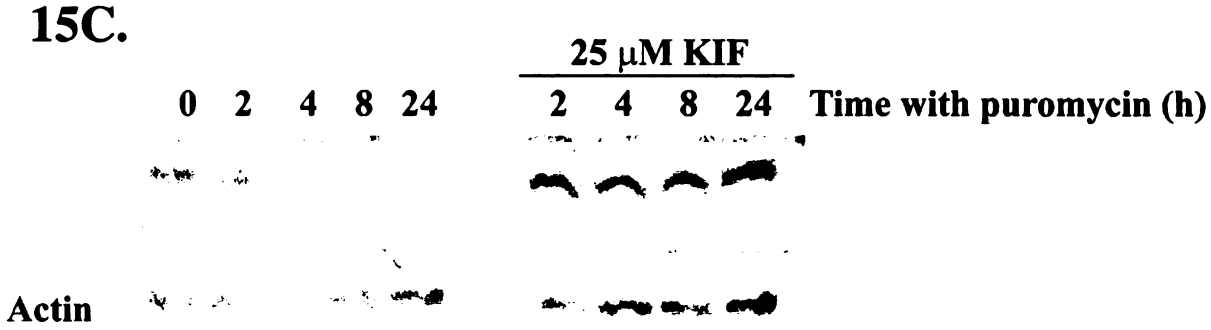

Figure 15. Glycosylation of *ins*594-612 ovCOX-1 and native huCOX-2 at Asn-594. *A (I)* Native ovCOX-1 (1), *ins*594-596 ovCOX-1 (2), *ins*594-612 ovCOX-1 (3), or *ins*594-612(N594A) ovCOX-1 (4) expression was induced with 10 μM ponasterone A in HEK293 cells for 24 h. *(II)* After protein induction of *ins*594-612 ovCOX-1 and *ins*594-612(N594A) ovCOX-1 cell lysates were prepared and boiled in SDS sample loading buffer for 10 min and then treated with or without Endo H (0.4 mU/μl) for at least 12 h. Proteins were resolved by SDS-PAGE on a 7% tris-acetate polyacrylamide gel and subjected to Western blotting. *B (I)*, native huCOX-2 (1) or N594A huCOX-2 (2) expression was induced with 10 μg/ml tetracycline in HEK293 cells for 24 h and 3 h, respectively. *(II)*, after protein induction as in *(I)* cells were rinsed in PBS and incubated for an additional 12 h in normal culture medium with or without 50 μM KIF. Thereafter, cell lysates were prepared and boiled in SDS sample loading buffer for 10 min and then treated with or without Endo H (0.4 mU/μl) for at least 12 h. Proteins were resolved and subjected to Western blotting as in *A*. Arrows indicate differences in molecular mass due to N-glycosylation. *C. ins*594-612 ovCOX-1 was induced in HEK293 cells as described in the legend to Fig. 2. The cells were then incubated with puromycin (50 μM) in the presence or absence of KIF (25 μM) for the indicated times. Cell lysates were prepared and subjected to SDS-PAGE and Western blotting as described in the legend to Fig. 11. The results shown are representative of two independent experiments.

Discussion

Substitution of the COX-1 coding region for COX-2 in transgenic mice partially rescues the typical phenotype of COX-2 null mice (252). Thus, a key difference between COX-1 and COX-2 is in their patterns of expression and not simply in their enzymatic properties. The difference in the profiles of COX-1 and COX-2 protein expression are at least partly attributable to differences in the regulation of transcription of the two genes (reviewed in (1,20,241)). In general, COX-1 gene expression is constitutive, and COX-2 expression is inducible. In addition, COX-2 mRNA with its repetitive AUUUA degradation sequences is subject to post-transcriptional control (145,253,254). In this report, we confirm and extend previous findings indicating that COX-1 is a stable protein, whereas COX-2 is degraded relatively rapidly, and that COX-2 can be ubiquitinated and degraded by the 26S proteasome (148,149,242). COX-2 is localized to the luminal surface of the ER (13-16), and so to be degraded, it must first be transported to the cytosol from the ER.

In the studies reported here, we have focused on the molecular basis for the relatively rapid rate of COX-2 degradation when compared with that of COX-1. Specifically, we evaluated the 19-aa cassette (Asn-594–Lys-612) that is unique to COX-2 for its potential role in degradation. This 19-aa insert is located 6 residues in from the COX-2 C terminus. It has only one recognizable consensus sequence, an *N*-glycosylation sequence involving Asn-594–Ser-596. We have demonstrated that the 19-aa cassette of COX-2, with an intact Asn-594 *N*-glycosylation site, targets COX-2 for proteasomal degradation. This is based on the following observations. *a*) A deletion mutant of huCOX-2 lacking 18 amino acids of the 19-aa insert (*del*595–612 huCOX-2) and a

functional *N*-glycosylation site at Asn-594 has native COX activity and the same subcellular location as native enzyme but is refractory to protein degradation. *b*) Point mutation of the Asn-594 *N*-glycosylation site (N594A huCOX-2) also stabilizes COX-2. *c*) Inserting the COX-2 19-aa cassette at the C terminus of ovCOX-1 (*ins*594–612 ovCOX-1) destabilizes ovCOX-1. *d*) Point mutation of Asn-594 in *ins*594–612 ovCOX-1 stabilizes this insertion mutant. *e*) The degradation of both native huCOX-2 and *ins*594–612 ovCOX-1 can be retarded by MG132, a 26S proteasome inhibitor. Although the Asn-594 *N*-glycosylation site is required for degradation, we found evidence that all or part of the remainder of the 19-aa insert is also necessary.

Our results suggest that glycosylation of Asn-594 of COX-2 is critical for initiating entry of the enzyme into the ERAD system for transport to the cytoplasm. The ERAD system is thought to involve unfolding of *N*-glycosylated proteins in the ER lumen and ATP-dependent retrograde transport across the ER membrane, and frequently, this is followed by ubiquitination of the transported protein by ubiquitin-protein isopeptide (E3) ligases associated with the cytosolic face of the ER membrane and subsequent degradation by the 26 S proteasome (165,183,206,243,244). The ERAD system is usually regarded as a quality control pathway for the clearance of misfolded, unassembled, or toxic proteins from the ER lumen (165,206,243,244,255). It has also been implicated in the degradation of native ER-associated proteins such as hydroxymethylglutaryl-CoA reductase, hepatic microsomal cytochrome P450 CYP3A4, and inositol 1,4,5-triphosphate receptor (232-234), all of which are ER transmembrane proteins. An ER luminal glycoprotein is selected for the ERAD pathway by a complex process that involves enzymatic processing of specific *N*-linked oligosaccharide groups on the surface of

glycoproteins (166,204,255,256). This requires the action of α1,2 ER mannosidase I whose inhibition by KIF leads to retention and stabilization of glycoproteins in the ER (199,200,248-251). In the current study, we show that KIF retards the degradation of COX-2 and a COX-1 mutant containing the 19-aa cassette of COX-2.

Spear and Ng (256) have recently shown that in a multiply glycosylated glycoprotein a single, specific *N*-linked oligosaccharide group serves as the determinant for entry into the ERAD pathway. In the present study, we have provided evidence suggesting that only one of the four *N*-glycosylation sites of COX-2 (*i.e.* Asn-594) is involved in COX-2 degradation; however, degradation also requires at least some amino acids downstream of the consensus *N*-glycosylation sequence. We presume that a carbohydrate moiety linked to Asn-594 along with adjacent amino acids of the 19-aa insert interact with the complex of proteins that provide entry into the ERAD system. Very little of the 19-aa cassette can be resolved in the COX-2 crystal structure (12), and therefore, the 19-aa insert is thought to lack secondary structure. The last resolved residue in the murine COX-2 crystal structure is Ser-596, the final amino acid in the *N*-glycosylation consensus sequence. Ser-596 is solvent-exposed and appears to be oriented in such a way that its C terminus would point toward the lipid bilayer. The COX-2 KDEL-like ER retention motif at the C terminus (19) also has to be on the protein surface to be recognized (18). Thus, the 19-aa cassette of COX-2 is likely to be solvent-exposed and situated close to the membrane surface.

In summary, we have identified a 19-aa cassette having a consensus *N*-glycosylation site at its N terminus that can target a protein to the ERAD system. Scanning mutagenesis should be helpful in identifying the critical residues in the 19-aa

cassette that work in conjunction with the Asn-594 *N*-glycosylation site to target COX-2 for degradation. It will also be important to characterize the oligosaccharide group linked to Asn-594.

Acknowledgments

We thank Dr. Anne Vojtek and Jennifer Taylor for their kind help with immunocytofluorescence. We are also grateful to Dr. Billy Tsai for his thoughtful suggestions relevant to this work. This work was supported in part by NIH Grant GM68848.

CHAPTER III

ASN-594 GLYCOSYLATION AND PROTEIN DEGRADATION OF COX-2 IS REGULATED BY ITS C-TERMINAL 27 AMINO ACID INSTABILITY ELEMENT

Summary

The C-terminal 19 amino acid cassette (19-aa) of COX-2 is required for the entry of the protein into the ER-associated degradation (ERAD) system. We have previously shown that the Asn-594 glycosylation site at the start of the 19-aa cassette is necessary, but not sufficient, to mediate COX-2 ERAD. Here, we demonstrate that the C-terminal 16 amino acid portion of 19-aa is also essential for COX-2 degradation. We also show a positive correlation between the extent of glycosylation at Asn-594 and the overall degradation of COX-2. Evidence is provided to demonstrate that the 19-aa cassette is part of a larger 27 amino acid sequence that dictates the intracellular stability of COX-2 by regulating glycosylation at Asn-594. Analysis of the region immediately upstream of Asn-594 suggests that an 8-residue sequence with α-helical structure impedes Asn-594 glycosylation, and in order for COX-2 to become glycosylated at Asn-594 there must be a change in the structure or conformation of this α-helix. We propose that this is elicited by the C-terminal 16-residue sequence of 19-aa. The upstream 8-residue sequence also appears to play a role in the processing of the *N*-glycan group at Asn-594 that preceeds translocation of COX-2 to the cytoplasm for proteasomal degradation. Therefore, the

interplay of the upstream 8-residue segment and the C-terminal 16 amino acid portion of 19-aa to regulate Asn-594 glycosylation and its *N*-glycan processing may control the timing and the extent of COX-2 protein degradation.

Introduction

Cyclooxygenases-1 and -2 (COX-1 and COX-2) catalyze the key committed step in prostanoid synthesis (1,3,7,17). These enzymes are multiply *N*-glycosylated ER resident proteins that exist as homodimers and exhibit ~60% identity in primary structure (1,3,7,17,150). They are also integral membrane proteins that monotopically insert into the lipid bilayer so that they are largely compartmentalized in the ER lumen or the contiguous lumen of the nuclear envelope (14-16). The mature forms of the COX isoforms are very similar in structure except that COX-2 has a unique 19-residue insertion (19-aa) near its C-terminus. Previously, we have shown that the 19-aa is essential for ER-associated degradation (ERAD) of COX-2 by the 26S proteasome (257). We have also demonstrated that the Asn-594 glycosylation site at the N-terminus of 19-aa is required for COX-2 ERAD (257). Immunoblotting of a variety of cell lines for COX-2 usually detects 72 and 74 kDa variably glycosylated forms of the enzyme due at least in part to alternative glycosylation at Asn-594 (148,151,258). Inhibition of co-translational *N*-glycosylation of COX-2 with tunicamycin at its four consensus glycosylation sites eliminates the cyclooxygenase (COX) and peroxidase (POX) activities of the enzyme (151). However, point mutation of the Asn-594 glycosylation site actually enhances COX-2 COX specific activity (151) most likely due to the increased stability of

the mutant enzyme (257). These results imply that while the Asn-594 glycosylation site is dispensable for proper co-translational protein folding, it is critical for the degradation of the enzyme.

In HEK293 cells stably expressing recombinant native human COX-2 the Asn-594 glycosylated form of the protein can only be detected upon addition of kifunensine, an ER α-1,2 mannosidase I inhibitor (257). This is an indication that Asn-594 glycosylated COX-2 is rapidly degraded by ERAD. It is well established that the ER possesses a quality control or surveillance system that selectively identifies glycoproteins with non-native structure so that they are retained in the ER long enough to achieve their native state (164-166,182-186). Glycoproteins that are irreversibly defective are degraded by ERAD, a process that involves unfolding of the protein and its export to the cytosol where it undergoes proteolysis by the 26S proteasome (164-166,182-186,188,189). COX-2 is the only ER luminal integral membrane protein that is known to be degraded via ERAD in its native or properly folded form. This raises the question as to why and how a properly folded glycoprotein is targeted for ERAD by the ER protein quality control system. We believe that a thorough structural and biochemical analysis of the C-terminal 19-aa of COX-2 may provide an answer to this conundrum.

Very little of the 19-aa can be resolved in the highest resolution mouse COX-2 X-ray crystal structure attained thus far (157). The last resolved residue in this 2.4 Å structure is Ser-596, the final amino acid in the Asn-594 *N*-glycosylation consensus sequence at the N-terminal end of 19-aa. The inability to resolve the remaining 16 residues of the 19-aa by X-ray crystallography may be an indication that this segment is largely disordered and lacks any degree of secondary structure. The Asn-594

glycosylation site is at the end of a two-turn helix that is linked to an upstream helix by a long 15-residue loop (Fig. 6). Asn-594 is not glycosylated in this structure presumably because the amide of its side chain is pointed upwards toward the upstream helix that is a distance of ~4.5 Å. Since the space between the helices is barely sufficient to accommodate an *N*-glycan group, a local conformational change, probably mediated by movement of the long and inherently flexible intervening loop, would have to occur to expose Asn-594 for *N*-glycosylation.

In our previous study, a HEK293 heterologous system was utilized to uncover the role of 19-aa in directing COX-2 protein degradation. In a different study, Dr. Masayuki Wada prepared fibroblast primary cultures from skin tissue of wild-type mice or a knock-in mouse carrying the mutant *del*595-612 murine (mu) COX-2 in place of the wild-type gene (Wada and Smith, unpublished results). To induce COX-2 expression, these primary cultures were first made quiescent by 24 h serum starvation followed by challenge with fetal bovine serum. NIH/3T3 fibroblasts that have been growth-arrested by serum starvation lack detectable COX-2 expression but constitutively express COX-1 (22). By immunoblotting analysis, Dr. Masayuki Wada made the interesting finding that while COX-1 was the only isoform that could be detected in growth-arrested primary cultures of wild-type mice, quiescent cultures prepared from *del*595-612 COX-2 mutant (-/-) mice constitutively expressed both COX isoforms. Fibroblasts from heterozygous (+/-) mice also constitutively expressed COX-2; however, the COX-2 protein levels were lower compared to the -/- cells indicating that protein expression was gene dose-dependent. Serum-stimulation of these quiescent primary cells resulted in the time-dependent accumulation of COX-2 protein in -/- cells in deep contrast to the more transient

expression of COX-2 in serum-treated wild-type cells. This is a confirmation that the 19-aa of COX-2 is essential for the degradation of the protein. More importantly, these results strongly argue that COX-2 ERAD that is mediated by 19-aa could represent a significant physiological mechanism for the regulation of COX-2 gene expression.

In the present study we set out to examine what specific features of the C-terminal 19-aa, in addition to Asn-594 glycosylation, are critical for targeting the enzyme to the ERAD system. The role of the helical region upstream of the Asn-594 glycosylation site in regulating Asn-594 glycosylation and COX-2 protein degradation was also investigated. Our findings have enabled us to identify a C-terminal 27 instability element of COX-2 that regulates the glycosylation of the enzyme at Asn-594, and subsequently, controls the timing and extent of protein degradation.

Experimental Procedures

Materials. Dulbecco's modified Eagle's medium (DMEM), fetal bovine serum (FBS), ponasterone A, and tetracycline were from Invitrogen. Bovine calf serum was from Hyclone. Cycloheximide, puromycin, and bacterial lipopolysaccharide (LPS) were obtained from Sigma. Kifunensine and MG132 were purchased from Calbiochem. Endoglycosidase H (Endo H) was purchased from Roche Applied Science.

Construction of Plasmids for Transfection. Recombinant human (hu) COX-2 cDNA was subcloned into the tetracycline-inducible vector pcDNA5/FRT/TO (Invitrogen). After subcloning, the QuickChange™ site-directed mutagenesis kit (Strategene) was used to create the following C-terminal mutants: *del*602-612 huCOX-2, *del*607-612 huCOX-2, P607A T608A huCOX-2, V609A huCOX-2, L610A huCOX-2,

L611A huCOX-2, K612A huCOX-2, V591P T592G huCOX-2, ovine (ov) COX-1 UPSTRM8 huCOX-2, and murine (mu) COX-2 UPSTRM8 huCOX-2. The COX-1 insertion mutant *ins*594-601 ovCOX-1 was created by QuikChange™ site-directed mutagenesis using *ins*594-612 ovCOX-1 as template. *Ins*594-612 ovCOX-1 mutant was previously made by overlap extension PCR and subcloned into the ecdysone-inducible pIND vector (Invitrogen). The COX-2 mutants, scrambled insert (S*ins*) 595-612 huCOX-2 and S*ins*597-612 huCOX-2 were created from the cDNA template for native huCOX-2 by overlap extension PCR and then subcloned into pcDNA5/FRT/TO using BamHI and XhoI sites. Correct cDNA orientation and mutations were confirmed by sequencing. The primers and the PCR conditions used to design the above mutants are shown in the 'Appendix' section.

Cell Culture and Transfection. NIH/3T3 fibroblasts at early passage (<6 passages) were cultured in DMEM supplemented with 10% bovine calf serum and 100 u/ml penicillin/streptomycin. To induce COX-2 expression, the cells were first made quiescent by serum starvation for 48 h in DMEM containing 0.2% bovine calf serum and thereafter treated with DMEM supplemented with 20% FBS for 4 h.

RAW 264.7 macrophage-like cells were cultured in DMEM supplemented with 10% FBS and 100 u/ml penicillin/streptomycin. To stimulate COX-2 expression, the cells were challenged with 200 ng/ml LPS for 12 h.

HEK293-derived cell lines stably expressing native or mutant COX constructs were generated using either the tetracycline-inducible and ecdysone-inducible mammalian expression systems (Invitrogen) according to the manufacturer's protocol. Constructs that were expressed under the control of a tetracycline-inducible promoter

were native huCOX-2, *del*602-612 huCOX-2, *del*607-612 huCOX-2, P607A T608A huCOX-2, V609A huCOX-2, L610A huCOX-2, L611A huCOX-2, K612A huCOX-2, V591P T592G huCOX-2, ovCOX-1 UPSTRM8 huCOX-2, muCOX-2 UPSTRM8 huCOX-2, S*ins*595-612 huCOX-2, and S*ins*597-612 huCOX-2. The *ins*594-601 ovCOX-1 construct was expressed under the control of the ecdysone-inducible promoter. Stably transfected HEK293 cells were cultured in DMEM supplemented with 10% FBS, 100 u/ml penicillin/streptomycin, and the appropriate pharmacological selective reagents. Inducible expression was achieved by by treatment with 10 μg/ml tetracycline or 10 μM ponasterone A (ecdysone analog) for 24 h in normal culture medium.

Protein Degradation and Drug Treatments. Quiescent 3T3 cells were serum-stimulated for 4 h then treated with 50 μM cycloheximide (CHX) for different times in the presence or absence of 25 μM kifunensine (KIF). RAW264.7 macrophage cells were challenged with 200 ng/ml LPS for 12 h then treated with 50 μM CHX in the presence or absence of treatment with 50 μM KIF. HEK293 cells stably and inducibly expressing wild-type or mutant cyclooxygenase constructs were grown to ~80% confluency, serum-starved for 24 h, and then treated with 10 μg/ml tetracycline or 10 μM ponasterone A in complete culture medium to induce expression. Afterwards, the cells were incubated for various times with 50 μM puromycin to block translation in the absence or presence of 20 μM MG132 or 25 μM KIF. Alternatively, stable transfectants of HEK293 cells were grown to ~80% confluency, treated with 10 μg/ml tetracycline for 24 h to induce expression, and thereafter treated for 12 h with 25 μM KIF.

Enyzmatic Deglycosylation. For complete deglycosylation, HEK293 whole cell lysates were denatured by boiling in NuPAGE SDS sample loading buffer (Invitrogen)

and then treated for at least 12 h with endoglycosidase H (Endo H) at a concentration of 0.4 mU/μl.

Western Transfer Blotting. After the appropriate treatments, NIH/3T3, RAW 264.7, and HEK293 cells were scraped into ice-cold PBS (phosphate-buffered saline), pH 7.4 containing 5 mM EDTA and a cocktail of protease inhibitors (Roche) and lysed by sonication. RIPA lysis buffer (10 mM Tris, pH 7.2, 150 mM NaCl, 5mM EDTA, 0.1% SDS, 1.0% Triton X-100, 1% deoxycholate) containing a protease inhibitor cocktail (Roche Applied Science) was also used for cell lysis. Protein concentrations were determined using the BCA protein assay kit (Pierce). The NuPAGE system (Invitrogen) was used to resolve the proteins in the whole cell lysates on a 7% tris-acetate polyacrylamide gel. After transfer to a nitrocellulose membrane, immunoblotting was performed with the appropriate primary antibody. Horseradish peroxidase-conjugated anti-rabbit or anti-mouse IgG antibodies (Bio-Rad) were used as secondary antibodies. Immunodetection was performed using the Western Lighting Chemiluminescent kit (Amersham Biosciences) followed by exposure to X-ray film. Densitometry analysis was performed using Quantity One software (Bio-Rad).

Antibodies for Western Analysis. A previously generated (13), peptide-specific, polyclonal primary antibody for murine (mu) COX-2 against the epitope Ser598-Lys612 was used in the current study to detect muCOX-2 expressed in NIH/3T3 and RAW264.7 cells. Peptide-specific, polyclonal primary antibodies for ovCOX-1 and huCOX-2 were synthesized by Covance Research Products against the following epitopes: Leu272-Gln283 of ovCOX-1 and Pro583-Asn594 of huCOX-2. A polyclonal antibody raised against whole muCOX-2, which also specifically detects native huCOX-2, was used to

immunoblot for the mutants V591P T592G huCOX-2, ovCOX-1 UPSTRM8 huCOX-2, and muCOX-2 UPSTRM8 huCOX-2.

Results

The C-terminal region of 19-aa is important for COX-2 degradation. It has previously been shown that the Asn-594 glycosylation site is necessary, but not sufficient, for enabling the proteasomal degradation of COX-2 (257). Therefore, an additional portion of 19-aa is required to mediate COX-2 degradation. We embarked on determining which amino acids of the C-terminal 19-aa are needed for this process. Initially, two C-terminal deletion mutants of human (hu) COX-2 were prepared, namely *del*602-612 huCOX-2 and *del*607-612 huCOX-2 (Fig. 16*a*, panel *I*). We also prepared an insertion mutant of ovine (ov) COX-1, *ins*594-601 ovCOX-1, that carried an identical truncated region of 19-aa as *del*602-612 huCOX-2 (Fig. 16*a*, panel *I*). These mutants were stably transfected into HEK293 cells and their degradation profiles examined. All three mutants, including *del*607-612 huCOX-2, were stable and did not degrade within the 24 h time frame of the experiment (Fig. 16*a*, panel *II*). These results indicated that removal of the last six residues of 19-aa was sufficient to eliminate COX-2 degradation. Preventing COX-2 degradation by trimming the 19-aa raised the possibility that a correct length for this insertion, rather than its primary structure, was needed to mediate protein turnover. To eliminate this possibility, we prepared two mutants of COX-2 that carried scrambled versions of the 19-aa (Fig. 16*b*, panel *I*). S*ins*597-612 huCOX-2 has an intact Asn-594 glycosylation site but the rest of the 19-aa has been scrambled. S*ins*595-612 huCOX-2 is not only mutated at Asn-594, but it also has a randomized version of the rest

of the 19-AA. After stably transfecting these scrambled mutants into HEK293 cells their protein stabilities were analyzed. Both mutants were much more stable than native huCOX-2 because they degraded very slowly with a half-life ($t_{1/2}$) > 24 h (Fig. 16*b*, panels *II* and *III*). Overall, these results suggest that there is primary structure information within the 19-aa cassette, in particular its last six residues, that is essential for dictating COX-2 protein degradation.

To identify which of the last six amino acids of 19-aa were important for enabling COX-2 degradation we performed alanine scanning mutagenesis of this region (Fig. 17*a*). The mutant P607A T608A huCOX-2 had a $t_{1/2}$ of ~8 h which was not far removed from that of the native huCOX-2 ($t_{1/2}$ ~5 h) (Figs. 17*b* and *c*). Its degradation kinetics was also similar to that of the native enzyme (Fig. 17*c*). The V609A huCOX-2 mutant also degraded with a $t_{1/2}$ of ~8 h (Figs. 17*b* and *c*). However, careful examination of its overall degradation profile revealed that V609A huCOX-2 was degraded less efficiently than both the native and P607A T608A huCOX-2 (Fig 17*c*). There seemed to be a significant loss of V609A huCOX-2 protein at the earlier time points after inhibiting protein translation. Thereafter, at the 12 h and 24 h time points, this mutant appeared to be relatively stable compared to native and P607A T608A huCOX-2 (Figs. 17*b* and *c*). Although the mutations L610A huCOX-2, L611A huCOX-2, and K612A huCOX-2 did not completely prevent COX-2 degradation, they significantly stabilized the enzyme; the $t_{1/2}$ for the degradation of all three mutants was >24 h (Figs. 17*b* and *c*). Collectively, these results point to a three amino acid sequence at the C-terminal end of 19-aa, namely Leu-610, Leu-611, and Lys-612, as being essential for enabling COX-2 degradation.

16A. (I)

^{580}FSVPDPELIKTVTI**NASSSRSGLDDINPTVLLK**ERSTEL^{618}	native huCOX-2
^{580}FSVPDPELIKTVTI**NASSSRSG**----------ERSTEL^{607}	*del*602-612 huCOX-2
^{580}FSVPDPELIKTVTI**NASSSRSGLDDIN**------ERSTEL^{612}	*del*607-612 huCOX-2
^{580}FHVPDPRQEDRPGV----------ERPPTEL^{600}	native ovCOX-1
^{580}FHVPDPRQEDRPGV**NASSSRSGLDDINPTVLLK**ERPPTEL^{619}	*ins*594-612 ovCOX-1
^{580}FHVPDPRQEDRPGV**NASSSRSG**----------ERPPTEL^{608}	*ins*594-601 ovCOX-1

A. (II)

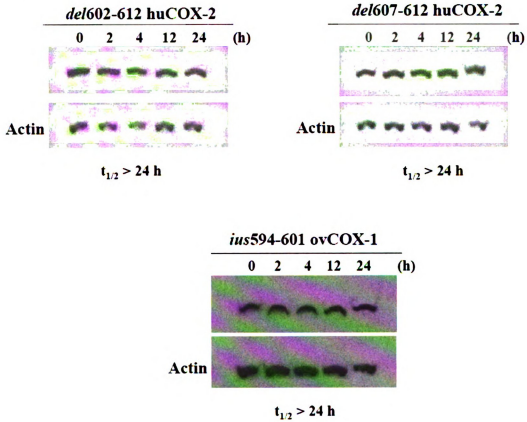

16B. (I)

^{580}FSVPDPELIKTVTI**NASSSRSGLDDINPTVLLK**ERSTEL^{618}	native huCOX-2
^{580}FSVPDPELIKTVTI**NAS**IRGPLTKLSDNSLVSDERSTEL^{618}	*Sins*597-612 huCOX-2
^{580}FSVPDPELIKTVTI**AASIRGPLTKLSDNSLVSD**ERSTEL^{618}	*Sins*595-612 huCOX-2

B. (II)

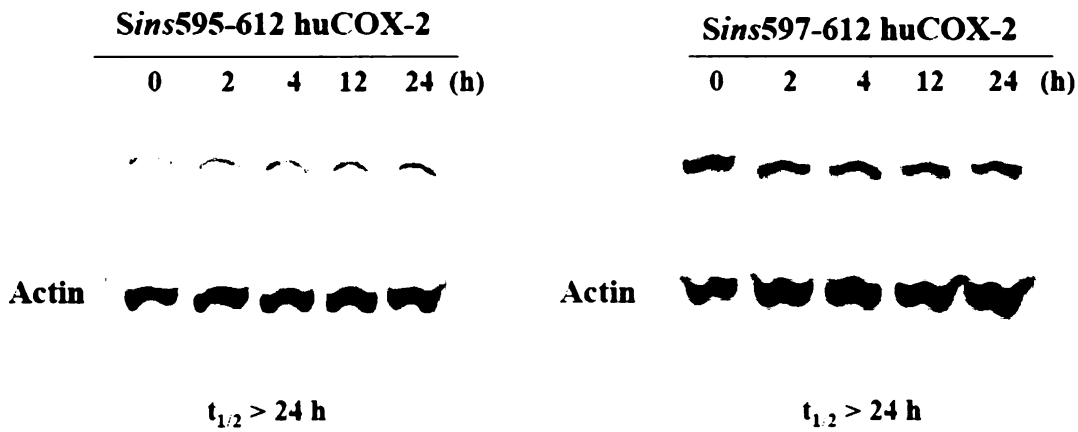

16B. (III)

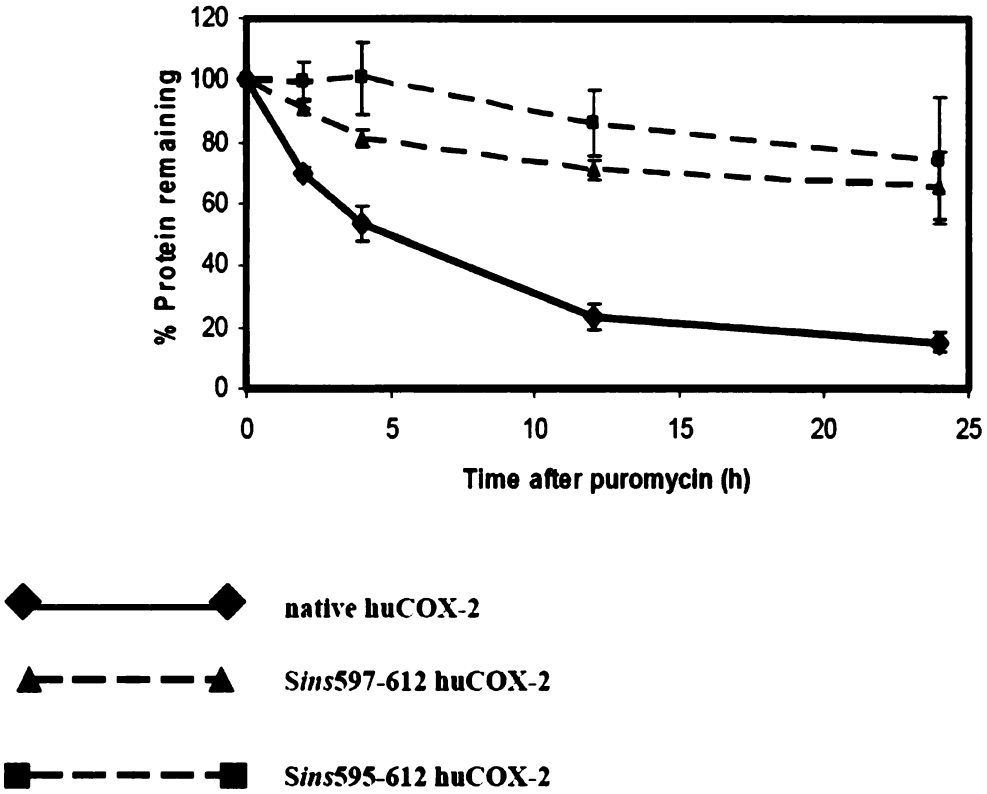

Figure 16. Deletion and scrambled mutations of the 19-AA cassette disrupt COX-2 degradation. *A (I)* and *B (I)*, Amino acid sequences of the C-termini of cyclooxygenase constructs that were stably transfected into HEK293 cells. The underlined sequence is the consensus *N*-glycosylation site at the start of the COX-2 19-aa cassette. The C-terminal sequences of native huCOX-2, native ovCOX-1, and *ins*594-612 ovCOX-1 are included for comparison. *A (II)* and *B (II)*, HEK293 cells stably and inducibly expressing the constructs shown in *(I)* were grown to ~80% confluency, subjected to serum-starvation for 24 h, and then treated with the appropriate inducing agent (10 μg/ml tetracycline or 10 μM ponasterone A) for 24 h. Puromycin (50 μM) was then added to block translation and COX-2 and actin protein levels were analyzed at different times by Western blotting. The Western blotting results in *A(II)* and *B(II)* are representative of two and three separate experiments, respectively, from which protein half-lives were determined. *B (III)*, Densitometry analysis of the degradation of native huCOX-2, S*ins*595-612 huCOX-2, and S*ins*597-612 huCOX-2. The results are based on at least three different experiments for each protein. The error bars denote +/- SE of the mean.

17A.

^{580}FSVPDPELIKTVTI**NASSSRSGLDDINPTVLLK**ERSTEL^{618}	native huCOX-2
^{580}FSVPDPELIKTVTI**NASSSRSGLDDINAAVLLK**ERSTEL^{618}	P607A T608A huCOX-2
^{580}FSVPDPELIKTVTI**NASSSRSGLDDINPTALLK**ERSTEL^{618}	V609A huCOX-2
^{580}FSVPDPELIKTVTI**NASSSRSGLDDINPTVALK**ERSTEL^{618}	L610A huCOX-2
^{580}FSVPDPELIKTVTI**NASSSRSGLDDINPTVLAK**ERSTEL^{618}	L611A huCOX-2
^{580}FSVPDPELIKTVTI**NASSSRSGLDDINPTVLLA**ERSTEL^{618}	K612A huCOX-2

B.

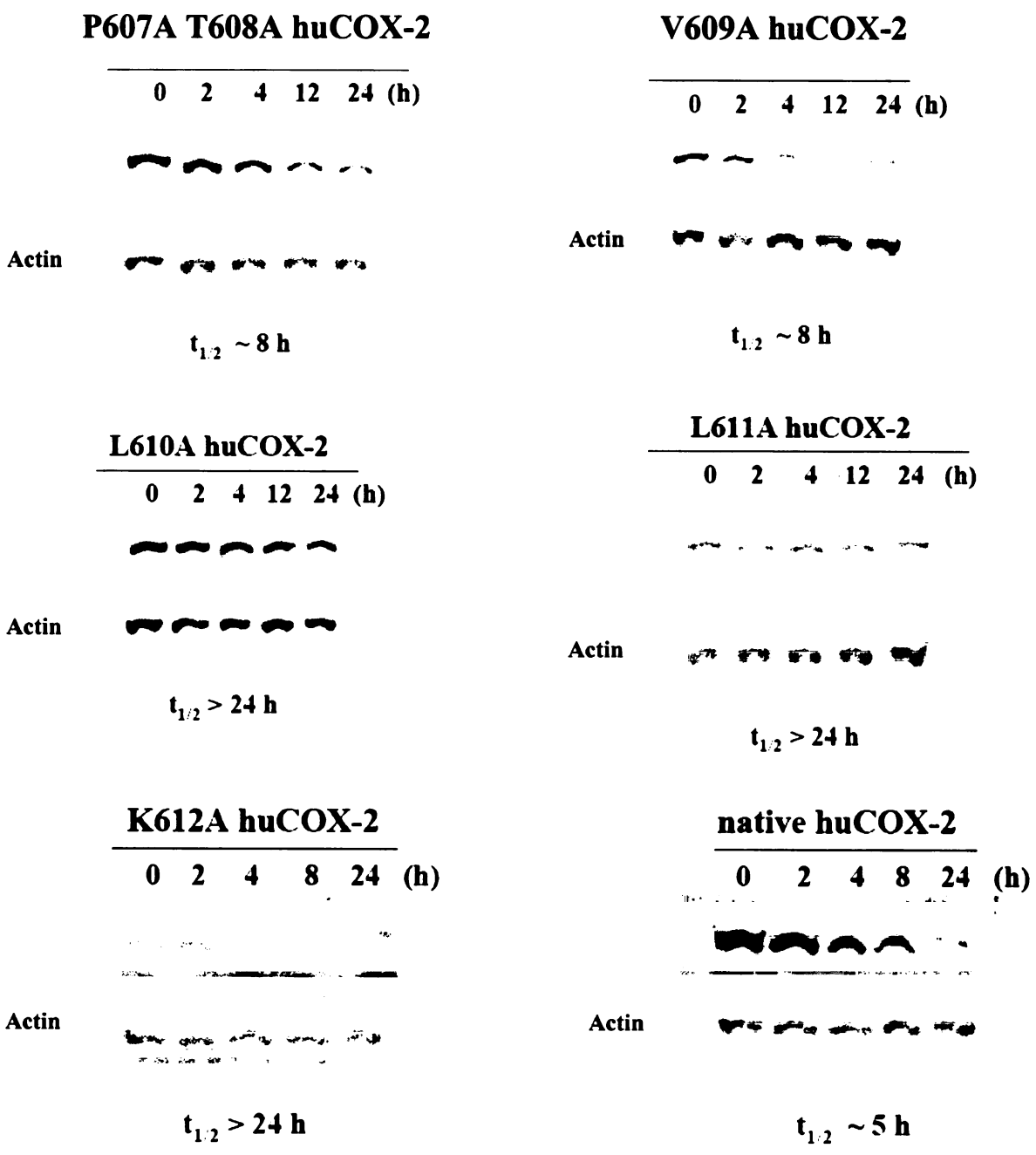

17C.

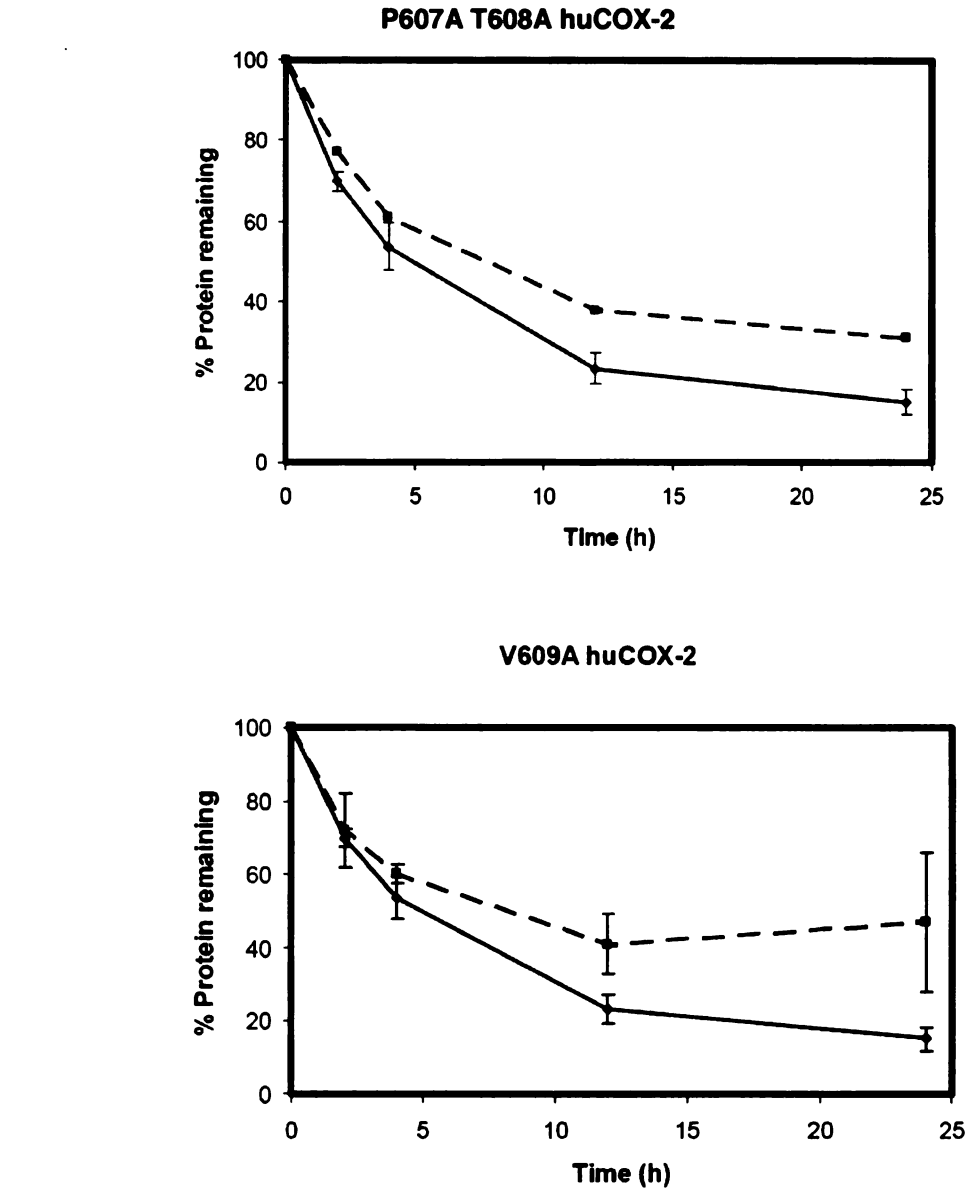
P607A T608A huCOX-2
% Protein remaining
Time (h)
V609A huCOX-2
% Protein remaining
Time (h)
native
mutant

17C. (cont'd)

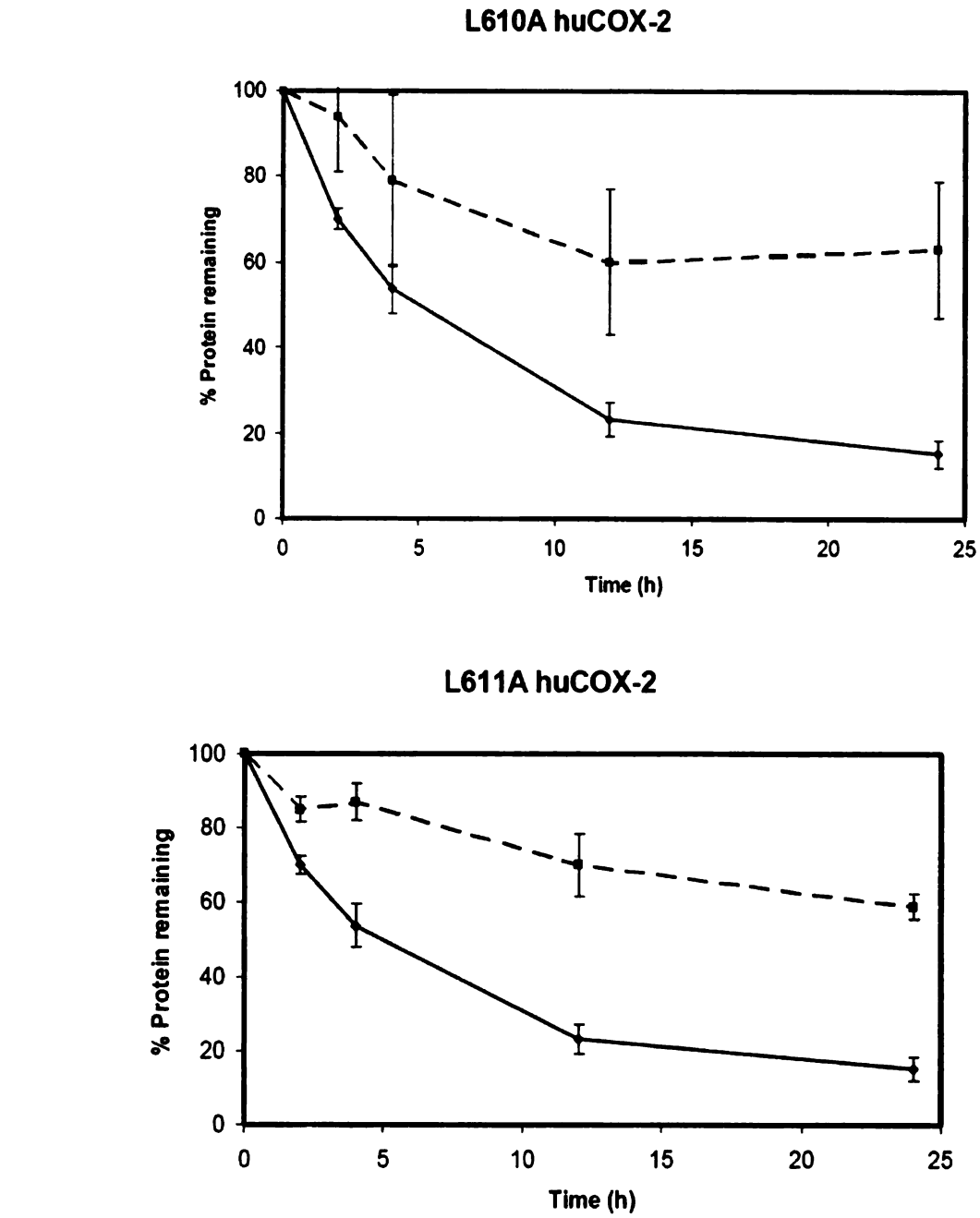
L610A huCOX-2
% Protein remaining
Time (h)
L611A huCOX-2
% Protein remaining
Time (h)
native
mutant

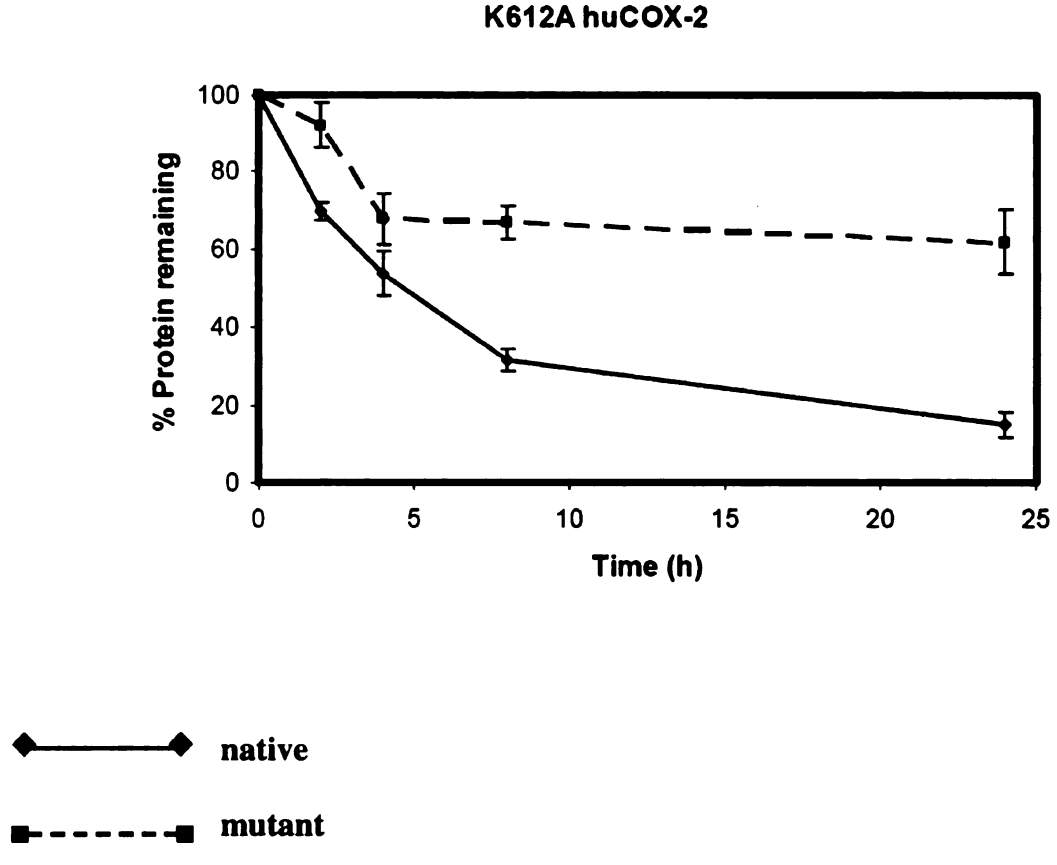

Figure 17. The C-terminal end of 19-aa is essential for COX-2 protein degradation. *A*, Alanine scanning mutants of the C-terminal portion of 19-aa that were stably transfected into HEK293 cells. The underlined sequence is the Asn-594 glycosylation site. *B*, HEK293 cells stably and inducibly expressing the constructs shown in *(A)* were grown to ~80% confluency, subjected to serum-starvation for 24 h, and then treated with 10 μg/ml tetracycline for 24 h. Thereafter, the time course of degradation of the proteins was determined as described in the legend to Fig. 16. Protein half-lives of all proteins except P607A T608A huCOX-2 were determined from at least three separate experiments. *C*, Densitometry analysis of the degradation of the mutants shown in *A* and *B*. The results for native huCOX-2 and for all mutants except P607A T608A huCOX-2 are based on at least three independent experiments. Densitometry analysis of P607A T608A huCOX-2 is based on a single experiment. The degradation profile of huCOX-2 has been included for comparison. The error bars denote +/- SE of the mean.

Glycosylation of Asn-594 correlates with COX-2 protein degradation. We previously reported that kifunensine, which inhibits ERAD by preventing *N*-glycan processing by ER α1,2 mannosidase I, stabilizes huCOX-2 stably expressed in HEK293 cells (257). At the same time kifunesine (KIF) leads to the appearance of a less mobile, alternatively glycosylated form of the native enzyme in HEK293, NIH/3T3, and RAW 264.7 cells even after protein translation has been inhibited (Figs. 18*a*, *b*, and *c*). This higher glycosylated form is not observed after KIF treatment of HEK293 cells expressing N594A huCOX-2 (257). Endo H treatment of native huCOX-2 expressing cells collapses both alternatively glycosylated forms to the 66 kDa fully deglycosylated form of the enzyme (Fig. 18*a*). Therefore, we believe that KIF stabilizes the 74 kDa Asn-594 glycosylated form of the native enzyme. The enhanced levels of the 74 kDa form upon KIF treatment could be used to assess Asn-594 glycosylation of COX-2 in HEK293 cells. Experiments were performed to determine if the deletion mutants *del*597-612 huCOX-2, *del*602-612 huCOX-2 and *del*607-612 huCOX-2, and the scrambled mutant S*ins*597-612 huCOX-2 are glycosylated at Asn-594. The deletion mutant *del*597-612 huCOX-2 has the same electrophoretic mobility as *del*595-612 huCOX-2, which lacks the Asn-594 glycosylation site (Fig. 19*a*, panel *I*). KIF treatment of cells expressing *del*597-612 huCOX-2 did not affect the mobility of this mutant suggesting that it is not glycosylated at Asn-594 (Fig. 19*a*, panel *II*). Similarly, *del*602-612 huCOX-2 and *del*607-612 huCOX-2 did not appear to be glycosylated at Asn-594 (Fig. 19*a*, panel *II*). The scrambled mutant S*ins*597-612 huCOX-2 carrying an intact Asn-594 glycosylation site had the same electrophoretic mobility as S*ins*595-612 huCOX-2 with or without KIF treatment

18A.

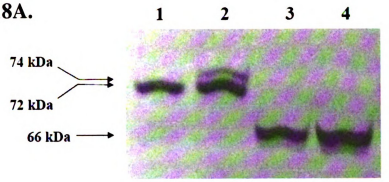

1. **tet-induced**
2. **tet-induced + 12 h KIF**
3. **EndoH cleavage of 1**
4. **EndoH cleavage of 2**

B.

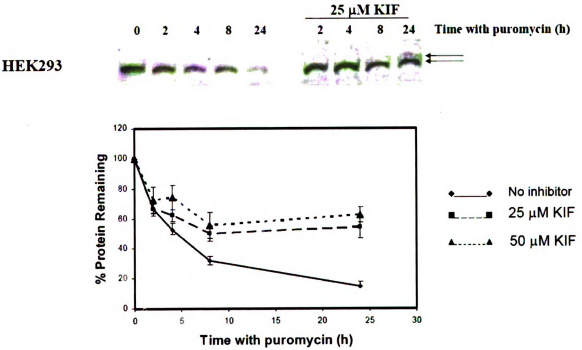

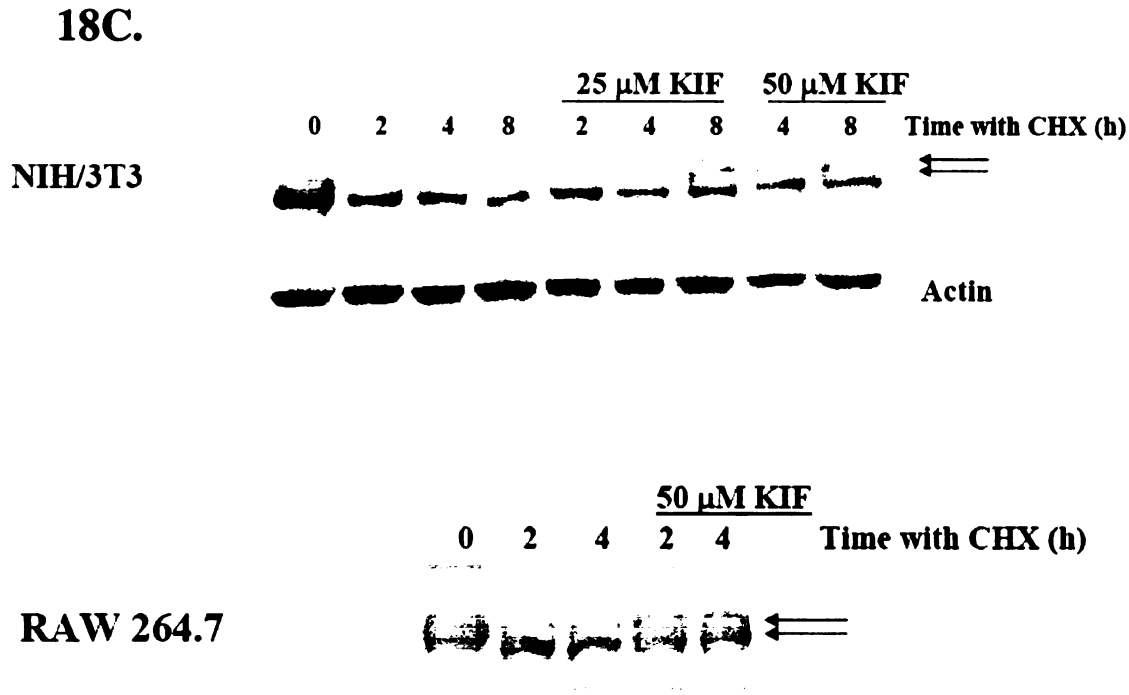

Figure 18. KIF treatment stabilizes the Asn-594 glycosylated form of COX-2. *A*, Native huCOX-2 expression in HEK293 cells was induced with 10 μg/ml tetracycline for 24 h . After protein induction cells were incubated for an additional 12 h in normal culture medium with or without 25 μM KIF. Thereafter, cell lysates were prepared and boiled in SDS sample loading buffer and then treated with or without Endo H (0.4 mU/μl) for at least 12 h. Proteins were resolved by SDS-PAGE on a 7% tris-acetate polyacrylamide gel and subjected to Western blotting. *B*, Native huCOX-2 expression was induced as described in the legend to Fig. 16. Puromycin (50 μM) was then added to block translation in the absence or presence of 25 μM KIF. Thereafter, COX-2 protein levels were analyzed at different times by Western blotting and densitometry. The densitometry analysis is based on three different experiments that were performed to examine the effect of 25 μM and 50 μM KIF on COX-2 degradation. The error bars denote +/- SE of the mean. *C*, Quiescent NIH/3T3 cells were stimulated with 20% FBS for 4 h to induce COX-2 expression. Cycloheximide (CHX; 50 μM final concentration) was added to the medium and the cells were incubated for the indicated times with or without additional treatment with 25 μM or 50 μM KIF. RAW264.7 cells were treated with 200 ng/ml LPS for 12 h to induce COX-2 expression. Thereafter, cells were treated with 50 μM CHX for the indicated times in the presence or absence of 50 μM KIF. Cell lysates were prepared and analyzed for COX-2 protein levels. Arrows in *B* and *C* show the 72 and 74 alternatively glycosylated forms of COX-2 detected by immunoblotting.

(Fig. 19*b*). Just like *del*597-612 huCOX-2, treatment with KIF did not result in the detection of a less mobile glycosylated form of S*ins*597-612 huCOX-2 (Fig. 19*b*). Collectively, these results indicate that mutations of the 19-aa that confer stability to COX-2 also prevent glycosylation of Asn-594. Consistent with this observation, the mutant V609A huCOX-2, which is degraded to a lesser extent compared to native huCOX-2, is also glycosylated less efficiently at Asn-594 in KIF-treated cells (Fig. 19*c*). Therefore, the C-terminal 16 amino acids of 19-aa appear to play an important role in effecting glycosylation of Asn-594. This could be one mechanism by which the 19-aa cassette mediates COX-2 protein degradation.

The helical region upstream of Asn-594 negatively regulates *N*-glycosylation. Previously, we showed that inserting the COX-2 19-aa near the C-terminus of ovCOX-1 yielded an unstable mutant *ins*594-612 ovCOX-1 that was degraded with a $t_{1/2}$ of ~3 h (257). A comparison of the molecular masses of *ins*594-612 ovCOX-1 with that of its stable, Asn-594-mutated counterpart *ins*594-612 (N594A) ovCOX-1 suggested that the former was fully glycosylated at Asn-594 (257). Unlike native huCOX-2, KIF treatment of HEK293 cells expressing *ins*594-612 ovCOX-1 failed to elicit the appearance of a higher glycosylated form of this ovCOX-1 mutant; instead, KIF significantly stabilized *ins*594-612 ovCOX-1 (257). The apparent disparity between native huCOX-2 and *ins*594-612 ovCOX-1 with respect to Asn-594 glycosylation suggested that the ease with which the two proteins became glycosylated at this site was different. The fact that the $t_{1/2}$ of *ins*594-612 ovCOX-1 is ~2 h shorter than that of native huCOX-2, also suggested that the efficiency of Asn-594 glycosylation appears to positively correlate with the rate of

19A. (I)

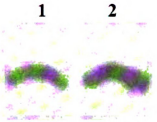

1. *del*595-612 huCOX-2
2. *del*597-612 huCOX-2

A. (II)

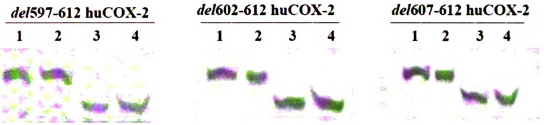

1. **tet-induced**
2. **tet-induced + 12 h KIF**
3. **EndoH cleavage of 1**
4. **EndoH cleavage of 2**

B.

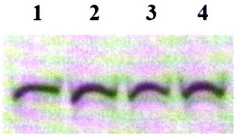

1. S*ins*595-612 huCOX-2
2. S*ins*597-612 huCOX-2
3. S*ins*595-612 huCOX-2 + 12 h KIF
4. S*ins*597-612 huCOX-2 + 12 h KIF

19C.

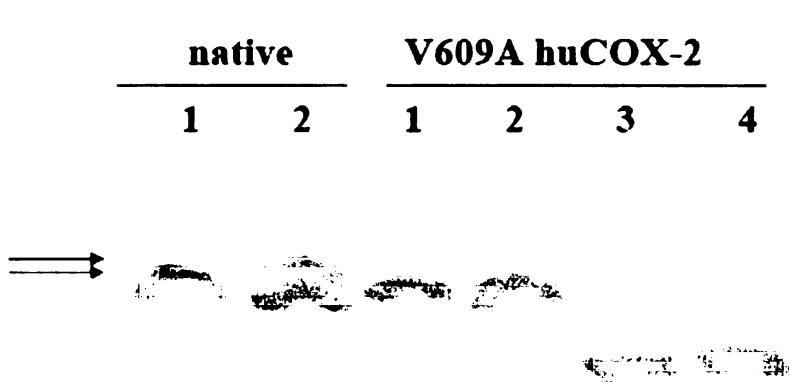

1. **tet-induced**
2. **tet-induced + 12 h KIF**
3. **EndoH cleavage of 1**
4. **EndoH cleavage of 2**

Figure 19. COX-2 stabilizing mutations of the 19-aa prevent glycosylation of Asn-594. *A (I)*, The expression of *del*595-612 huCOX-2 or *del*597-612 huCOX-2 was induced with 10 μg/ml tetracycline for 24 h. *(II)*, After protein induction as in *(I)* cells were incubated for an additional 12 h in normal culture medium with or without 25 μM KIF (*del*597-612 huCOX-2) or 50 μM KIF (*del*602-612 huCOX-2 and *del*607-612 huCOX-2). Thereafter, cell lysates were prepared and boiled in SDS sample loading buffer for 10 min and then treated with or without Endo H (0.4 mU/μl) for at least 12 h. Proteins were resolved by SDS-PAGE and subjected to Western blotting as in *18A*. *B*, Expression of S*ins*595-612 huCOX-2 or S*ins*597-612 huCOX-2 was induced as in *A(I)*. After protein induction cells were incubated for an additional 12 h with or without 25 μM KIF. Proteins were resolved by SDS-PAGE and subjected to Western blotting as in *18A*. *C*, Expression of native huCOX-2 or V609A huCOX-2 was induced as in *A(I)*. After protein induction cells were incubated for an additional 12 h with or without 25 μM KIF. Cell lysates were then prepared and boiled in SDS sample loading buffer for 10 min and then treated with or without Endo H (0.4 mU/μl) for at least 12 h. Proteins were resolved by SDS-PAGE and subjected to Western blotting as in *18A*. Arrows indicate differences in molecular mass due to *N*-glycosylation.

COX degradation. Native huCOX-2 and *ins*594-612 ovCOX-1 have very similar sequences downstream of Asn-594; therefore, we decided to probe the region upstream of Asn-594 in huCOX-2 for its ability to negatively regulate *N*-glycosylation. In the muCOX-2 X-ray crystal structure, the Asn-594 glycosylation site is at the C-terminal end of a 9-residue α-helical region (Figs. 20*a* and *b*). This helix (helix A) is connected to a nearby helix (helix B) by a long 15-residue loop; four of these residues are presumed to be part of the loop because they cannot be resolved in the crystal structure (Figs. 20*a* and *b*). The amide side chain of Asn-594 appears to be pointed upwards in the direction of helix B which is at a distance of ~4.5 Å (Fig. 20*c*). The length of two GlcNAc residues of an *N*-glycan group is ~8 Å. Therefore, helix B is situated such that it may impede the transfer of an *N*-glycan group to the amine group of the amide chain of Asn-594. Furthermore, a nearby disulfide bridge formed between Cys-569 of helix B and Cys-575 of the loop may also impede Asn-594 glycosylation because it is situated ~4.7 Å away (Fig. 20*c*). Moreover, the disulfide bridge may limit the flexibility of the loop, thereby, constraining helix A into a conformation in which Asn-594 cannot become glycosylated. The loop and the disulfide bridge can both be seen in the X-ray crystal structure of ovCOX-1, indicating that they are conserved in both isoforms (Fig. 20*d*). The last resolved residue in the ovCOX-1 structure is Pro-583, which is part of the loop; therefore, the region that would be immediately upstream of Asn-594 in *ins*594-612 ovCOX-1 (ie. Asp-584 to Val-593) cannot be resolved, suggesting a lack of secondary structure. Furthermore the presence of proline and glycine at two consecutive positions, 591 and 592, respectively, makes it highly improbable that this region would possess any secondary structure. It is therefore likely that *ins*594-612 ovCOX-1 is fully glycosylated

at Asn-594 because this glycosylation site is situated in a loop that is long enough to be very flexible even in the presence of the disulfide linkage (Fig. 20*e*).

To test this hypothesis, we prepared and stably transfected huCOX-2 mutants bearing various modifications of an 8-residue sequence (UPSTRM8) immediately upstream of Asn-594. The mutation V591P T592G huCOX-2 introduces a proline and a glycine into UPSTRM8 to disrupt the helix that is presumably formed by this region of huCOX-2. This mutation was also designed to mimic the corresponding region of ovCOX-1 (Fig. 21*a*). A second mutant was made in which the whole UPSTRM8 region of huCOX-2 was replaced with the corresponding region of ovCOX-1 (Fig. 21*a*). This mutant is designated ovCOX-1 UPSTRM8 huCOX-2. The initial rates of degradation of V591P T592G huCOX-2 ($t_{1/2}$ ~4-5 h) and ovCOX-1 UPSTRM8 huCOX-2 ($t_{1/2}$ ~3 h) were similar to that of the native enzyme (Figs. 21*b* and *c*). However, overall, both mutants appeared to be degraded to a greater extent than native huCOX-2 (Fig. 21*c*). For instance, essentially all of V591P T592G huCOX-2 or ovCOX-1 UPSTRM8 huCOX-2 was degraded by the 24 h time point, while ~15% of native huCOX-2 remained (Fig. 21*c*). Also, these mutations resulted in the detection of the 74 kDa glycosylated form even without KIF treatment (Figs. 21*b*, 22*a*, and 22*b*). This interesting observation led us to hypothesize that disrupting helix A facilitated Asn-594 glycosylation, and consequently, enhanced the overall degradation of the protein. If this is true, then replacing the UPSTRM8 region of huCOX-2 with that of muCOX-2 should not change the glycosylation pattern at Asn-594. As shown in Fig. 21*a* substantial differences exist between the UPSTRM8 regions of muCOX-2 and huCOX-2. Nonetheless, we expected that helix A of muCOX-2 would be conserved in huCOX-2. The initial degradation rate

of the mutant muCOX-2 UPSTRM8 huCOX-2 ($t_{1/2}$ ~4-5 h) was similar to that of native huCOX-2 and the ovCOX-1 UPSTRM8 mutants (Figs 21*b* and *c*). Moreover, the extent of the overall degradation of this mutant appeared to be intermediate between that of the native huCOX-2 and the ovCOX-1 UPSTRM8 mutants (Fig. 21*c*). The Asn-594 glycosylation pattern of muCOX-2 UPSTRM8 huCOX-2 was similar to that of the native huCOX-2 in that unlike the ovCOX-1 UPSTRM8 mutants, very little of the Asn-594 glycosylated form of this mutant could be detected in the absence of KIF or MG132 treatment (Figs. 22*a* and *b*). The modest detection of Asn-594-glycosylated muCOX-2 UPSTRM8 huCOX-2 is consistent with the observation that the extent of its overall degradation is slightly greater than that of native huCOX-2. Nonetheless, these results are consistent with our expectation that the UPSTRM8 regions of muCOX-2 and huCOX-2 have conserved helical secondary structure which appears to negatively regulate Asn-594 glycosylation. It is important to note that the putative helix A formed by the UPSTRM8 of huCOX-2 may actually be 2 residues longer since, unlike muCOX-2 UPSTRM8, this region lacks a proline residue at its N-terminus (Fig. 21*a*).

Just like native huCOX-2, the degradation of all three UPSTRM8 huCOX-2 mutants involved entry into the ERAD system because the 26S proteasome inhibitor MG132 and the ER α1,2-mannosidase I inhibitor KIF stabilized these mutants (Figs. 22*a*, *b*, and *c*). These findings lead us to propose that the UPSTRM8 of huCOX-2 acts in concert with the downstream 19-aa to control the timing of the entry of the protein into the ERAD system and the extent of protein degradation by regulating glycosylation of Asn-594.

20A.

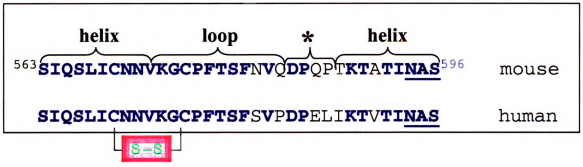
helix
loop
*
helix
563 SIQSLICNNVKGCPFTSFNVQDPQPTKTATINAS 596
mouse
SIQSLICNNVKGCPFTSFSVPDPELIKTVTINAS
human
S-S

B.


Helix B
Asn-570
Cys-569
Thr-590
Ser-596
Helix A
Helix B
Asn-570
Cys-569
Ser-596
Helix A

C.

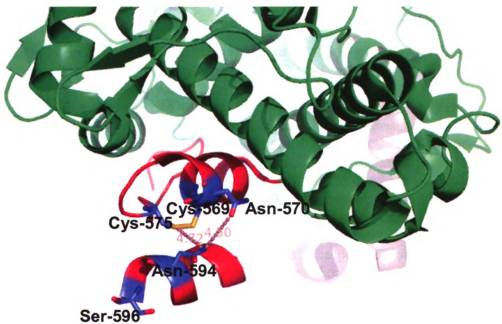
Cys-569
Asn-570
Cys-575
Asn-594
Ser-596

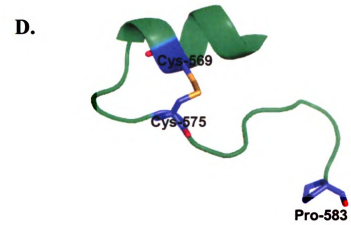

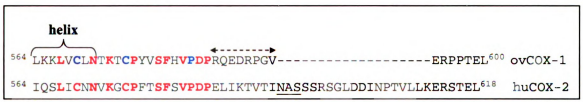

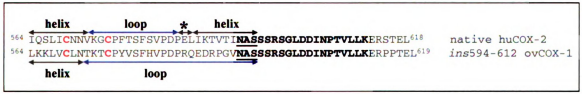

Figure 20. Structure of the C-terminal region of COX-1 and COX-2. *A*, Amino acid sequences of the C-terminal regions of muCOX-2 and huCOX-2 that are located upstream of the Asn-594 glycosylation site (underlined). Residues that are colored blue are conserved between the two species. Segments that form helices in the muCOX-2 X-ray structure are highlighted. The region marked with an asterisk is not resolved in the muCOX-2 X-ray structure and is very likely to be a continuation of the resolved loop. The disulfide linkage between Cys-569 and Cys-575 is also shown. *B*, Ribbon diagrams depicting the structure of the C-terminal region of muCOX-2 whose sequence is shown in *A*. The last resolved residue in the muCOX-2 X-ray structure is Ser-596, the final amino acid of the Asn-594 glycosylation site. Asn-594 is situated in a helix (Helix A) that is positioned right under an adjacent helix (Helix B). The amide chain of Asn-594 appears to be pointed upward in the direction of helix B. The position of the disulfide linkage relative to Asn-594 is shown. *C*, A ribbon diagram showing the distances between Asn-594 and Asn-570 of helix B (4.5 Å), and Asn-594 and the disulfide linkage between the loop and helix B (4.7 Å). *D, Top,* Structure of the C-terminal region of ovCOX-1. The last resolved residue in the X-ray structure of ovCOX-1 is Pro-583. The conserved

disulfide linkage between Cys-569 and Cys-575 is shown. *Bottom*, Amino acid sequences of the C-termini of ovCOX-1 and huCOX-2. The sequence in ovCOX-1 that forms a helix is shown. The sequence highlighted with a dashed double arrow is the region of ovCOX-1 that is not resolved in the X-ray crystal structure whose corresponding region is resolved in the X-ray structure of muCOX-2. Conserved residues between ovCOX-1 and huCOX-2 are highlighted in red. The conserved cysteines that form the disulfide bridge in either isoform are colored blue. The last resolved residue, Pro-583, is also colored blue. *E*, Comparison of the C-termini of native huCOX-2 and *ins*594-612 ovCOX-1. Segments expected to form a helix are highlighted with black double arrows. Segments expected to form a loop are highlighted with blue double arrows. The area of native huCOX-2 marked with an asterisk is likely to be a continuation of the helix. The conserved Cys-569 and Cys-575 are colored red.

21A.

^{580}FSVPDPELIKTVTI**NASSSRSGLDDINPTVLLK**ERSTEL^{618}	native huCOX-2
^{580}FSVPDPELIKTPGI**NASSSRSGLDDINPTVLLK**ERSTEL^{618}	V591P T592G huCOX-2
^{580}FSVPDPRQEDRPGV**NASSSRSGLDDINPTVLLK**ERSTEL^{618}	ovCOX-1 UPSTRM8 huCOX-2
^{580}FSVPDPQPTKTATI**NASSSRSGLDDINPTVLLK**ERSTEL^{618}	muCOX-2 UPSTRM8 huCOX-2

B.

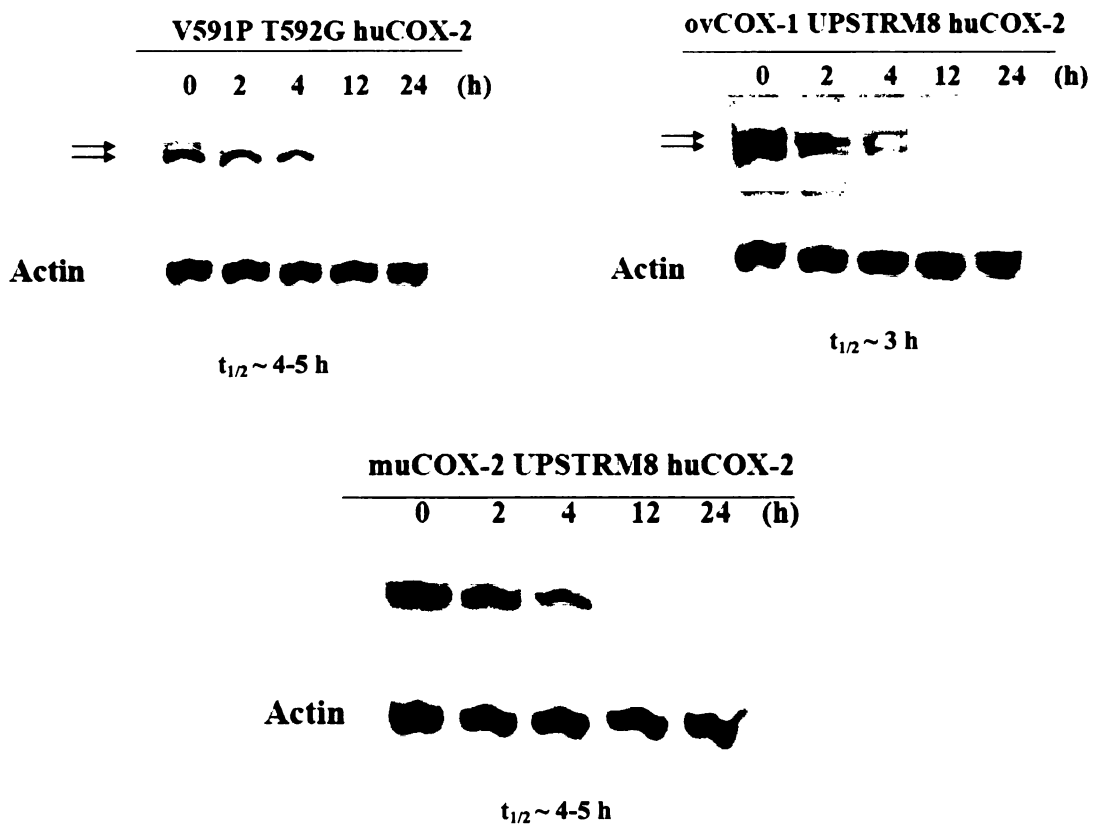

21C.

ovCOX-1 UPSTRM8 huCOX-2

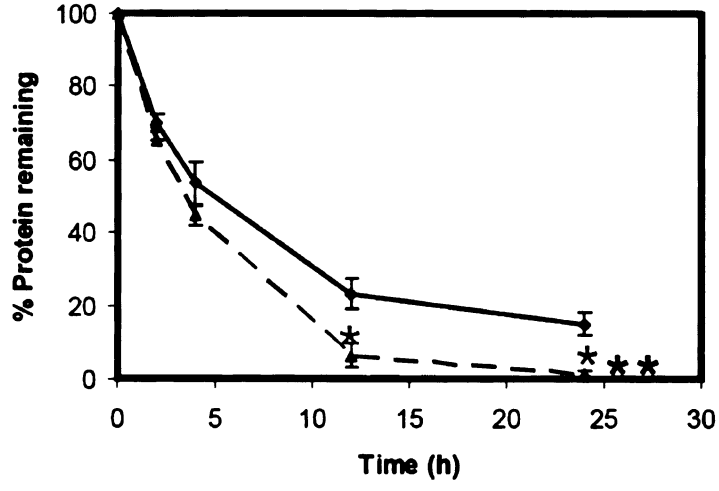

native

mutant

V591P T592G huCOX-2

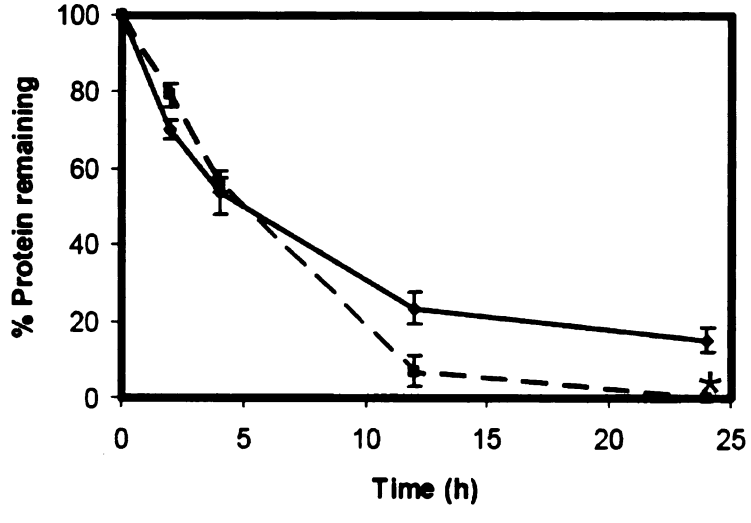

native

mutant

21C. (cont'd)

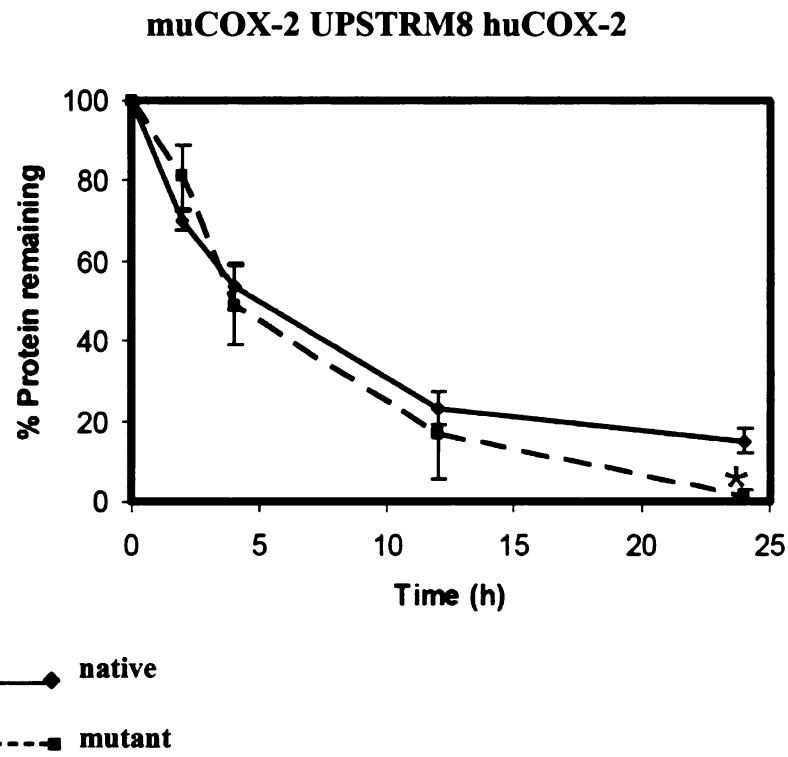

Figure 21. Degradation of the UPSTRM8 huCOX-2 mutants. *A*, Amino acid sequences of the C-termini of UPSTRM8 huCOX-2 mutants that were stably transfected into HEK293 cells. The underlined sequence is the Asn-594 glycosylation site. *B*, After stably transfecting the UPSTRM8 huCOX-2 constructs shown in *A*, protein expression was induced as described in the figure legend to Fig. 16. Thereafter, cells were treated with 50 μM puromycin for the indicated times and remaining levels of COX-2 and actin were analyzed by Western blotting. The Western blotting results are based representative of three separate experiments from which protein half-life measurements were made. Arrows indicate differences in molecular mass due to *N*-glycosylation. *C*, Densitometry analysis of the degradation of the UPSTRM8 huCOX-2 mutants relative to native huCOX-2. Densitometry is based on three separate experiments. Error bars denote +/- SE of the mean. Red asterisk indicates that the difference in % protein levels between the mutant and native protein at a given time point is statistically significant based on a Student's paired *t*-Test (p value < 0.01). Black asterisks indicate that the overall degradation of the mutant relative to the native protein is statistically significant based on a Student's paired *t*-Test (p value < 0.05).

22A. (I)

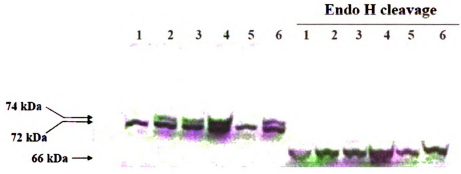

1. native huCOX-2
2. native huCOX-2 + KIF
3. V591P T592G huCOX-2
4. V591P T592G huCOX-2 + KIF
5. muCOX-2 UPSTRM8 huCOX-2
6. muCOX-2 UPSTRM8 huCOX-2 +KIF

A. (II)

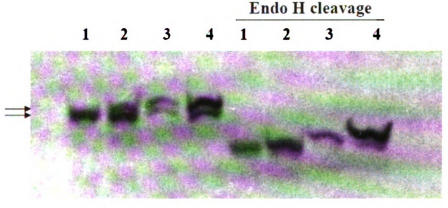

1. native huCOX-2
2. native huCOX-2 + KIF
3. ovCOX-1 UPSTRM8 huCOX-2
4. ovCOX-1 UPSTRM8 huCOX-2 + KIF

22B. (I)

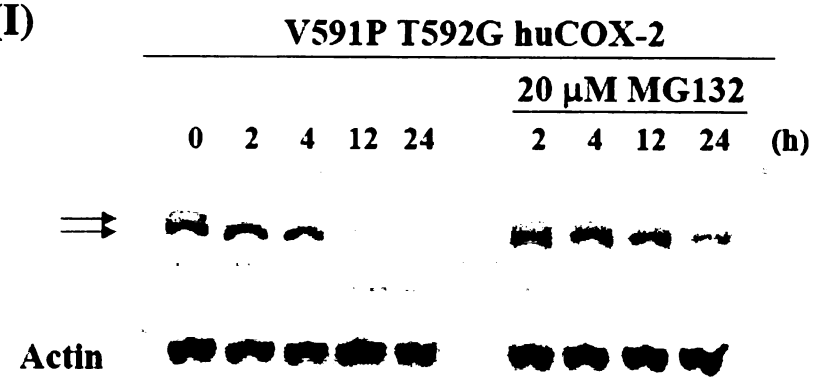

B. (II)

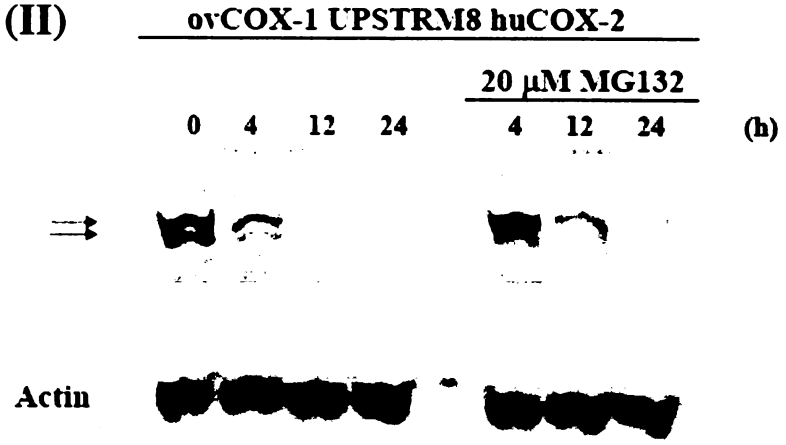

B. (III)

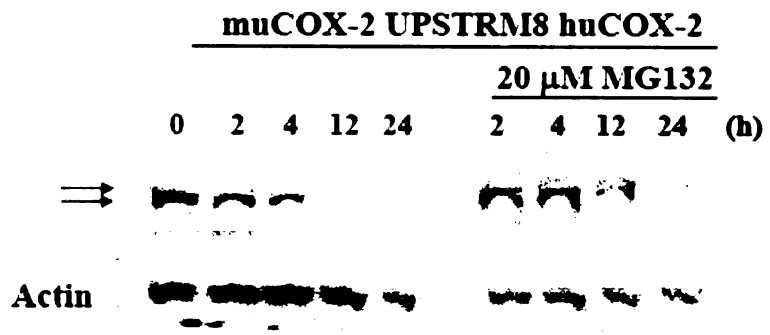

22B. (IV)

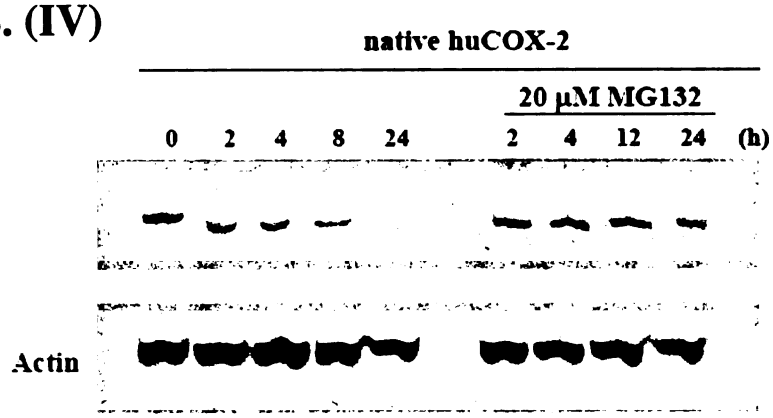

C.

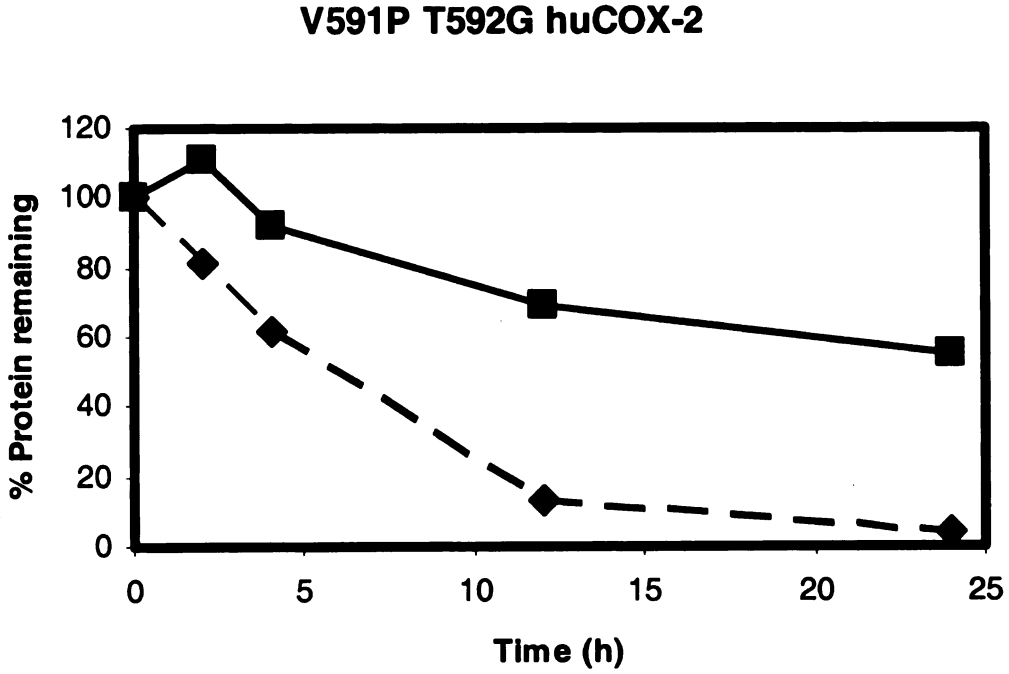

No protease inhibitor

20 μM MG132

22C. (cont'd)

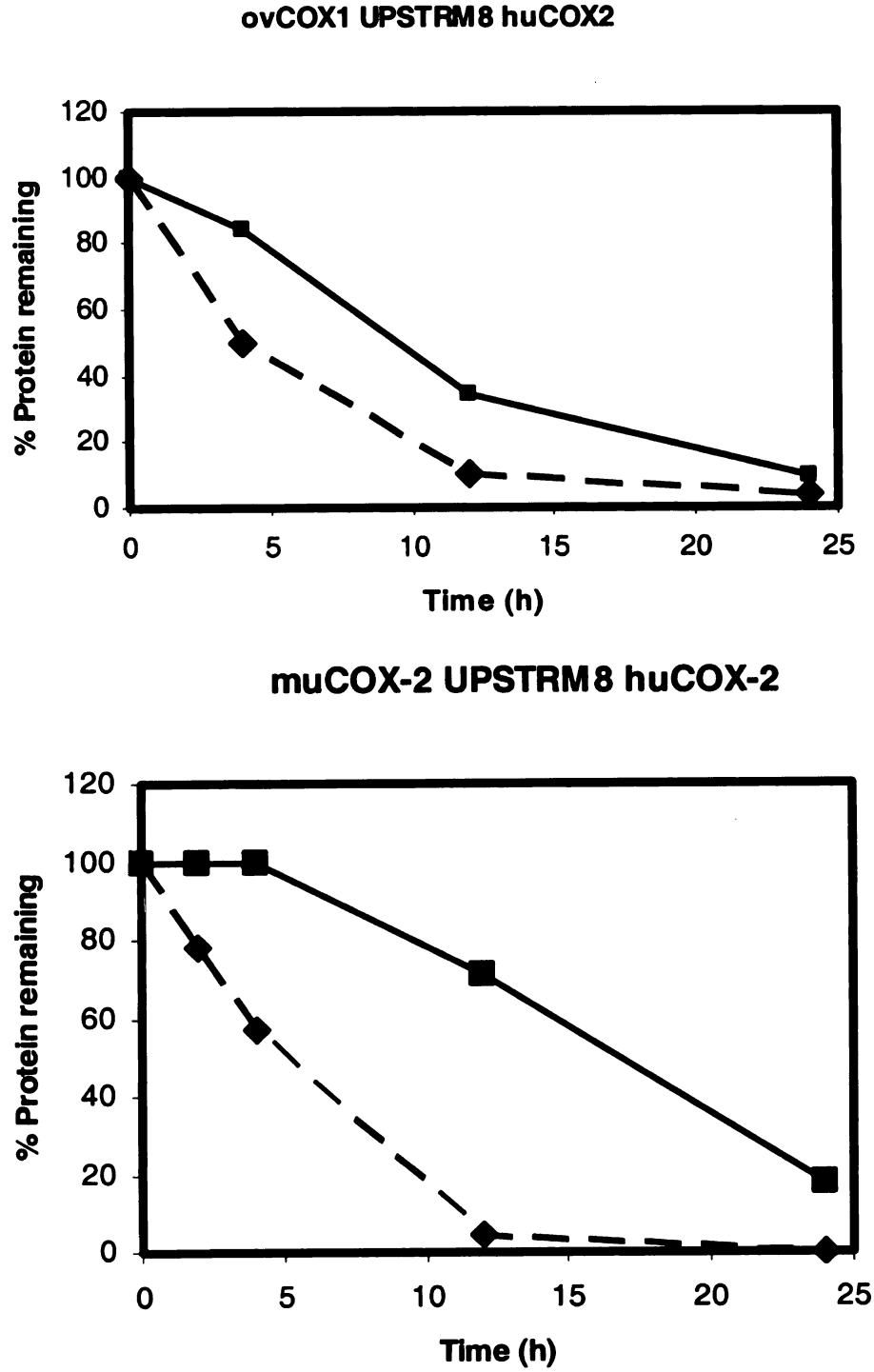
ovCOX1 UPSTRM8 huCOX2
% Protein remaining
120
100
80
60
40
20
0
0
5
10
15
20
25
Time (h)
muCOX-2 UPSTRM8 huCOX-2
% Protein remaining
120
100
80
60
40
20
0
0
5
10
15
20
25
Time (h)
No protease inhibitor
20 μM MG132

22C. (cont'd)

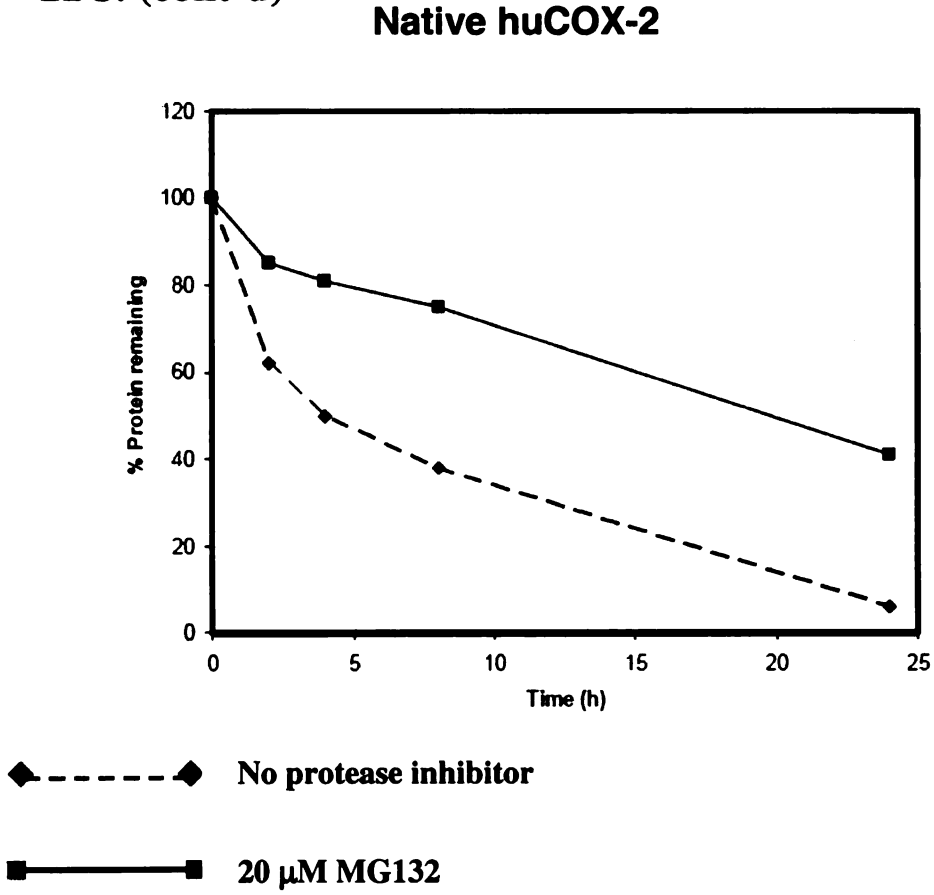

Figure 22. Asn-594 glycosylation of the UPSTRM8 huCOX-2 mutants and their degradation by the ERAD pathway. *A (I)* and *(II)*, The expression of native huCOX-2 or the UPSTRM8 huCOX-2 mutants was induced with 10 μg/ml tetracycline for 24 h. After protein induction cells were incubated for an additional 12 h in normal culture medium with or without 25 μM KIF. Thereafter, cell lysates were prepared and boiled in SDS sample loading buffer for 10 min and then treated with or without Endo H (0.4 mU/μl) for at least 12 h. Proteins were resolved by SDS-PAGE and subjected to Western blotting as in *18A*. Arrows indicate differences in molecular mass due to *N*-glycosylation. *B (I)*, *(II)*, *(III)*, and *(IV)*, HEK293 cells stably expressing the UPSTRM8 huCOX-2 mutants were grown to ~80% confluency, subjected to serum-starvation for 24 h, and then treated with 10 μg/ml tetracycline for 24 h. Puromycin (50 μM) was then added to block translation with or without additional treatment with 20 μM MG132. Thereafter, COX-2 and actin protein levels were analyzed at different times by Western blotting. Arrows indicate differences in molecular mass due to *N*-glycosylation. *C*, Quantitative analysis of the effect of 20 μM MG132 on the protein stability of native huCOX-2 and the UPSTRM8 huCOX-2 mutants.

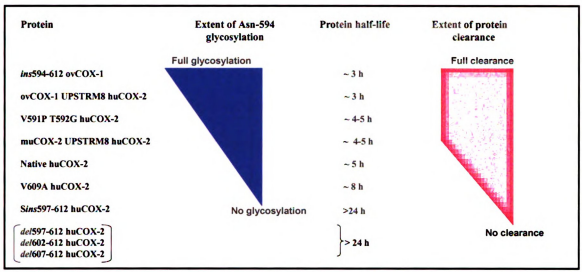

Table 2. Relationship between the extent of Asn-594 glycosylation and overall protein degradation. The extents of Asn-594 glycosylation and protein clearance are arbitrary and are based on Western blotting and densitometry data. Protein clearance is a relative measure of how much protein is remaining at the end of the 24 h experiment.

Discussion

Inhibiting the *N*-glycosylation of COX-2 during its synthesis and maturation in the ER severely compromises its catalytic activity (151). Therefore, co-translational *N*-glycosylation of COX-2 appears to be required for the proper folding of the enzyme. It is well known that there are ER-resident chaperones, namely calnexin and calreticulin, that associate with folding or misfolded glycoprotein substrates mainly by binding to their exposed *N*-linked oligosaccharide groups (166). Asn-594, the last *N*-glycosylation site of COX-2, is usually variably glycosylated (148,151,258), and is not required for the enzyme to achieve a catalytically competent conformation (151). Previously, we have shown that the Asn-594 glycosylation site is essential for the ER-associated degradation (ERAD) of COX-2 (257). In the present study, we have addressed the question of whether glycosylation of Asn-594 is essential for enabling COX-2 ERAD. We provide evidence that Asn-594 glycosylation is regulated by interplay of an upstream segment, approximately 8 residues long and a downstream 16-residue sequence that forms part of the 19-aa cassette. Furthermore, we observed a positive correlation between the extent of Asn-594 glycosylation and the overall degradation of the protein (Table 2). This is based on the following findings: a) 19-aa deletion mutants of huCOX-2 that have an intact Asn-594 glycosylation site but lack various portions of the 19-aa appear not to be glycosylated at Asn-594 and are completely stable; b) scrambling the 16-amino acid sequence downstream of the Asn-594 glycosylation site prevents glycosylation of Asn-594 and yields a mutant that is degraded much slower than native COX-2; c) inserting the huCOX-2 19-aa near the C-terminus of ovCOX-1 results in the complete glycosylation of Asn-594, and the COX-1 mutant has a shorter $t_{1/2}$ (~3 h) compared to native huCOX-2

(~5 h)(257); and d) replacing the 8-residue sequence immediately upstream of Asn-594 in huCOX-2 with the corresponding region of ovCOX-1 facilitates Asn-594 glycosylation concomitant with a shorter $t_{1/2}$ (~ 3 h) and more effective clearance of the protein.

Both the 72 and 74 kDa alternatively glycosylated forms of COX-2 can be readily detected by immunoblotting in various cell types, including NIH/3T3 fibroblasts and RAW264.7 macrophages. However, heterologous expression of recombinant huCOX-2 in HEK293 cells yields predominantly the 72 kDa form. The 74 kDa Asn-594-glycosylated huCOX-2 form can be detected in these cells after treatment with kifunensine (KIF), an inhibitor of ER α1,2 mannosidase I, which we have shown to stabilize COX-2 (257). ER α1,2 mannosidase I catalyzes the committed step in the ERAD pathway (259,260). Its activity releases irreversibly misfolded glycoproteins from the calnexin/calreticulin folding cycle by cleaving a single mannose residue from an *N*-linked $Man_9GlcNAc_2$ (198-200). A putative Man_8-binding lectin Yos9p or the ER-degradation mannosidase I-like protein (EDEM) will bind $Man_8GlcNAc_2$ and facilitate the delivery of protein having a processed *N*-glycan to a membrane retrotranslocon for export out of the ER and into the cytosol for proteasomal degradation (201-204,206,207,248). The identity of this membrane retrotranslocon has not been determined. KIF inhibition of ER α1,2 mannosidase I prevents the retrotranslocation and proteasomal degradation of aberrant glycoproteins by causing them to be retained in the ER (199,200,248-251). Since KIF inhibits COX-2 degradation and leads to accumulation of the Asn-594 glycosylated form of the enzyme in HEK293, NIH/3T3, and RAW264.7 cells, we reason that COX-2 ERAD requires Asn-594 glycosylation and subsequent processing of the attached *N*-glycan group by ER α1,2 mannosidase I.

Even though ERAD is considered to be an ER quality control mechanism for the elimination of aberrantly folded glycoproteins, COX-2 appears to be degraded from a properly folded conformation. Sifers and co-workers have proposed that glycoprotein ERAD (GERAD) requires at least two signal determinants: a) an *N*-glycan component, and b) non-native protein structure (259). Their proposal is based on the observation that inhibiting the glycosylation of misfolded glycoproteins prevents their degradation (261). However, it is still unclear how GERAD quality control is able to selectively eliminate terminally defective glycoproteins while sparing folding glycoproteins that have yet to achieve their native protein structure. It is possible that the intimate physical interaction of folding glycoproteins with ER resident molecular chaperones protects them from being degraded. Taking into consideration both the criteria for GERAD and our overall findings, we provide a model for the initiation of COX-2 degradation by Asn-594 glycosylation (Figs 23, 24, and 25). In this model, COX-2 synthesis and maturation in the ER involves co-translational glycosylation of its first three *N*-glycosylation sites, but not Asn-594. Glycosylation of these sites as the COX-2 nascent protein grows from the Sec61 translocon would serve the purpose of recruiting the chaperones calnexin and/or calreticulin to assist in protein folding. COX-2 maturation also entails formation of disulfide bonds, membrane insertion, heme incorporation, and assembly into a homodimer. This yields a catalytically competent COX-2 having an Asn-594 site that may not be easily accessible for glycosylation because it is situated in an ordered helix (helix A) such that its amide group is protected by an adjacent helix (helix B) ~4.5 Å away. A disulfide bridge between Cys-569 of helix B and Cys-575 of a 15-residue loop connects helices A and B. This covalent modification may further contribute to

constraining helix A into a conformation which prevents glycosylation of Asn-594. However, this disulfide bridge is also present in COX-1 and we have found that the COX-1 insertion mutant *ins*594-612 ovCOX-1 appears to be fully glycosylated at Asn-594. Therefore, we propose that the degradation of COX-2 is initiated by a local conformational change in the helix A-loop-helix B region that enables the post-translational glycosylation of the protein at Asn-594. This conformational change probably involves the last 16 amino acids of the 19-aa cassette since this region appears to be required for Asn-594 to become glycosylated. The mechanism by which the C-terminal 16 amino acid segment of 19-aa promotes glycosylation of Asn-594 is yet to be determined. It is possible that after this putative loop region may form hydrophobic and electrostatic interactions with helix A, thereby, causing helix A to change conformation so that it is no longer stacked against helix B. Alternatively, the C-terminal 16 amino acids of 19-aa may serve as a docking site for a protein complex that will remodel the helix A-loop-helix B region so that the side chain of Asn-594 is exposed for glycosylation. Based on our experimental results, it is unlikely that cleavage of the disulfide bridge between the intervening loop and helix B is required for Asn-594 to become glycosylated. Otherwise, one of the proteins in this complex may be a protein disulfide isomerase that would catalyze the breakage of the disulfide bond between the loop and helix B. Oligosaccharyltransferase (OST) could also be part of this complex. Since OST is a membrane-bound complex that is associated with the protein translocon

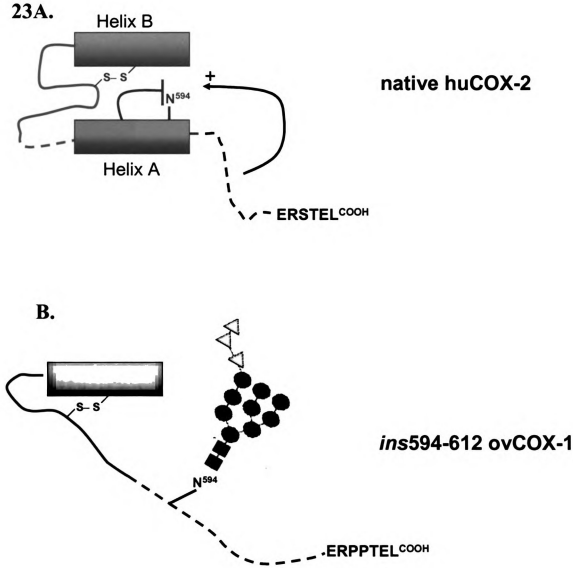

Figure 23. Schemes illustrating how the C-terminus of COX-2 may regulate Asn-594 glycosylation. *A*, In native huCOX-2, Asn-594 glycosylation may be hindered by the ordered helical conformation of the region immediately upstream of Asn-594. The C-terminal 16 amino acid segment of 19-aa appears to promote glycosylation of Asn-594. *B*, Since *ins*594-612 ovCOX-1 lacks secondary structure in the vicinity of Asn-594, this residue is easily accessible to glycosylation. Asn-594 glycosylation of *ins*594-612 ovCOX-1 may not require reduction of the disulfide bond. The green continuous line represents the loop that is resolved in the X-ray structures of muCOX-2 and ovCOX-1. The green dashed line is the putative loop region upstream of Asn-594 that is not resolved in either isoform. The black dashed line represents the C-terminal 16-amino acid segment of 19-aa.

24.

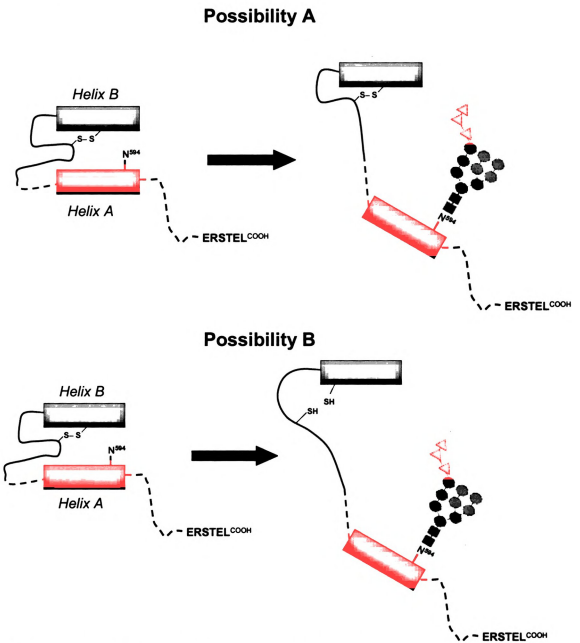

Figure 24. Two possibilities of how Asn-594 of native huCOX-2 may become accessible to glycosylation. The loop region from Cys-575 to helix A could be long and flexible enough to enable movement of helix A to permit Asn-594 glycosylation (Possibility A). Alternatively, reduction of the disulfide bond may also be needed to sufficiently expose Asn-594 for glycosylation (Possibility B). In either case, the C-terminal 16 amino acid segment of 19-aa would be required to mediate Asn-594 glycosylation.

25.

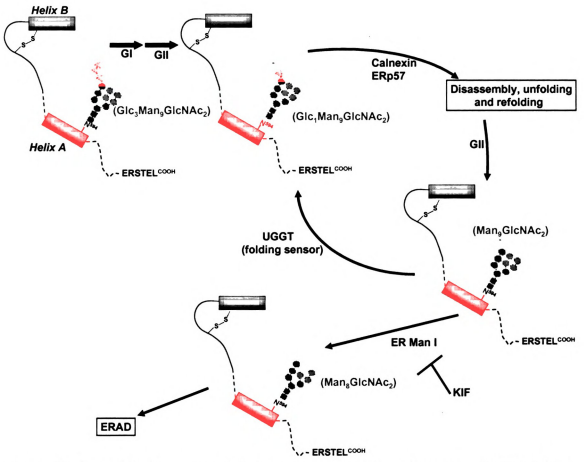

Figure 25. A model of how Asn-594 glycosylation mediates the entry of COX-2 into the ERAD pathway. An *N*-glycan group consisting of $Glc_3Man_9GlcNAc_2$ is transferred *en bloc* from ER membrane-bound dolichol pyrophosphate to Asn-594. This occurs after the helix A-loop-helix B region has been remodeled to permit glycosylation. The remodeling process could be mediated by a complex of proteins that dock onto the 16-amino acid segment of 19-AA. Glucosidases I and II (GI and GII) will cleave off the two terminal glucose residues leaving a monoglucosylated *N*-glycan that is specifically recognized by calnexin, a membrane-bound lectin binding chaperone. The heterodimer complex of calnexin and ERp57 will participate in the disassembly, unfolding, and refolding of the protein in an attempt to correct the structural modification to the native enzyme. The protein will be maintained in the calnexin cycle by the actions of GII and the folding sensor and glucosyltransferase UGGT. Since COX-2 is irreversibly glycosylated at Asn-594, the protein will eventually be released from the calnexin cycle by ER α1,2 mannosidase I (ER Man I) which cleaves off the α1,2-linked mannose to form $Man_8GlcNAc_2$. This will initiate ERAD of Asn-594 glycosylated COX-2. Processing of the $Man_9GlcNAc_2$ oligosaccharide group by ER Man I is the committed step of ERAD and is inhibited by KIF.

(262,263), the C terminal region of mature COX-2 has to be in the vicinity of the membrane for Asn-594 to become post-translationally glycosylated. Introduction of the local conformational change in the helix A-loop-helix B region and the subsequent glycosylation of Asn-594 may constitute the signals needed to initiate COX-2 GERAD.

The above model for COX-2 degradation could be tested in several ways. We have preliminary evidence that COX-2 undergoes post-translational glycosylation at Asn-594. This is based on the observation that in addition to preventing COX-2 ERAD in HEK293 cells, KIF treatment causes the accumulation of what appears to be the Asn-594 glycosylated form, even in the absence of protein synthesis; this COX-2 glycosylated form is barely detectable in untreated HEK293 cells. Accumulation of the 74 kDa Asn-594 glycosylated form of COX-2 in KIF-treated cells may inhibit further glycosylation of Asn-594. This would explain why KIF also stabilizes the 72 kDa form of the native enzyme. To the best of our knowledge, the only published report of post-translational *N*-glycosylation is that of the secretory glycoprotein human coagulation factor VII (FVII). FVII has two consensus glycosylation sites, and, like COX-2, exists as two alternatively glycosylated forms of 54 and 56 kDa (264). Using ^{35}S pulse chase analysis, Steenstrup and co-workers elegantly demonstrated that the 54 kDa form is a precursor for the 56 kDa form, and by Endo H treatment were able to show that the difference between the two forms was due to *N*-glycosylation. Similarly, it will be important to perform ^{35}S pulse chase analysis to confirm that the 72 kDa form of COX-2 is indeed the precursor for the 74 kDa form in KIF-treated cells. It would also be interesting to examine the effect of mutagenesis of Cys-575 on the extent of Asn-594 glycosylation and the overall degradation of COX-2.

In conclusion, we have identified a potential mechanism for the initiation of COX-2 ERAD that involves Asn-594 glycosylation, its negative regulation by an 8-residue segment that is immediately upstream, and its positive regulation by the last 16 amino acids of the 19-aa cassette. The upstream 8-residue sequence may also play a role in the processing of the *N*-glycan group at Asn-594 that preceeds translocation of COX-2 to the cytoplasm for proteasomal degradation. We reason that both the 19-aa cassette and the upstream 8-residue sequence form a 27 amino acid sequence that constitutes the instability element responsible for controlling the intracellular stability of COX-2.

Acknowledgments

We thank Dr. Randal Kaufman and Dr. Billy Tsai for helpful suggestions relevant to this study.

CHAPTER IV

SUBSTRATE DEPENDENT COX-2 PROTEIN DEGRADATION

Summary

Cyclooxygenases (COX-1 and COX-2) catalyze the committed step in prostanoid synthesis. Previously, we showed that the unique C-terminal 19 amino acid cassette of COX-2 enables degradation of this COX isoform in a proteasome-dependent manner. Here, we demonstrate that COX-2 degradation in NIH/3T3 and HEK293 cells is enhanced by treatment with exogenous arachidonic acid (AA) at concentrations as low as 5-20 μM. At similar concentrations AA did not cause significant COX-1 degradation in either cell type. Endogenous COX-2 degradation in serum-treated NIH/3T3 cells was enhanced by treatment with 10 μM calcium ionophore (A23187) and was almost completely blocked by cyclooxygenase (COX) inhibitors. AA-induced COX-2 degradation was retarded by COX inhibitors. The 26S proteasome inhibitor MG132, which blocks basal COX-2 protein turnover in HEK293 cells, did not affect the AA-dependent degradation of the protein. Moreover, AA-dependent degradation of COX-2 occurred independently of its C-terminal 19 amino acid cassette. Only fatty acid substrates of COX-2 were able to enhance degradation. Also, a G533A COX-inactive point mutant of COX-2 was resistant to AA-induced degradation even though it underwent substrate-independent degradation at the same rate as native COX-2. Loss of COX specific activity and prostaglandin product formation was also observed in COX-2-expressing cells treated with AA. We propose that substrate-dependent inactivation of

COX-2 causes structural damage to the enzyme that subsequently leads to its degradation.

Introduction

Cyclooxygenases-1 and -2 (COX-1 and COX-2) are membrane-bound, ER-resident hemoproteins that catalyze the committed step in prostanoid synthesis (1,3,7,17,150). Although encoded by different genes, COX-1 and COX-2 are structural isoforms that share ~60% identity in primary structure. COX-1 is a stable protein that is constitutively expressed in resting cells of many tissues, most notably in platelets and vesicular gland (1,257,265,266). In contrast, COX-2 is a stimulus-inducible protein that is quite unstable and whose expression is observed to be short-lived in epithelial, endothelial, smooth muscle, and fibroblast cells (20,21,23,24,257). The short half-life of COX-2 protein mimics that of the COX-2 mRNA. Both the COX-2 mRNA and protein have been found to possess instability elements that target them for rapid degradation. At the 3' untranslated region (UTR) of COX-2 mRNA are multiple AUUUA elements that are known to target the message for rapid exonuclease cleavage (20,129). COX-1 mRNA lacks these 3' UTR AU-rich elements which would explain the prolonged expression of COX-1 mRNA in megakaryocytes and vascular endothelial cells (117,118,267). We have recently reported that a unique C-terminal 19-amino acid insertion near the C-terminus of COX-2 confers the enzyme with a short half-life by rapidly and selectively initiating its proteasomal degradation (257). This cassette is part of a larger 27 amino acid sequence that appears to be essential for directing ER-associated degradation of the enzyme. It could therefore be postulated that the evolution of COX-2 must have entailed the

development of post-transcriptional and post-translational mechanisms that contribute to the sophisticated tight regulation of the synthesis of COX-2-derived prostanoids.

The principal endogenous fatty acid substrate of COX-1 and -2 is arachidonic acid ($20:4^{\Delta 5,8,11,14}$) which is mobilized from the *sn*-2 position of membrane phospholipids upon the activation of cytosolic phospholiase $A_2\alpha$ ($cPLA_2\alpha$) with bradykinin, thrombin, growth factors, calcium ionophore, or cytokines (1,3,8,36-41,43). The cyclooxygenase isoforms have two catalytic activities that occur at two spatially distinct active sites. At the cyclooxygenase (COX) active site, arachidonic acid (AA) is oxygenated to form the hydroperoxide and endoperoxide prostaglandin G_2 (PGG_2) (1,3,7). This prostaglandin intermediate is then moved to the peroxidase (POX) site where its hydroperoxy group undergoes a two-electron reduction to form the alcohol prostaglandin H_2 (PGH_2) (1,3,7,156). PGH_2 is a common substrate for downstream terminal prostanoid synthases that act upon it differently to form various prostanoids.

The POX and COX activities of COX-1 and -2 undergo irreversible suicide inactivation *in vitro* during catalysis. POX and COX self inactivation is mechanism-based because it proceeds from heme and tyrosyl radical intermediates that are formed during the POX and COX reactions, respectively (3,156). The specific structural changes in the holoenzyme that lead to suicide inactivation remain unknown. Mevkh *et al.* noted that COX-1 self inactivation is accompanied by dramatic changes in protein structure as is manifested by the increased susceptibility of the inactive enzyme to trypsin cleavage and the increased number of exposed histidine residues subject to chemical covalent modification (162). It has not been established whether the COXs can undergo suicide inactivation *in vivo*. If so, this could serve as an additional regulatory mechanism for

prostanoid synthesis. In this regard it would be interesting to investigate whether the inactive forms of COX-1 and -2 are more susceptible to degradation compared to the native forms. It is well established that misfolded or structurally damaged proteins that are present in the ER can be targeted for degradation by a process known as ER-associated degradation (ERAD) (164-166,182-186). It is possible that COX-2 might selectively undergo suicide inactivation at endogenous hydroperoxide or AA levels that would be insufficient to inactivate COX-1. If indeed the inactive protein gets degraded, this could partly explain the short-lived nature of COX-2 protein. The present study examined the impact of COX catalysis *in vivo* on the protein stabilities of COX-1 and COX-2. We demonstrate that COX-2 protein degradation that is mediated by the C-terminal 19 amino acid insertion can be substantially enhanced by COX substrates in NIH/3T3 and HEK293 cells in a proteasome-independent manner. We also provide evidence that substrate-dependent degradation of COX-2 requires a functional COX active site and proceeds from substrate-induced inactive forms of the enzyme.

Experimental Procedures

Materials. Dulbecco's modified Eagle's medium (DMEM), fetal bovine serum (FBS), ponasterone A, and tetracycline were obtained from Gibco/Invitrogen. Bovine calf serum (BCS) was from Hyclone. Arachidonic acid (AA), eicosapentaenoic acid (EPA), eicosadienoic acid (EDA), oleic acid (OA), linoleic acid (LA), 2-arachidonoyl glycerol ether (2-AG ether), dihomo-γ-linolenic acid (DHLA), (R/S)-flurbiprofen, (S)-flurbiprofen, (R)-flurbiprofen, and NS-398 were from Cayman Chemicals. (S)-flurbiprofen and NS-398 are time-dependent, irreversible inhibitors of cyclooxygenase (COX) activity whereas (R)-flurbiprofen is a competitive COX inhibitor. Cycloheximide, puromcyin, and glutathione (GSH) were purchased from Sigma. Calcium ionophore (A23187), bradykinin, and MG132 were purchased from Calbiochem. [1-^{14}C] arachidonic acid (55 mCi/mmol) was from American Radiolabeled Chemicals. Microsomal PGES-1 (mPGES-1) was kindly provided by Dr. Michael Garavito of Michigan State University.

Construction of Plasmids for Transfection. Recombinant ovine (ov) COX-1 cDNA and N-terminal hexahistidine-tagged ovCOX-1 cDNA were subcloned into pIND (Invitrogen). cDNAs for human (hu) COX-2, N-terminal hexahistidine-tagged huCOX-2, and N-terminal hexahistidine-tagged murine (mu) COX-2 were subcloned into pcDNA5/FRT/TO (Invitrogen). pIND is ecdysone-inducible whereas pcDNA5/FRT/TO is tetracycline-inducible. After subcloning, the Quick-Change™ site-directed mutagenesis kit (Stratagene) was used to create the following huCOX-2 mutants: G533A huCOX-2, N594A huCOX-2, and *del*595-612 huCOX-2. Correct cDNA orientation and mutations were confirmed by sequencing.

Cell Culture and Transfection. NIH/3T3 fibroblasts at early passage (<6 passages) were cultured in DMEM supplemented with 10% BCS and 100 u/ml penicillin/streptomycin. To induce COX-2 expression, the cells were first made quiescent by serum starvation for 48 h in DMEM containing 0.2% BCS and thereafter treated with DMEM supplemented with 20% FBS for 4 h.

Stable HEK293 transfectants of native or mutant COX-2 constructs were generated using the Flp-In T-Rex tetracycline-inducible expression system (Invitrogen). Native ovCOX-1 or His-tagged ovCOX-1 were stably transfected into the ecdysone-inducible expression system (Invitrogen). All these transfections were conducted according to the manufacturer's protocol. Stably transfected HEK293 cells were cultured in DMEM supplemented with 10% FBS, 100 u/ml penicillin/streptomycin, and the appropriate pharmacological selective reagents. Inducible expression was achieved by a 24 h serum starvation in serum-free medium followed by treatment with 10 μg/ml tetracycline or 10 μM ponasterone A (ecdysone analog) for an additional 24 h in normal culture medium.

Fatty acid and Drug Treatments. Quiescent 3T3 cells were serum-stimulated for 4 h then treated with 50 μM cycloheximide (CHX) or 50 μM puromycin for different times in the presence or absence of 20 μM arachidonic acid (AA), 100 μM flurbiprofen (FB), 20 μM NS-398, or a combination of 20 μM AA and one of the following: 100 μM flurbiprofen (FB), 20 μM NS-398, or 20 μM MG132. Alternatively, after serum-stimulation the cells were treated for different times with 50 μM cycloheximide (CHX) or 50 μM puromycin in the presence or absence of 10 μM A23187 or 10 μM bradykinin with or without 100 μM flurbiprofen , 20 μM NS-398, or 20 μM MG132.

HEK293 cells inducibly expressing wild-type or mutant cyclooxygenase constructs were grown to 80% confluency, serum-starved for 24 h, and then treated with 10 μg/ml tetracycline or 10 μM ponasterone A in complete culture medium for 24 h to induce expression. Afterwards, the cells were incubated for various times with 50 μM puromycin to block translation in the absence or presence of the polyunsaturated fatty acids AA, EPA, EDA, 2-AG ether, LA, DHLA, OA, or the COX inhibitor flurbiprofen. To examine the effect of COX, proteasome, lysosomal, and ER to Golgi trafficking inhibitors on AA-induced protein turnover, cells expressing native huCOX-2, *del*594-612 huCOX-2, or N594A huCOX-2 were treated for 4 h with 50 μM puromycin with or without AA in combination with one of the following: 20 μM MG132, 100 μM flurbiprofen, 50 μM (S)-flurbiprofen, 50 μM (R)-flurbiprofen, 20 μM NS-398, 50 μM leupeptin, 25 μM E64, or 5 μg/ml brefeldin A.

Microsome Preparation and Trypsin Cleavage. HEK293 cells stably expressing *del*595-612 huCOX-2 or N594A huCOX-2 were lysed by sonication in 0.1 M Tris-Cl buffer, pH 8.0. The lysates were centrifuged at 5,000 rpm for 10 min at 4°C to precipitate unbroken cells. Thereafter, microsomes were prepared by ultraentrifugation at 55,000 rpm for 1 h at 4°C. The microsomes were resuspended in 0.1 M Tris-Cl buffer, pH 8.0 and 200 μg of this resuspension was incubated in a 100 μl reaction mixture containing 0.1 M Tris-Cl, pH 8.0, 10 μM hematin, and 1 mM phenol in the absence of substrate, or with 100 μM AA, or a combination of 100 μM AA and 100 μM FB. The incubation was performed at 37°C for 4 h. 100 μg of microsomes were treated with 5 μg trypsin before or after solubilization with 1% Tween-20. Trypsin treatment was performed at 37°C for 20 min.

Western Transfer Blotting. After the appropriate treatments, NIH/3T3 and HEK293 cells were harvested by centrifugation at 2000 rpm for 3 min. Cell pellets were stored at -80°C until needed. RIPA lysis buffer (10 mM Tris, pH 7.2, 150 mM NaCl, 5mM EDTA, 0.1% SDS, 1.0% Triton X-100, 1% deoxycholate) containing a protease inhibitor cocktail (Roche Applied Science) was used for cell lysis. Protein concentrations were determined using the BCA protein assay kit (Pierce). The NuPAGE system (Invitrogen) was used to resolve the proteins in the whole cell lysates on a 7% tris-acetate polyacrylamide gel. After transfer to a nitrocellulose membrane, immunoblotting was performed with the appropriate primary antibody. Horseradish peroxidase-conjugated anti-rabbit or anti-mouse IgG antibodies (Bio-Rad) were used as secondary antibodies. Immunodetection was performed using the Western Lighting Chemiluminescent kit (Amersham Biosciences) followed by exposure to X-ray film. Densitometry analysis was performed using Quantity One software (Bio-Rad).

Cyclooxygenase Inactivation Assay. Cultured HEK293 cells stably expressing His-tagged ovCOX-1 or His-tagged muCOX-2 were incubated for 10 min with different concentrations of AA ranging from 2.5 μM to 50 μM. After incubation the cells were washed with 1X PBS (phosphate buffered saline) and harvested by centrifugation at 2000 rpm for 3 min. Cell pellets were resuspended in 0.1 M Tris, pH 8.0 buffer containing 1 mM EDTA and a protease inhibitor cocktail and lysed by sonication. Protein concentration in the lysates was determined by BCA assay (Pierce). COX activity assays were performed at 37°C by monitoring the initial rate of oxygen uptake using an oxygen electrode as described previously (268). Reactions were initiated by adding cell lysate to

the assay chamber containing 3 ml of 0.1 M Tris-HCl, pH 8.0, 1 mM phenol, 5 μM hematin, and 100 μM AA.

Microsomes were prepared from the lysates of His muCOX-2-epxressing cells by ultracentrifugation at 55,000 rpm for 1 h at 4°C. The microsomes were resuspended in 0.1 M Tris-HCl, pH 8.0 containing 1 mM EDTA and 20% glycerol and a BCA assay (Pierce) was perfomed to determine protein concentration. The microsomal fractions were then used to perform COX radioactive TLC assays to examine COX product formation as previously described (269). Briefly, microsomes (0.5 mg) were incubated in a 100-μl reaction mixture containing 0.1 M Tris-HCl, pH 8.0, 1 mM phenol, 10 μM hematin, and 10 μM [1-^{14}C]arachidonic acid at room temperature for 1 min. To assay for PGE_2 formation microsomal PGES-1 (mPGES-1) and 60 μM GSH were included in some of the reaction samples. The reactions were terminated by adding 300 μl of an ice-cold mixture of ethylether, methanol, and 0.2 M citric acid (30:4:1). The organic phase of the reaction mixture, containing the radioactive products, was isolated and applied directly onto a TLC silica plate at 4°C. The plate was developed in ethyl acetate, 2,2,4-trimethylpentane, acetic acid, and water (110:50:20:100) and exposed to x-ray film, and radioactive products were visualized by autoradiography.

Results

COX Inhibitors Retard COX-2 Degradation in NIH/3T3 cells. About nine years ago Smith and co-workers made the interesting finding that serum-stimulating quiescent NIH/3T3 cells in the presence of the non-selective NSAIDs flurbiprofen and aspirin, or the COX-2 selective inhibitor NS-398 dramatically enhanced inducible COX-2 protein expression without affecting COX-2 mRNA levels ((14), Arakawa and Smith, unpublished results). In contrast, constitutive COX-1 protein expression was not affected. These results suggested that COX inhibitors promote the stability of COX-2 protein in NIH/3T3 cells by preventing the degradation of the enzyme. After successfully reproducing these findings (Fig. 26*a*) I tested hypothesis that NSAIDs inhibit the rapid degradation of COX-2. In a cycloheximide chase experiment (R/S)-flurbiprofen, (R)-flurbiprofen, and (S)-flurbiprofen nearly completely retarded COX-2 degradation in NIH/3T3 cells within the time frame of the experiment (Fig. 26*b*). There is no evidence to date that NSAIDs directly inhibit the 26S proteasome. Since proteasome inhibitors partly inhibit COX-2 degradation in 3T3 cells (257), my findings suggest the possibility of a second non-proteasome-dependent pathway for COX-2 protein turnover. Moreover, flurbiprofen inhibits COX-2 degradation in 3T3 cells to a greater extent than the proteasome inhibitors MG132 and epoxomicin (data not shown). Therefore, it is likely that COX inhibitors prevent both the proteasomal and non-proteasomal degradation of COX-2 in 3T3 cells.

Proteasomal Degradation of COX-2 in HEK293 cells is not inhibited by NSAIDS. We have previously reported that heterologously expressed COX-2 undergoes proteasomal degradation in HEK293 cells in a manner that is dependent upon the C-

terminal 19 amino acid cassette of the protein (257). To determine if COX inhibitors stabilize COX-2 in HEK293 cells, COX-2 protein degradation was examined in these cells in the presence or absence of treatment with 20 μM NS-398 or 100 μM flurbiprofen. We were surprised to find that, unlike 3T3 cells, neither NS-398 nor flurbiprofen significantly stabilized COX-2 in HEK293 cells (Fig 26*c*). Furthermore, inducible COX-2 expression in these cells was not enhanced by treatment with 20 μM NS-398 (Fig. 26*d*).

Serum-stimulation of quiescent 3T3 cells results in the coordinate induction of COX-2 and the mobilization of free AA due to activation of $cPLA_2\alpha$ (77). Therefore, it is reasonable to expect that serum-treatment of quiescent 3T3 cells will stimulate COX-2 COX catalysis. During catalysis COX-2 may undergo suicide inactivation, a process that could initiate the rapid degradation of the enzyme. Resting HEK293 cells lack detectable phosholipase A_2 activity so that heterologously expressed COX-2 is more likely to be in its latent form (33,58). This may explain the discrepancy that is observed in the two cell lines with respect to the effect of COX inhibitors on COX-2 protein turnover. It is possible that COX-2 is degraded in serum-treated 3T3 cells by at least two distinct mechanisms: (a) COX substrate-induced protein turnover which is inhibited by COX inhibitors; and (b) a proteasome-dependent basal degradation of the resting enzyme that is directed by the C-terminal 19 amino acid cassette.

Substrate-dependent Degradation of COX-2. To test the hypothesis that COX fatty acid substrates can induce COX-2 protein turnover, we analyzed the effect of treatment with exogenous AA on the degradation of native huCOX-2, *del*595-612

26A.

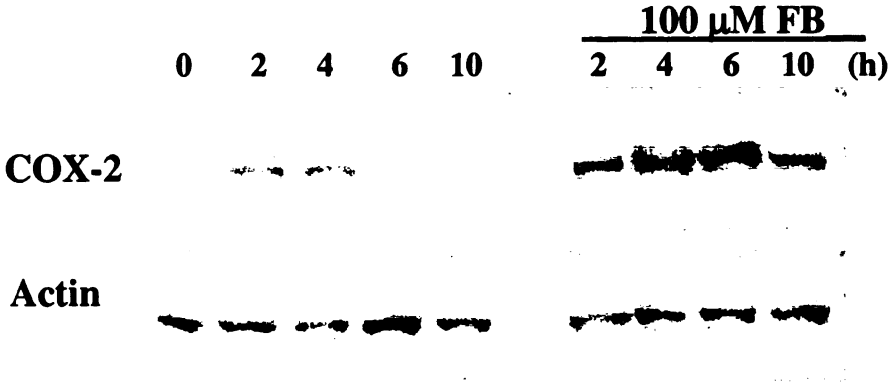
100 μM FB
0 2 4 6 10
2 4 6 10 (h)
COX-2
Actin

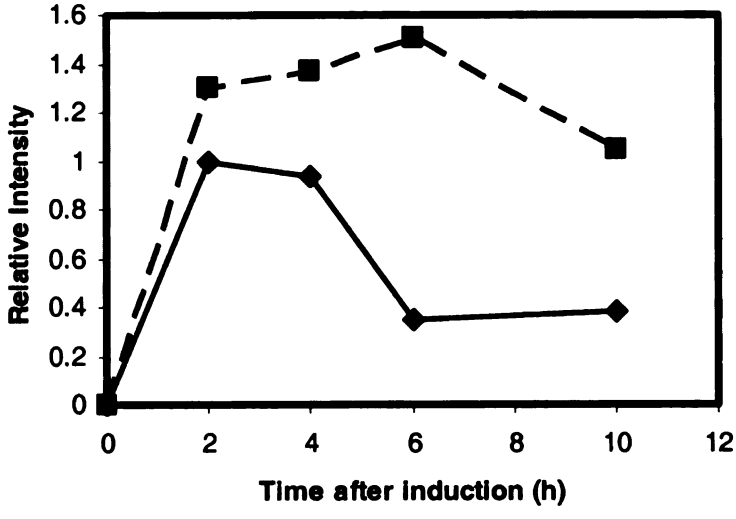
Relative Intensity
1.6
1.4
1.2
1
0.8
0.6
0.4
0.2
0
0 2 4 6 8 10 12
Time after induction (h)

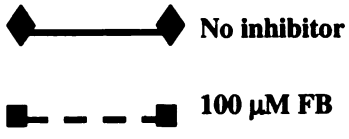
No inhibitor
100 μM FB

26B.

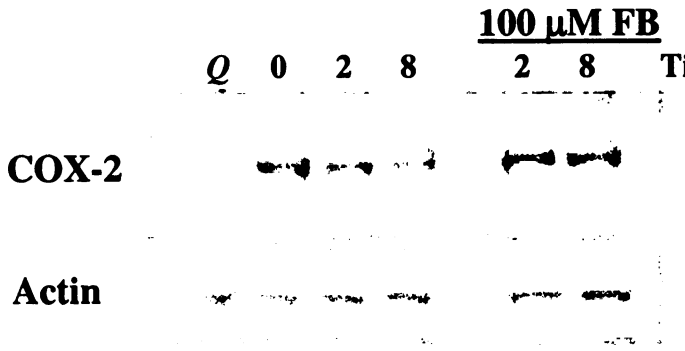

	100 μM FB				
	0	2	8	2	8 (h)
Densitometry (%)	100	58	35	102	103

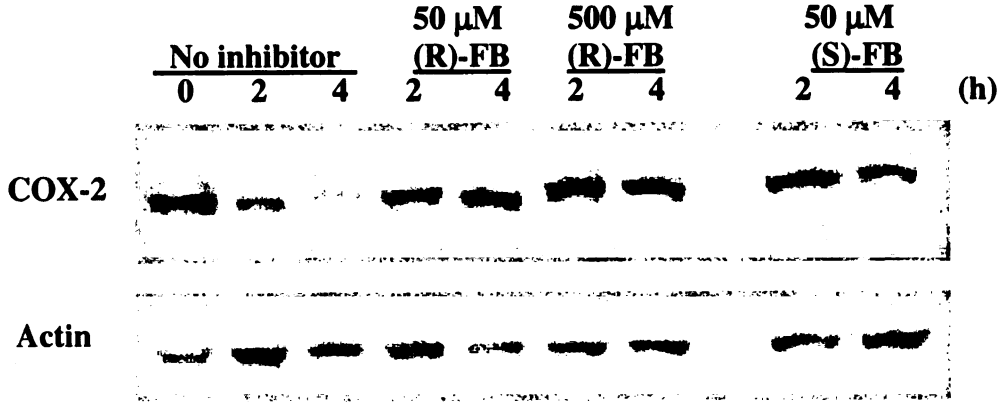

	0	No Inhibitor		50 μM (R)-FB		500 μM (R)-FB		50 μM (S)-FB		
		2	4	2	4	2	4	2	4	(h)
Densitometry (%)	100	39	36	65	83	80	69	65	48	

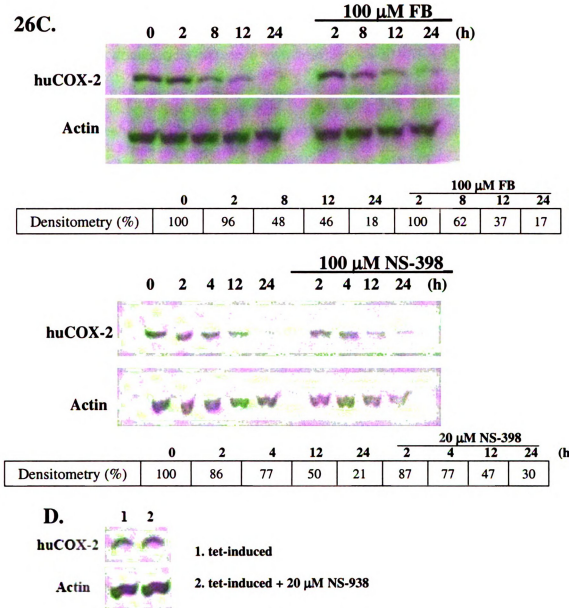

Figure 26. Cyclooxygenase inhibitors prevent the rapid degradation of COX-2 in serum-treated NIH/3T3, but not HEK293, cells. (A) NIH/3T3 cells were made quiescent by 48 h serum-starvation and serum-induced for different times in the absence or presence of 100 μM flurbiprofen (FB). (B) Quiescent (*Q*) 3T3 cells were serum-induced for 4 h then treated with 50 μM cycloheximide (CHX) with or without 100 μM FB, 50 μM (R)-FB, 500 μM (R)-FB, or 50 μM (S)-FB. (C) HEK293 cells stably expressing huCOX-2 were serum-starved for 24 h and treated with 10 μg/ml tetracycline in normal complete medium for an additional 24 h to induce COX-2 expression. Upon COX-2 induction, cells were treated with 50 μM puromycin to block translation with or without 100 μM FB or 20 μM NS-398. (D) COX expression was induced in HEK293 cells with tetracycline (tet) in the absence (1) or presence (2) of treatment with 20 μM NS-398. After the treatments in *(A)-(D)* the cells were harvested, lysed, and analyzed by Western blotting for COX-2 and actin.

huCOX-2, and N594A huCOX-2 in HEK293 cells. The basal degradation of native huCOX-2 was dramatically enhanced by treatment with 20 μM AA (Fig. 27*a*, panel *I*). An AA dose response of COX-2 degradation revealed that protein turnover could be substantially enhanced by fatty acid concentrations as low as 5 μM (Fig. 27*b*, panel *I*). The mutants *del*595-612 huCOX-2 and N594A huCOX-2, which are usually stable under basal conditions, also rapidly degraded upon treatment with 10 μM AA (Fig. 27*a*, panels *II* and *III*, and Fig. 27*b*, panel *II*). Therefore, substrate-induced degradation of COX-2 is not mediated by the C-terminal 19-amino acid cassette. Since removal of the cassette does not affect COX-2 catalytic activity, these results imply that substrate-induced degradation could be a consequence of substrate turnover at the COX active site. To test this hypothesis, we examined the effect of COX inhibitors on substrate-induced COX-2 degradation in HEK293 cells. We also analyzed a panel of polyunsaturated fatty acids only some of which are COX-2 substrates. Flurbiprofen, (R)-flurbiprofen, (S)-flurbiprofen, and NS-398 significantly blocked the AA-induced degradation of huCOX-2 in 293 cells (Figs. 27*c* and *d*). Moreover, these NSAIDS selectively inhibited COX-2 degradation that was substrate-dependent without affecting the basal degradation of the enzyme (Figs. 27*c* and *d*). In contrast, the degradation of *del*595-612 huCOX-2 and N594A huCOX-2, which was only observed upon exogenous AA treatment, was nearly completely blocked by flurbiprofen and (S)-flurbiprofen (Fig. 27*e*).

In order to be utilized as substrate by COX-2, exogenous AA would have to penetrate the cell, move to the ER membrane by diffusion or carrier-mediated transport, and be delivered to COX-2 on the luminal side of the membrane. This transport and delivery process should be very rapid since prostaglandin product formation is

known to reach a plateau within minutes after treatment with exogenous AA in cultured cells expressing COX activity (270). Therefore, a brief challenge of cells with exogenous AA should be sufficient to induce COX-2 degradation. HEK293 cells stably expressing huCOX-2 were exposed to 20 μM AA for 5 min or 4 h. After aspirating the AA-containing medium, cells that were treated for 5 min with AA were washed with 1X PBS then treated with the protein translation inhibitor puromycin with or without flurbiprofen for an additional 4 h. It was observed that regardless of the duration of AA treatment (5 min or 4 h), COX-2 degradation was enhanced to a similar extent (Fig. 27*f*). Flurbiprofen added after the 5 min treatment with AA did not protect the enzyme from degradation as well as when the inhibitor was added together with substrate. These observations indicate that a short-term incubation of cells with AA, during which prostaglandin products are expected to be formed, is sufficient to further destabilize COX-2.

Like native huCOX-2, the N-terminal hexahistidine (His_6)-tagged huCOX-2 was susceptible to AA-induced degradation that could be inhibited by NSAIDS (Figs. 28*a* and *b*). The IC_{50} values for the inhibition of huCOX-2 COX activity by flurbiprofen and NS-398 are 0.51 μM and 1.77 μM, respectively (271). I found that 10 μM FB and 500 nM NS-398 significantly inhibited the degradation of His_6-tagged huCOX-2 induced by 15 μM AA (Fig. 28*b*). Just like AA, the COX-2 polyunsaturated fatty acid (PUFA) substrates EPA and DHLA enhanced COX-2 degradation albeit at higher concentrations than AA (Figs. 28*c* and *d*, panel II). In contrast, 2-AG ether, a derivative of the COX-2 substrate 2-arachidonyl glycerol, and OA did not affect COX-2 protein turnover (Fig.28*d*, panels *II* and *III*). Similarly, LA and EDA which are known to be poor COX-2 substrates did not induce COX-2 degradation even at concentrations as high as 50-100 μM

27A. (I)

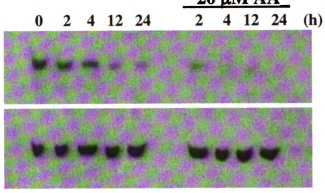
20 μM AA
0 2 4 12 24 2 4 12 24 (h)
huCOX-2
Actin

(II)

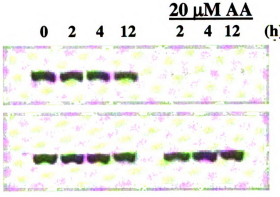
20 μM AA
0 2 4 12 2 4 12 (h)
del595-612 huCOX-2
Actin

(III)

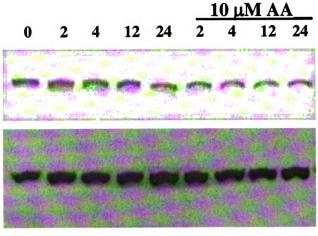
10 μM AA
0 2 4 12 24 2 4 12 24 (h)
N594A huCOX-2
Actin

27B. (I)

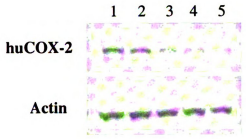

1. 24 h induction
2. " + 4 h puromycin
3. " + " + 5 μM AA
4. " + " + 10 μM AA
5. " + " + 20 μM AA

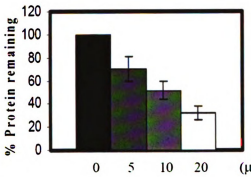

B. (II)

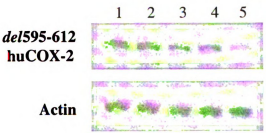

1. 24 h induction
2. " + 4 h puromycin
3. " + " + 5 μM AA
4. " + " + 10 μM AA
5. " + " + 20 μM AA

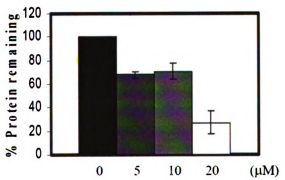

27C.

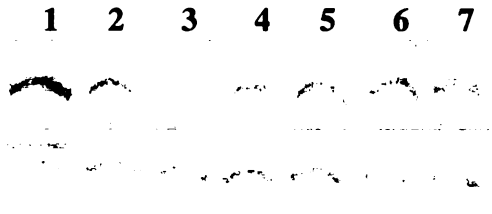

	1	2	3	4	5	6	7
Densitometry (%)	100	51.2	17.6	26.4	39.4	45.6	44.3

1. 24 h induction
2. " + 4 h puromycin
3. " + " + 10 μM AA
4. " + " + " + 20 μM MG132
5. " + " + " + 50 μM R-FB
6. " + " + " + 50 μM S-FB
7. " + " + " + 100 μM FB

D.

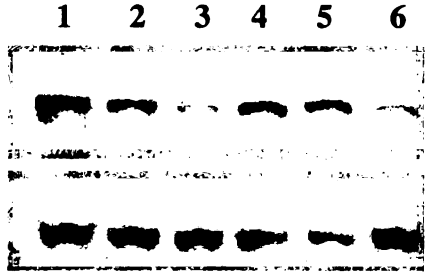

1. 24 h induction
2. " + 4 h puromycin
3. " + " + 20 μM AA
4. " + " + " + 20 μM NS-398
5. " + " + " + 100 μM FB
6. " + " + " + 20 μM MG132

27E.

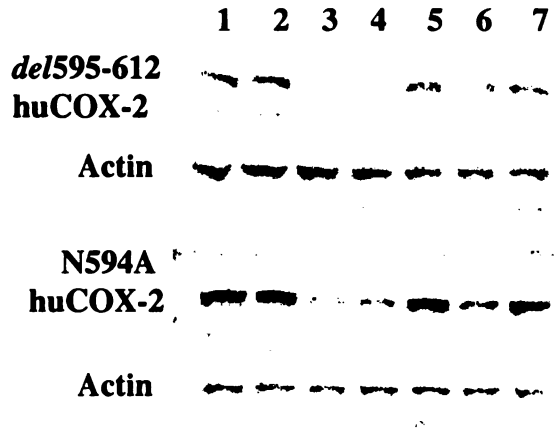

1. 24 h induction
2. " + 4 h puromycin
3. " + " + 20 μM AA
4. " + " + " + 20 μM MG132
5. " + " + " + 100 μM FB
6. " + " + " + 50 μM R-FB
7. " + " + " + 50 μM S-FB

F.

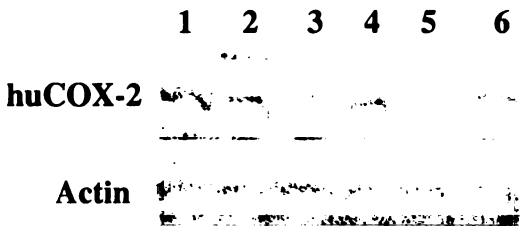

	1	2	3	4	5	6
Densitometry (%)	100	78.3	50.7	77.0	36.3	37.4

1. 24 h induction
2. " + 4 h puromycin
3. " + " + 20 μM AA
4. " + " + " + 100 μM FB
5. " + 5 min puromycin + 20 μM AA; 1X PBS wash; 4 h puromycin
6. " + " + " ; " ; " + 100 μM FB

Figure 27. COX-2 degradation in HEK293 cells is enhanced by exogenous AA treatment. (A) After serum-starvation and challenge with tetracycline to induce expression HEK293 cells stably expressing native huCOX-2 (I), *del*595-612 huCOX-2 (II), or N594A huCOX-2 (III) were treated with 50 μM puromycin for the indicated times with or without the addition of 10 μM or 20 μM AA. Alternatively, the cells were treated for 4 h with puromycin, a combination of puromycin and different concentrations of AA (5 μM, 10 μM, or 20 μM) (B), or a combination of puromycin, AA, and the indicated inhibitors (C, D, and E). (F) After a 24 h COX-2 induction with 10 μg/ml tetracycline cells were treated with 50 μM puromycin and 20 μM AA for 5 min or 4 h in the presence or absence of 100 μM FB. Following the 5 min treatment with AA, cells were washed with PBS and treated for an additional 4 h with puromycin in the presence or absence of 100 μM FB. After the treatments in *(A)-(F)* protein levels were analyzed by Western blotting and densitometry analysis. The results in B(I) and B(II) are representative of three independent experiments and the graph error bars denote 1 SE of the mean. The result in F is representative of two different experiments.

(Fig. 28*d*, panels *I*, *II*, and *III*). Thus, COX-2 degradation in 293 cells is selectively induced by COX PUFA substrates. Collectively, these results suggest that substrate binding to the COX active site is a prerequisite for the substrate-dependent degradation of COX-2.

G533A huCOX-2 is Refractory to Substrate-dependent Degradation. In a standard *in vitro* oxygen electrode assay, G533A huCOX-2 has less than 5% of the COX specific activity of native enzyme with AA as substrate (17,272). We stably expressed G533A huCOX-2 in HEK293 cells and analyzed its degradation profile after treatment with exogenous AA. Under basal conditions G533A huCOX-2 degraded with a half-life that was similar to that of the native huCOX-2 (Fig. 29*a*). However, this mutant was resistant to degradation that was induced by COX substrate (Figs. 29*b* and *c*). Our findings suggest that a functional COX active site is required for substrate-induced degradation of COX-2.

Substrate-dependent COX-2 Degradation in NIH/3T3 cells. We attempted to reproduce the enhancement of COX-2 degradation by fatty acid substrate in a different cell type. Serum-stimulation of quiescent 3T3 cells induced endogenous COX-2 degradation which was enhanced by treatment with 20 μM exogenous AA (Fig. 30*a*, panels *I* and *II*). Flurbiprofen significantly blocked both the endogenous degradation of COX-2 and AA-induced degradation of the protein (Fig. 30*b*). We also conducted experiments to determine if further stimulating endogenous AA release with bradykinin or A23187 in addition to serum-induction would also cause an enhancement of COX-2 degradation. In one experiment, treatment with 10 μM A23187 modestly enhanced COX-2 degradation albeit to a similar extent as treatment with 20 μM AA (Fig. 30*c*). The enhancement of COX-2 degradation by both A23187 and AA was inhibited by NS-398.

28A.

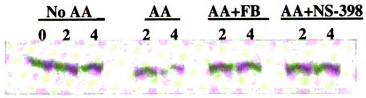

B.

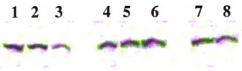

1. tet-induced
2. " + 4 h puromycin
3. " + " + 20 μM AA
4. " + " + " + 10 μM FB
5. " + " + " + 30 μM FB
6. " + " + " + 100 μM FB
7. " + " + " + 500 nM NS-398
8. " + " + " + 20 μM NS-398

C.

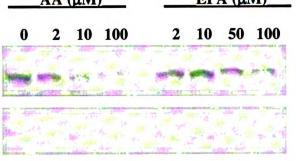

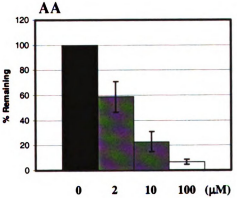

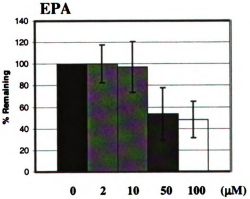

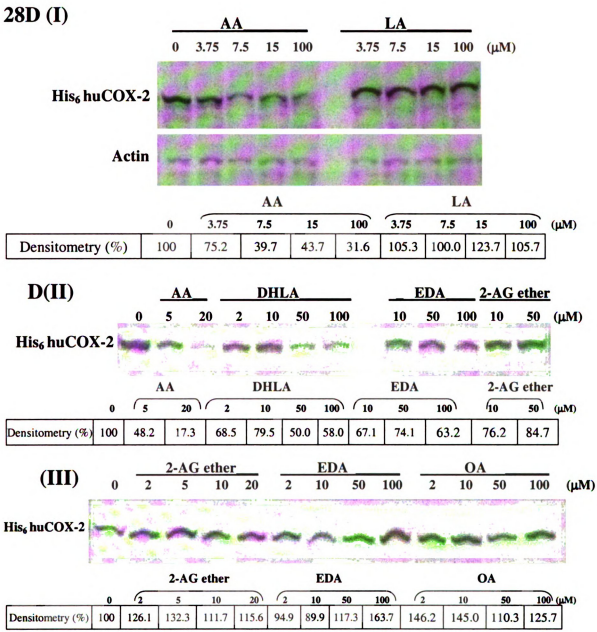

Figure 28. COX-2 degradation is selectively induced by PUFA COX substrates for the enzyme. N-terminal His_6-tagged huCOX-2-expressing HEK293 cells were treated as in 27(A) to induce protein expression. (A) Cells were treated for the indicated times with 50 μM puromycin with or without 20 μM AA, or a combination of puromcyin, AA, and the indicated concentrations of FB or NS398. (B) After induction of His huCOX-2 (1), cells were treated for 4 h with 50 μM puromycin only (2), or in combination with 15 μM AA (3) and 10 μM FB (4), 30 μM FB (5), 100 μM FB (6), 500 nM NS-398 (7), or 20 μM NS-398 (8). In (C) and (D) puromycin treatment was followed by treatment with different concentrations of AA, linoleic acid (LA), eicosapentaenoic acid (EPA), 2-arachidonyl glycerol ether (2-AG ether), dihomo-γ-linolenic acid (DHLA), eicosadienoic acid (EDA), and oleic acid (OA). COX-2 protein levels were analyzed by Western blotting and densitometry. The result in C is representative of at least three independent experiments and the graph error bars denote 1 SE of the mean.

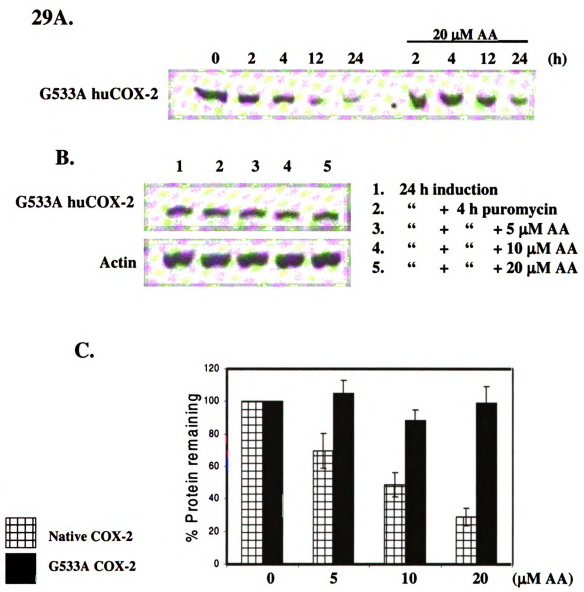

Figure 29. The G533A cyclooxygenase-inactive COX-2 mutant is not susceptible to substrate-dependent degradation. (A) Degradation of G533A huCOX-2 was examined with or without addition of 20 μM AA. (B) Cells expressing G533A huCOX-2 were treated for 4 h with 50 μM puromycin plus different concentrations of AA (5 μM, 10 μM, or 20 μM). Protein levels were analyzed by Western blotting. (C) Densitometry was performed on the levels of native huCOX-2 or G533A huCOX-2 and normalized to those of actin. Densitometry analysis for each protein is based on at least three independent experiments. The error bars denote 1 SE of the mean.

In contrast, bradykinin at 10 μM did not facilitate COX-2 protein turnover. It is possible that A23187 may cause more release of endogenous AA than bradykinin and that the amount of bradykinin-induced free AA may not be sufficient to facilitate COX-2 degradation in serum-stimulated 3T3 cells.

Substrate-dependent Degradation of COX-1. COX-1 is known to be a very stable protein (257). This is consistent with the observation that NIH/3T3 cells that have been made quiescent by serum deprivation for 48 h continue to express the enzyme. Furthermore, stimulating quiescent 3T3 cells with serum will induce COX-1 mRNA (22). However, serum-stimulation of 3T3 cells in the presence of flurbiprofen does not lead to an accumulation of COX-1 protein. Collectively, these results imply that the constitutive expression of this COX isoform observed in many tissues is likely to be mainly due to the stability of the enzyme rather than a continuous balance of protein synthesis and degradation. Experiments were performed to determine if COX-1 protein turnover could be induced by COX fatty acid substrate. In NIH/3T3 cells, treatment with 20 μM AA did not affect the stability of endogenous COX-1 protein (Fig. 31*a*). This was a surprising result because treatment of quiescent 3T3 cells with 10 μM AA results in prostanoid product formation due to COX-1 activity. Therefore, at the AA concentrations that were used in our experiments COX-1 is catalyzing oxygenation. In HEK293 cells, treatment with $\geq$20 μM of AA resulted in a modest loss of COX-1 protein (Figs. 31*b* and *c*). If indeed COX-2 degradation due to AA challenge is a consequence of suicide inactivation during COX catalysis, it is possible that COX-1 may be more resistant to COX substrate-induced inactivation *in vivo* compared to COX-2. Alternatively, the inactive form(s) of COX-1 formed during COX catalysis may be less susceptible to degradation.

30A. (I)

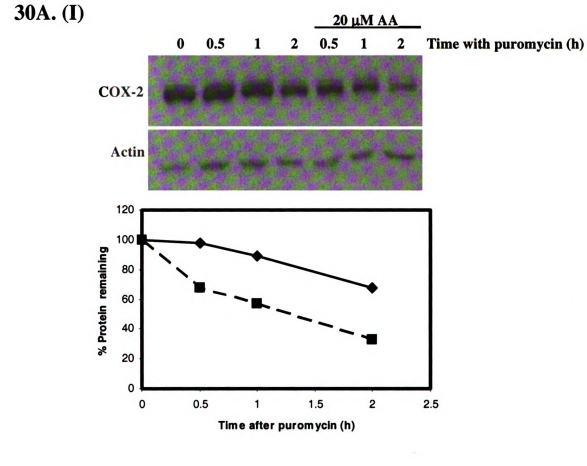
20 μM AA
0 0.5 1 2 0.5 1 2 Time with puromycin (h)
COX-2
Actin
% Protein remaining
120
100
80
60
40
20
0
0 0.5 1 1.5 2 2.5
Time after puromycin (h)
No substrate
20 μM AA

30A. (II)

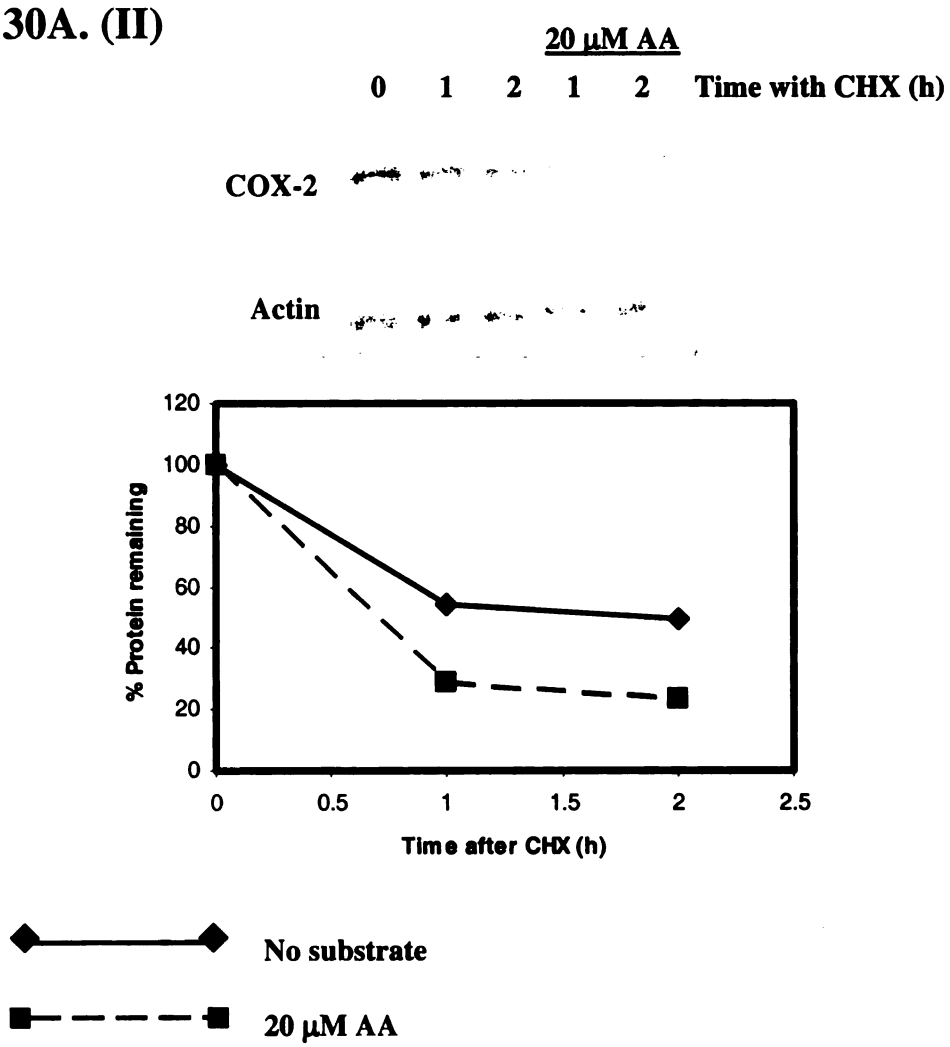
20 μM AA
0 1 2 1 2 Time with CHX (h)
COX-2
Actin
120
100
80
60
40
20
0
% Protein remaining
0 0.5 1 1.5 2 2.5
Time after CHX (h)
No substrate
20 μM AA

30B.

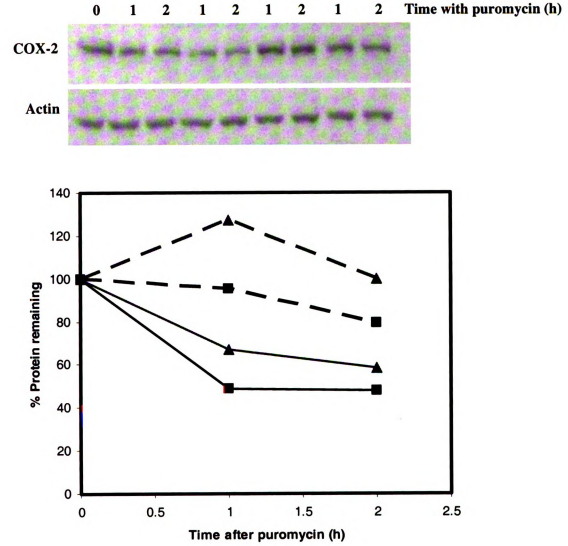
0 1 2 1 2 1 2 1 2 Time with puromycin (h)
COX-2
Actin
% Protein remaining
Time after puromycin (h)
No substrate
20 μM AA
20 μM AA + 100 μM FB
100 μM FB

30C.

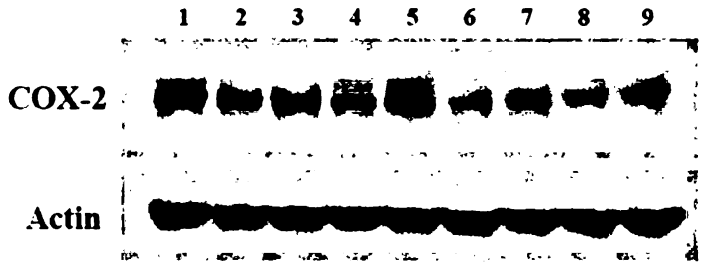

	1	2	3	4	5	6	7	8	9
Densitometry (%)	100	73	80	87	94	62	76	59	80

Figure 30. The enhancement of COX-2 degradation in NIH/3T3 cells by exogenous and endogenous AA is inhibited by NSAIDs. (A and B) Serum-starved, quiescent 3T3 cells were serum-stimulated for 4 h to induce COX-2 expression. Thereafter, cells were treated with 50 μM puromycin or 50 μM CHX for the indicated times in the presence or absence of 20 μM AA, 100 μM FB, or a combination of both AA and FB. After Western analysis, densitometry was performed on the levels of COX-2 and normalized to those of actin. (C) After inducing COX-2 expression (1) as in A and B, cells were treated with 50 μM CHX (2) in the presence or absence of the following: 20 μM NS-398 (3), 10 μM bradykinin (4) , 10 μM bradykinin + 20 μM NS398 (5), 10 μM A23187 (6), 10 μM A23187 + 20 μM NS-398 (7), 20 μM AA (8), or 20 μM AA + 20 μM NS-398 (9). Densitometry was performed on COX-2 protein levels and normalized to those of actin.

31A.

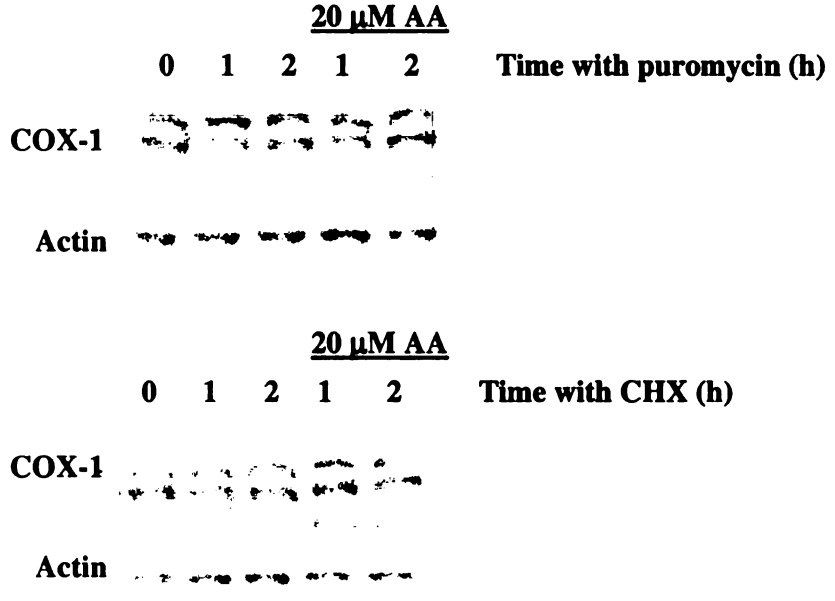

31B.

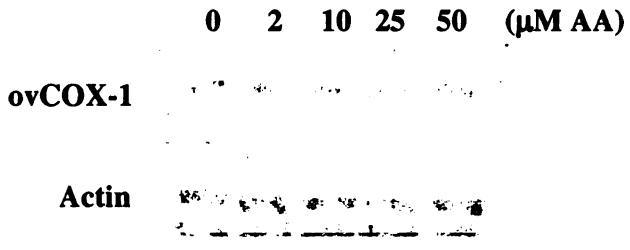

	0	2	10	25	50 (μM AA)
Densitometry (%)	100	81	78	74	69

C.

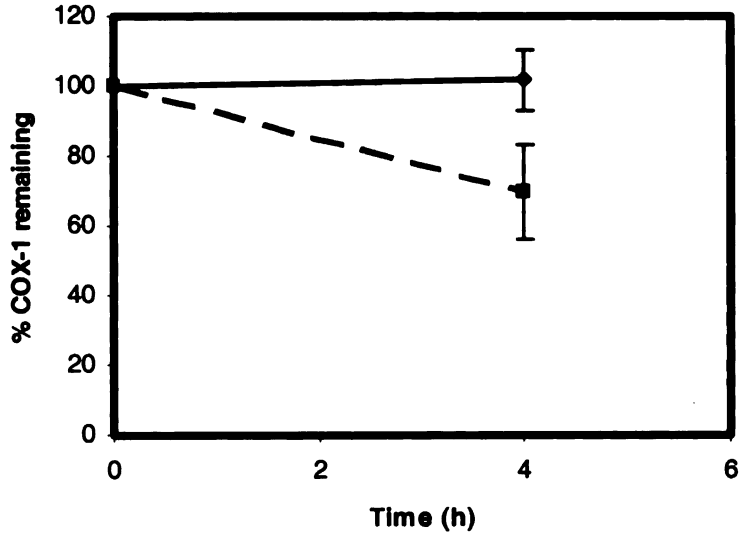

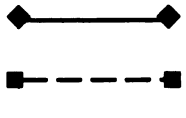

Figure 31. COX-1 stability is not significantly affected by exogenous AA. (A) Quiescent 3T3 cells were serum-stimulated for 4 h then treated with 50 μM puromycin or 50 μM CHX for the indicated times with or without the addition of 20 μM AA. (B) 293 cells stably expressing ovCOX-1 were treated with 50 μM puromycin for 4 h with or without the addition of different concentrations of AA. (C) Densitometry of the effect of 20 mM AA on ovCOX-1 stability in 293 cells. Quantitative analysis is based on six independent experiments. The graph error bars denote 1 SE of the mean.

Substrate-dependent Degradation of COX-2 is not Proteasome- or Lysosome-dependent. We tested an inhibitor of the 26S proteasome and selective inhibitors of lysosomal degradation in an attempt to identify the pathway responsible for substrate-dependent COX-2 protein turnover. The 26S proteasome inhibitor MG132 failed to inhibit substrate-induced COX-2 degradation in both 3T3 and 293 cells (Figs. 27*c*, 27*d*, 27*e*, and 32*a*). Similarly, the lysosomal degradation inhibitors E64 and leupeptin, and brefeldin A, an inhibitor of ER to Golgi trafficking, failed to prevent AA-induced COX-2 degradation in 293 cells (Figs. 32*a* and *b*). Therefore, substrate-dependent degradation of COX-2 does not appear to require the proteolytic activity of the proteasome or lysosome.

Experiments were carried out to determine if the protease(s) responsible for cleaving COX-2 in a substrate-dependent manner was ER-associated. Microsomes prepared from 293 cells expressing *del*595-612 huCOX-2 or N594A huCOX-2 were incubated with or without 100 μM AA in a reaction buffer containing 10 μM hematin and 1 mM phenol. After 4 h at 37°C the samples were analyzed by Western blotting to determine whether there was loss of COX-2 protein as a consequence of substrate treatment. There was no observable change in the levels of *del*595-612 huCOX-2 or N594A huCOX-2 in microsomes that were exposed to AA (Fig. 32*c*). It is possible that the microsomes that we prepared were not sufficiently intact to retain any ER luminal protease(s) responsible for COX-2 proteolytic cleavage. To test the integrity of the microsomes, I treated solubilized or non-solubilized microsomes with trypsin. Limited digestion of COX-2 with trypsin yields a single cleavage at its C-terminus that produces a ~2-3 kDa C-terminal fragment. The C-terminal trypsin cleavage site is within the epitope for the primary antibody used to detect COX-2. Since COX-2 is an ER luminal protein it

should not be cleaved by trypsin if the microsomes are intact. However, both *del*595-612 huCOX-2 and N594A huCOX-2 were proteolytically cleaved by trypsin in non-solubilized microsomes (Fig. 32*d*). These results indicated that the prepared microsomes were permeable and/or wrong-side-out. Therefore, we cannot eliminate the possibility that there could be an ER-associated protease involved in substrate-dependent COX-2 degradation. The protease is likely to be a luminal enzyme or it may be ER membrane-associated but requires luminal co-factors for its catalytic activity.

COX Self-inactivation Preceeds Substrate-dependent COX-2 Degradation. Both COX-1 and COX-2 are known to undergo irreversible, mechanism-based COX inactivation during *in vitro* catalysis (3,156). It is possible that the self-inactivation of COX-2 in HEK293 cells and NIH/3T3 cells treated with AA would accompany the formation of cyclooxygenase oxygenation products. If indeed the enzyme self-inactivates *in vivo* during catalysis, it would reflect damage at the COX active site. Structurally damaged COX-2 would likely be more susceptible to degradation than the native enzyme, which could explain why AA treatment facilitates COX-2 protein turnover in HEK293 and NIH/3T3 cells.

I decided to examine whether COX-1 and COX-2 undergo self-inactivation *in vivo* during COX catalysis. For this purpose, I utilized HEK293 cells stably expressing N-terminal His-tagged versions of ovCOX-1 (His ovCOX-1) or murine COX-2 (His muCOX-2). These cells were treated for 10 min with varying concentrations of AA (0, 2.5, 10, 25, and 50 μM). Thereafter, the cells were washed with PBS, pH 7.4 and centrifuged at 2000 rpm for 3 min. Cell pellets were resuspended in 0.1 M Tris, pH 7.4 and sonicated. The COX activity of the whole cell lysates was then assayed using an

32A.

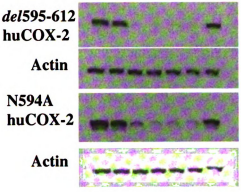

1. tet-induction
2. " + 4 h puromycin
3. " + " + 20 μM AA
4. " + " + " + 50 μM Leup
5. " + " + " + 25 μM E64
6. " + " + " + 20 μM MG132
7. " + " + " + 20 μM NS-398

B.

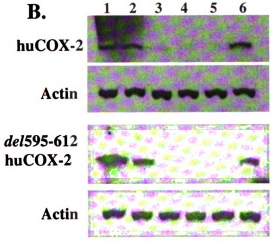

1. tet-induction
2. " + 4 h puromycin
3. " + " + 20 μM AA
4. " + " + " + 5 μg/ml BFA
5. " + " + " + 5 μg/ml BFA
6. " + " + " + 20 μM NS-398

32C.

1,4. No substrate
2,5. 100 μM AA
3,6. 100 μM AA + 100 μM FB

32D.

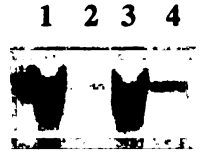

1. unsolubilized
2. unsolubilized + trypsin tmt.
3. solubilized
4. solubilized + trypsin tmt.

Figure 32. Inhibitors of proteasomal and lysosomal degradation do not prevent substrate-dependent COX-2 protein turnover. (A) HEK293 cells stably expressing *del*595-612 huCOX-2 and N594A huCOX-2 were treated as in 27A to induce protein expression (1). Thereafter, cells were treated for 4 h with 50 μM puromycin (2) or in combination with 20 μM AA (3), 20 μM AA + 50 μM leupeptin (4), 20 μM AA + 25 μM E64 (5), 20 μM AA + 20 μM MG132 (6), or 20 μM AA + 20 μM NS398 (7). (B) Cells stably expressing native huCOX-2 and *del*595-612 huCOX-2 were treated as in 27A to induce protein expression (1). This was followed by treatment with 50 μM puromycin only (2) or in combination with 20 μM AA (3), 20 μM AA + 5 μg/ml brefeldin A (4), 20 μM AA + 5 μg/ml brefeldin A (5), or 20 μM AA + 20 μM NS398 (6). (C) Microsomes were prepared from 293 cells stably expressing *del*595-612 huCOX-2 or N594A huCOX-2 as described in the text. Thereafter, the microsomes were resuspended in 0.1 M Tris-Cl buffer, pH 8.0 and 200 μg of this resuspension was incubated in a 100 μl reaction mixture containing 0.1 M Tris-Cl, pH 8.0, 10 μM hematin, and 1 mM phenol with no substrate (1,4) or with 100 μM AA (2,5) and 100 μM FB (3,6). The incubation was performed at 37°C for 4 h. (D) After resuspension, 100 μg of microsomes were treated with 5 μg trypsin before or after solubilization with 1% Tween-20. Trypsin treatment was performed at 37°C for 20 min. After the treatments in A-D protein levels were analyzed by Western blotting.

oxygen electrode. Microsomes were also prepared from the whole cell lystates and assayed for prostaglandin product formation by radioactive TLC. There was a dramatic concentration-dependent decrease in COX activity of His_6-tagged muCOX-2-expressing whole cell lysates (Fig. 33*a*), which could not be a result of a decline in His_6-tagged muCOX-2 protein levels during the 10 min duration of AA pretreatment (data not shown). In contrast, the decline in COX activity observed with His_6-tagged ovCOX-1-expressing HEK293 cells was less dramatic (Fig. 33*a*). For instance, His_6-tagged muCOX-2-expressing lysates pretreated with 10 μM had a ~40% decrease in specific activity compared to only ~20% for His_6-tagged ovCOX-1-expressing lysates pretreated with the same concentration of AA. The observations made with the oxygen electrode assays are consistent with results from radioactive COX TLC assays which demonstrated that prostaglandin product formation of His_6-tagged muCOX-2-expressing microsomes prepared from cells that were treated with 10 μM or 25 μM AA was significantly reduced (Fig. 33*b*). Overall, these findings indicate that, at least in HEK293 cells, both COX-1 and COX-2 undergo substrate-induced catalytic inactivation with COX-2 appearing to be the more susceptible isoform.

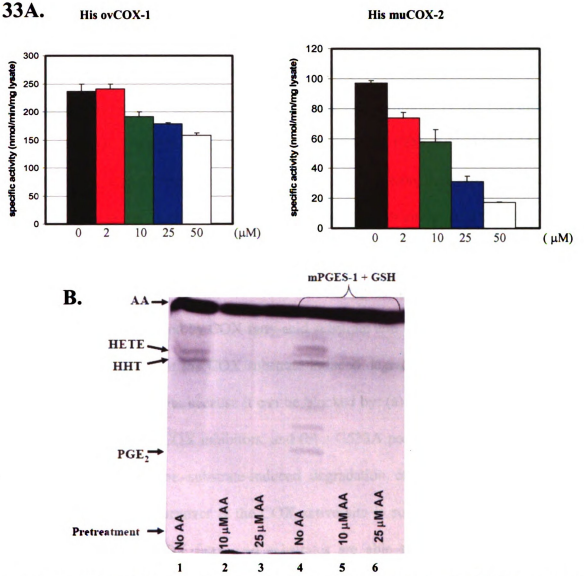

Figure 33. COX activity and prostaglandin product formation of His ovCOX-1 and His muCOX-2 cells pretreated with exogenous AA. Upon induction of His ovCOX-1 or His muCOX-2, cultured 293 cells stably expressing these enzymes were incubated with the indicated concentrations of AA for 10 min. Afterwards, the cells were washed with 1X PBS, harvested and centrifuged at 2000 rpm for 3 min. Cell pellets were resuspended in 0.1 M Tris-Cl, pH 8.0 and lysed by sonication. (A) The COX activity of the whole cell lysates was measured by an oxygen electrode assay in a standard reaction mixture containing 100 μM AA, 1 mM phenol, and 5 μM hematin dissolved in 0.1 M Tris-Cl, pH 8.0. (B) Microsomes were isolated from the whole cell lysates pretreated with 0 μM (1, 4), 10 μM (2, 5) or 25 μM AA (3, 6) and prepared for radioactive TLC as described in the text. Equivalent amounts of microsomes (0.5 mg) were incubated in a 100-μl reaction mixture containing 0.1 M Tris-HCl, pH 8.0, 1 mM phenol, 10 μM hematin, and 10 μM [1-^{14}C]arachidonic acid at room temperature for 1 min. To assay for PGE_2 formation microsomal PGES-1 (mPGES-1) and 60 μM GSH were included in reaction samples 4, 5 and 6. After the reactions were terminated as described in the text the radioactive products were isolated, resolved by TLC, and analyzed by autoradiography. HETE–hydroxyeicosatetraenoic acid; HHT – hydroxyheptadecatrienoic acid.

Discussion

The secondary and tertiary structures of COX-2 are more susceptible to guadinium hydrochloride chemical denaturation compared with COX-1, demonstrating a difference in the inherent structural stabilities of the COX isoforms (150). This difference in protein stability parallels that observed *in vivo* where COX-1 is very stable under conditions in which COX-2 is rapidly degraded (257). We have previously attributed the short protein half-life of COX-2 to a unique C-terminal 19-amino acid cassette (19-aa) that is required for ER-associated degradation of the enzyme in HEK293 cells. In the present study we have shown that COX-2 undergoes a second distinct form of degradation that is induced by COX fatty acid substrate and is independent of the 19-aa. We also demonstrate that the COX substrate-induced degradation of COX-2 requires a functional COX active site because it can be blocked by: (a) both competitive and time-dependent, irreversible COX inhibitors, and (b) a G533A point mutation that inactivates COX catalysis. That the substrate-induced degradation of COX-2 is dependent on substrate binding and turnover at the COX active site is suggested by the finding that only known COX-2 COX fatty acid substrates are able to facilitate COX-2 protein turnover. Furthermore, a 5 min brief challenge of COX-2-expressing cells with AA, during which prostaglandin products are expected to be formed, is sufficient to significantly enhance COX-2 degradation. Overall, these findings enable us to postulate that COX substrate-dependent degradation of COX-2 is initiated at the COX active site by the binding of fatty acid substrate. It is not clear whether the inactivity observed with G533A COX-2 is due to a defect in substrate binding or substrate turnover. This point mutant has some residual COX activity with AA as substrate (~5% relative to the native

enzyme) (17,272) suggesting that it may bind AA but inefficiently bis-oxygenate the substrate to form PGG_2.

Proteasome activity appears to be dispensable for the COX substrate-dependent degradation of COX-2. We have previously shown that COX-2 degradation in NIH/3T3 cells is partly proteasome-independent in NIH/3T3 cells, but largely proteasome-dependent in HEK293 cells (257). Also noteworthy is the finding that COX inhibitors dramatically prevented the basal degradation of COX-2 in serum-induced NIH/3T3 cells but did not affect the proteasome-dependent degradation of the enzyme in HEK293 cells. Collectively, these findings suggest that COX inhibitors may not inhibit the proteasome-dependent degradation of COX-2 that is initiated by the C-terminal 27 amino acid instability element. Therefore, there appears to be a second distinct mechanism for COX-2 protein turnover present in NIH/3T3 cells that is triggered by the endogenous release of AA. HEK293 cells lack detectable phospholipase A_2 activity whereas NIH/3T3 cells can activate $cPLA_{2\alpha}$ in response to serum treatment (33,58,77). This could explain why COX inhibitors do not retard the basal, proteasome-dependent degradation of COX-2 in HEK293 cells. In NIH/3T3 cells, endogenously released AA will be utilized as COX substrate by COX-2, thereby, initiating the substrate-dependent degradation of the enzyme. Addition of exogenous free AA or A23187, but not bradykinin, further enhanced the NSAID-inhibitable degradation of COX-2 in serum-treated 3T3 cells. In this regard, it is possible that a copious amount of endogenous AA was released upon serum-stimulation that was sufficient to induce substantial degradation of COX-2, so that adding an additional stimulus like bradykinin did not dramatically affect COX-2 protein levels. It would be interesting to determine if the effect of bradykinin and A23187 on COX-2

degradation can be amplified in 3T3 cells that have been induced to express COX-2 with phorbol ester instead of serum. Since phorbol ester is not a major activator of $cPLA_{2\alpha}$ in fibroblast cells it should induce a relatively smaller release of AA compared to serum resulting in a proportionate attenuation of the endogenous COX-2 degradation. If indeed endogenous COX-2 degradation is partly induced by $cPLA_2$-mobilized AA in serum-treated NIH/3T3 cells, it would also be reasonable to test the effect of $cPLA_2$ inhibition on the degradation of the protein.

COX-1 and COX-2 undergo irreversible suicide inactivation during COX catalysis under cell-free conditions (3,156,162,163). Whether or not these enzymes undergo suicide inactivation in intact cells has not yet been clarified. Riese *et al.* have provided evidence to suggest that COX-2 may inactivate in RAW264.7 macrophage cells that have been challenged with a combination of LPS and IFN-γ (273). In their study, they observed that while COX-2 expression levels remained at maximal levels 24-48 h after induction with LPS and IFN-γ, the specific activity of the enzyme was transient during this time period. *In vitro* COX inactivation is accompanied by significant changes in the structural conformation of the enzyme, suggesting that this process is a culmination of the destruction of the native structure of heme-protein complex (162). The concept of inactivation-coupled structural damage due to COX catalysis becomes important in the context of COX protein stability since it is well known that the ER has a sophisticated quality control system that recognizes and selectively eliminates structurally-damaged ER-associated proteins (164-166,182-186). In the present study, evidence has been provided to show that both COX-1 and -2 can inactivate in intact HEK293 cells upon exposure to exogenous AA. From this finding we propose that the inactivation-coupled

structural damage to COX-2 as a consequence of substrate turnover at the COX active site precedes the substrate-dependent degradation of the enzyme (Fig. 34). We are yet to determine whether this model is also applicable to COX-1. It is interesting to observe that although the COX substrate-dependent degradation of COX-1 in HEK293 is relatively modest compared to COX-2, it appears to be proportionate to its COX substrate-induced inactivation.

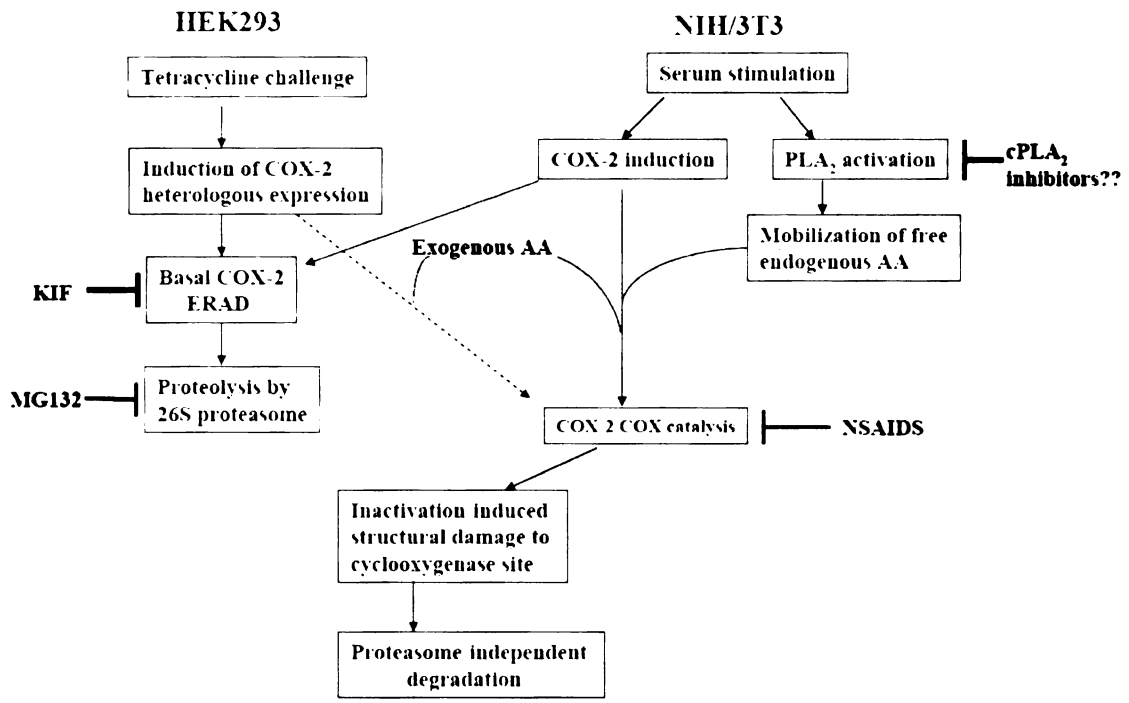

Figure 34. Model for the basal and COX substrate-initiated degradation of COX-2 in HEK293 (red) and serum-treated NIH/3T3 cells (blue). Proteasome-dependent glycoprotein ERAD is the predominant pathway for COX-2 degradation in HEK293 cells which essentially lack phospholipase A_2 (PLA_2) activity. Addition of exogenous AA to COX-2-expressing HEK293 cells will activate a second distinct proteasome-independent, NSAID-inhibitable degradation pathway that involves COX catalysis. The degradation of endogenous inducible COX-2 in serum-treated NIH/3T3 cells may occur via both pathways. If COX-2 degradation in these cells is further enhanced by endogenous AA release, then phospholipase A_2 inhibitors should stabilize the protein to the same extent as NSAIDS.

It seems unlikely that the COX substrate-dependent loss of COX-2 protein as determined by immunoblotting is due to the formation of COX reactive oxygenated side products that covalently modify a region(s) of the COX-2 protein that serves as an epitope for antibody detection. In examining the effect of COX substrate on the stability of COX-2 we utilized two different antibodies for immunoblotting. In NIH/3T3 cells a peptide-directed antibody against the epitope S598-K612 of muCOX-2 was used to detect serum-induced COX-2. In HEK293 cells an antibody against Q583-N594 of huCOX-2 was used to detect tetracycline-inducible stably expressed COX-2. Both antibodies yielded similar results even though they are directed against different epitopes on the protein. Therefore, we believe that the substrate-dependent decrease in COX-2 immunoreactivity in both cell lines reflects the degradation of the enzyme. We were unable to identify the degradation pathway or the protease(s) responsible for the substrate-induced proteolytic cleavage of COX-2. We have found that the proteolytic activities of the 26S proteasome and the lysosome, and trafficking between the ER and Golgi appear to be dispensable for this process. It is likely that the protease(s) involved in substrate-induced cleavage of COX-2 may be resident in the ER. It may not have been possible to identify the ER- or microsome-associated proteolytic activity because the microsomes that were used in our studies were not intact; trypsin cleavage analysis suggested that the microsomes were likely to be wrong-side-out.

Very few enzymes have been hitherto identified as ER-resident proteases. Signal peptidase, which is known to be physically associated with the Sec61 translocon, cleaves N-terminal ER targeting sequences of proteins as they are imported into the ER (274-276). Signal peptide peptidase (SPP) is an ER membrane-associated aspartyl protease that

cleaves the signal peptide fragments generated by signal peptidase (277). Recently, SPP has been shown to be essential for the retrotranslocation and subsequent proteasomal degradation of major histocompatibility complex (MHC) Class I heavy chains that is induced by the US2 protein of cytomegalovirus (278). However, this study did not clarify whether the protease activity of SPP *per se* was required for this process. ER aminopeptidases-1 and -2 (ERAP-1 and -2) are ER luminal, interferon-γ-inducible metallopeptidases that are believed to be involved in the final proteolytic processing of short proteasome-generated peptide fragments that will be loaded onto MHC Class I molecules for antigen presentation on the surface of an antigen presenting cell (279-282). There are no reports thus far implicating ERAP-1 and -2 in the degradation of whole proteins. The membrane remodeling enzyme Δ^9 steroyl-CoA desaturase is an ER integral membrane protein that is rapidly degraded ($t_{1/2}$ ~3-4 h) under basal conditions in a proteasome-independent manner (283,284). Heinemann *et al* have purified and characterized a 90 kDa plasminogen-related protease with Arg/Lys specificity that it is responsible for the rapid degradation of steroyl-CoA desaturase (284,285). This protease is unlikely to act in the ER lumen because the sequence determinant of steroyl-CoA desaturase that directs its rapid turnover is found on the cytosolic N-terminal portion of the enzyme (286). Although the mechanism for steroyl-CoA proteolysis is still unclear, there is evidence to show that the protein gets cleaved within a putative membrane binding region, most likely by the ER plasminogen-related protease (283). It has been suggested that the N-terminal instability sequence of steroyl-CoA desaturase may help to bring the membrane protease to close vicinity with the enzyme (286). Recently, Donoso *et al.* have shown that the degradation of a misfolded mutant form of BiP is initiated in

the ER lumen by a serine protease that is yet to be identified (287). In this regard, it is likely that a proteolytic system exists in the ER that may serve as an alternative or a complement to the ERAD-proteasome pathway in the quality control of structurally defective ER-associated proteins. Therefore, we speculate that the catalytically inactivated form(s) of COX-2 is degraded by this putative ER protease system.

In conclusion, we have found that AA, the principal PUFA COX-2 substrate, induces both the COX catalytic inactivation and the rapid degradation of the enzyme. We have also observed that inhibition of COX-2 COX catalysis using site-directed mutagenesis and pharmacological approaches prevent AA-dependent degradation. Based on these observations we have proposed that the AA-dependent degradation of COX-2 is a consequence of structural damage to the COX active site. In the future, it will be important to measure and compare the kinetic constants for the catalytic inactivation of the COX isoforms in intact cells. The proposition that COX-2 degradation in NIH/3T3 cells is enhanced by serum-induced mobilization of free AA will need to be tested further using inhibitors of $cPLA_2$. A protocol for preparing intact microsomes will also be designed in an effort to identify the ER-associated protease(s) that degrades catalytically inactive COX-2. Indeed, the unconventional COX substrate-dependent quality control of COX-2 may serve as an additional physiological mechanism for the metabolic regulation of prostanoid synthesis.

CONCLUSION

The structural basis for the selection of normal short-lived proteins for rapid proteolysis in an intracellular environment where they coexist with many stable proteins is not clearly defined. We have identified a 27 amino acid instability element close to the C-terminal end of COX-2 that regulates the proteasomal degradation of this ER-resident membrane-bound protein by mediating its entry into the ERAD system. We believe that COX-2 is the only known ER luminal integral membrane protein that is degraded via ERAD from its native or properly folded form. The ERAD pathway is an important protein quality control pathway that is not well characterized in mammalian cells. ERAD components in the ER lumen that participate in the initial selective recognition of an ERAD substrate and the mechanism by which they do so are not clearly defined. The identity of the ER membrane retrotranslocon is also yet to be determined. Therefore, since COX-2 is one of the very few mammalian proteins that are known to undergo proteasomal degradation from the ER it could serve as a suitable reporter substrate for studying ERAD in a mammalian system.

We have also identified a second distinct mechanism for COX-2 degradation that is preceded by the COX substrate (AA)-induced suicide inactivation of the enzyme. Intracellular COX-1 appears to be less susceptible to substrate-induced suicide inactivation and degradation. COX-1 is a stable protein that is constitutively expressed in many cells. It is also able to utilize endogenous AA at higher concentrations than COX-2. Therefore, based on our experimental data we reason that the housekeeping function of COX-1 might extend to include regulating the intracellular levels of free AA. The proteolysis of COX-2 in response to two distinct signals, namely a structural and a

metabolic signal, reflects the tight and elaborate control of COX-2 expression at all three levels of gene regulation. Since the differential expression profiles of COX-1 and COX-2 are thought to contribute to their specialized biological functions, our observations may provide a clue to the unsolved mystery of why mammals have two COX isoforms.

APPENDIX

Table 3. C-terminal mutants designed by QuickChange™ site-directed mutagenesis

Mutation	Primers	Template
G533A huCOX-2	Forward: 5'CTCCTTGAAAGCACTTA TGGGTAATG 3' Reverse: 5'CATTACCCATAAGTGCTTT CAAGGAG 3'	huCOX-2
N594A huCOX-2	Forward: 5' GTCACCATCGCAGCAAGTT CTTCCCGC 3' Reverse: 5' GCGGGAAGAACTTGCTG CGATGGTGAC 3'	huCOX-2
P607A T608A huCOX-2	Forward: 5' CTA GAT GAT ATC AAT GCA GCA GTA CTA CTA AAA GAA 3' Reverse: 5' TTC TTT TAG TAG TAC TGC TGC ATT GAT ATC ATC TAG 3'	huCOX-2
V609A huCOX-2	Forward: 5' GAT GAT ATC AAT CCC ACA GCA CTA CTA AAA GAA CGT 3' Reverse: 5' ACG TTC TTT TAG TAG TGC TGT GGG ATT GAT ATC ATC 3'	huCOX-2
L610A huCOX-2	Forward: 5' GAT ATC AAT CCC ACA GTA GCA CTA AAA GAA CGT TCG 3' Reverse: 5' CGA ACG TTC TTT TAG TGC TAC TGT GGG ATT GAT ATC 3'	huCOX-2

Table 3 (cont'd)

L611A huCOX-2	Forward: 5' ATC AAT CCC ACA GTA CTA GCA AAA GAA CGT TCG ACT 3' Reverse: 5' AGT CGA ACG TTC TTT TGC TAG TAC TGT GGG ATT GAT 3'	huCOX-2
K612A huCOX-2	Forward: 5' CCCACAGTACTACTA GCAGAACGTTCGACT 3' Reverse: 5' AGTCGAACGTTCTGCTAGT AGTACTGTGGG 3'	huCOX-2
*del*595-612 huCOX-2	Forward: 5' ACAGTCACCATCAAT GAACGTTCGAC 3' Reverse: 5' CTACAGTTCAGTC GAACGTTCATTG 3'	huCOX-2
*del*597-612 huCOX-2	Forward: 5' ACCATCAATGCA AGTGAACGTTCGACT 3' Reverse: 5' AGTCGAACGTTCACTTGCATT GATGGTGAC 3'	huCOX-2
*del*602-612 huCOX-2	Forward: 5'CTTCCCGCTCCGGAG AACGTTCGACTGAA 3' Reverse: 5' TTCAGTCGAACGTTCTC CGGAGCGGGAAG 3'	huCOX-2
*del*607-612 huCOX-2	Forward: 5'GATGATATCAAT GAACGTTCGACTGAA 3' Reverse: 5'TTCAGTCGAACGTTCA TTGATATCATC 3'	huCOX-2

Table 3 (cont'd)

MuCOX-2 UPSTRM8 huCOX-2	Forward: 5' AGT GTT CCA GAT CCA CAG CCT ACC AAA ACA GCC ACC ATC AAT GCA AGT 3' Reverse: 5' ACT TGC ATT GAT GGT GGC TGT TTT GGT AGG CTG TGG ATC TGG AAC ACT 3'	huCOX-2
ovCOX-1 UPSTRM8 huCOX-2	Forward: 5' AGT GTT CCA GAT CCA CGT CAG GAG GAC AGG CCT GGG GTG AAT GCA AGT TCT TCC 3' Reverse: 5' GGA AGA ACT TGC ATT CAC CCC AGG CCT GTC CTC CTG ACG TGG ATC TGG AAC ACT 3'	huCOX-2
V591P T592G huCOX-2	Forward: 5' GAG CTC ATT AAA ACA CCC GGC ATC AAT GCA AGT TCT 3' Reverse: 5' AGA ACT TGC ATT GAT GCC GGG TGT TTT AAT GAG CTC 3'	huCOX-2
*ins*594-596 ovCOX-1	Forward: 5' GACAGGCCTGGGGTGGAGA ATGCAAGTCGGCCACCCACA 3' Reverse: 5' TGTGGGTGGCCGACTTGCA TTCTCCACCCCAGGCCTGTC 3'	ovCOX-1
*ins*594-601 ovCOX-1	Forward: 5' TCCCGCTCCGGAGAGCGG CCACCC 3' Reverse: 5' GGGTGGCCGCTCTCCGGAGC GGGA 3'	*ins*594-612 ovCOX-1
*ins*594-612 (N594A) ovCOX-1	Forward: 5' GACAGGCCTGGGGTGGCAGC AAGTTCTTCCCGC 3' Reverse: 5' GCGGGAAGAACTTGCTGC CACCCCAGGCCTGTC 3'	*ins*594-612 ovCOX-1

Table 4. C-terminal mutants designed by overlap-extension PCR mutagenesis

Mutation	Primers	Template
*ins*594-612 ovCOX-1	**Mutation Primers** Forward: 5' GACAGGCCTGGGGTGAATGC AAGTTCTTCCCGCTCCGGACTAGATGAT ATCAATCCCACAGTACTACTAAAAGAG CGGCCACCCACA 3' Reverse: 5' TGTGGGTGGCCGCTCTTTTAG TAGTACTGTGGGATTGATATCATCTAGT CCGGAGCGGGAAGAACTTGCATTCACC CCAGGCCTGTC 3' **Common Primers** Forward: 5' GCGTTTAAACTTAAGCTT 3' Reverse: 5' GAGCTCGGTACCAAGCTT 3'	ovCOX-1
S*ins*594-612 huCOX-2	**Mutation primers** Forward: 5' ACAGTCACCATCGCTGCTA GTATTAGAGGTCCTTTAACTAAACTTAG TGATAATAGTCTTGTTAGTGATGAACGT TCGACTGAACTG 3' Reverse: 5' CAGTTCAGTCGAACGTTCATC ACTAACAAGACTATTATCACTAAGTTTA GTTAAAGGACCTCTAATACTAGCAGCG ATGGTGACTGT 3' **Common primers** Forward: 5' GCTTGGTACCGAGCTCGGA TCC 3' Reverse: 5' CGGGCCCTCTAGACTCGAG CGGCC 3'	huCOX-2

Table 4 (cont'd)

S*ins*597-612 huCOX-2	**Mutation primers** Forward: 5' GTCACCATCAATGCAAGTAT TAGAGGTCCTTTAACTAAACTTAGTGAT AATAGTCTTGTTAGTGATGAACGTTCGA CTGAACTG 3' Reverse: 5' CAGTTCAGTCGAACGTTCAT CACTAACAAGACTATTATCACTAAGTTT AGTTAAAGGACCTCTAATACTTGCATTG ATGGTGAC 3' **Common primers** Forward: 5' GCTTGGTACCGAGCTCGGA TCC 3' Reverse: 5' CGGGCCCTCTAGACTCGAG CGGCC 3'	huCOX-2

A. Conditions for QuickChange™ site-directed mutagenesis

Cycles	Temperature (°C)	Time (min)
1	94	3
20	94	1
	52	1
	68	20
1	72	7

B. Site-directed mutagenesis by overlap-extension PCR

1) Mutation step

a) PCR reaction set-up:

- 50 ng DNA template
- 5 µl 10X Vent DNA polymerase reaction buffer
- 25 picomoles each of forward common primer* and reverse mutation primer (Reaction A), or 25 picomoles each of reverse common primer* and forward mutation primer (Reaction B)
- 1.25 µl of 40 mM dNTP mix
- 1 µl Vent DNA polymerase (2.5 U/µl)
- Add ddH_2O to final volume of 50 µl

* The common primers carry the restriction sites

b) PCR conditions:

Cycles	Temperature (°C)	Time (min)
1	94	3
30	94	1
	52	1
	72	5
1	72	5

- After the PCR reaction is completed, treat with Reactions A and B with 1 µl DpnI for at least 37°C for at least 4 h
- Purify the PCR fragments by gel extraction and measure DNA concentration

2) Extension step

a) Reaction set-up:

- Equal amounts of the purified PCR fragments from Reactions A and B
- 5 µl Vent DNA 10X polymerase reaction buffer
- 1.25 µl 40 mM dNTP mix
- 1 µl Vent DNA polymerase
- Bring total volume to 50 µl with ddH_2O

b) PCR conditions

Cycles	Temperature (°C)	Time (min)
1	94	3
6	94	1
	52	1
	72	5

3) Amplification step

a) Reaction set-up:

To the reaction obtained from the extension step, add:

- 25 picomoles of each of the common primers
- 1 µl Vent DNA polymerase

b) PCR conditions

Cycles	Temperature (°C)	Time (min)
1	94	3
30	94	1
	52	1
	72	5
1	72	5

- Purify the PCR product using a PCR purification kit
- Perform a restriction digestion with the appropriate enzymes and ligate onto vector of interest.

BIBLIOGRAPHY

1. Smith, W. L., DeWitt, D. L., and Garavito, R. M. (2000) *Annu Rev Biochem* **69**, 145-182

2. Narumiya, S., and FitzGerald, G. A. (2001) *J Clin Invest* **108**(1), 25-30

3. Rouzer, C. A., and Marnett, L. J. (2003) *Chem Rev* **103**(6), 2239-2304

4. Wang, D., Mann, J. R., and DuBois, R. N. (2005) *Gastroenterology* **128**(5), 1445-1461

5. Grosser, T., Fries, S., and FitzGerald, G. A. (2006) *J Clin Invest* **116**(1), 4-15

6. Honda, T., Segi-Nishida, E., Miyachi, Y., and Narumiya, S. (2006) *J Exp Med* **203**(2), 325-335

7. van der Donk, W. A., Tsai, A. L., and Kulmacz, R. J. (2002) *Biochemistry* **41**(52), 15451-15458

8. Leslie, C. C. (2004) *Biochem Cell Biol* **82**(1), 1-17

9. Murakami, M., Kambe-Ohkura, T., and Kudo, I. (2002) *Adv Exp Med Biol* **507**, 15-19

10. Kudo, I., and Murakami, M. (2002) *Prostaglandins Other Lipid Mediat* **68-69**, 3-58

11. Picot, D., Loll, P. J., and Garavito, R. M. (1994) *Nature* **367**(6460), 243-249

12. Kurumbail, R. G., Stevens, A. M., Gierse, J. K., McDonald, J. J., Stegeman, R. A., Pak, J. Y., Gildehaus, D., Miyashiro, J. M., Penning, T. D., Seibert, K., Isakson, P. C., and Stallings, W. C. (1996) *Nature* **384**(6610), 644-648

13. Otto, J. C., and Smith, W. L. (1994) *J Biol Chem* **269**(31), 19868-19875

14. Spencer, A. G., Woods, J. W., Arakawa, T., Singer, II, and Smith, W. L. (1998) *J Biol Chem* **273**(16), 9886-9893

15. MirAfzali, Z., Leipprandt, J. R., McCracken, J. L., and DeWitt, D. L. (2006) *J Biol Chem* **281**(38), 28354-28364

16. Spencer, A. G., Thuresson, E., Otto, J. C., Song, I., Smith, T., DeWitt, D. L., Garavito, R. M., and Smith, W. L. (1999) *J Biol Chem* **274**(46), 32936-32942

17. Yuan, C., Rieke, C. J., Rimon, G., Wingerd, B. A., and Smith, W. L. (2006) *Proc Natl Acad Sci U S A* **103**(16), 6142-6147

18. Munro, S., and Pelham, H. R. (1987) *Cell* **48**(5), 899-907

19. Song, I., and Smith, W. L. (1996) *Arch Biochem Biophys* **334**(1), 67-72

20. Tanabe, T., and Tohnai, N. (2002) *Prostaglandins Other Lipid Mediat* **68-69**, 95-114

21. Perkins, D. J., and Kniss, D. A. (1997) *Biochem J* **321 (Pt 3)**, 677-681

22. DeWitt, D. L., and Meade, E. A. (1993) *Arch Biochem Biophys* **306**(1), 94-102

23. Rich, G., Yoder, E. J., and Moore, S. A. (1998) *J Cell Physiol* **176**(3), 495-505

24. Zaric, J., and Ruegg, C. (2005) *J Biol Chem* **280**(2), 1077-1085

25. Funk, C. D. (2001) *Science* **294**(5548), 1871-1875

26. Zhang, Y., Shaffer, A., Portanova, J., Seibert, K., and Isakson, P. C. (1997) *J Pharmacol Exp Ther* **283**(3), 1069-1075

27. Samad, T. A., Moore, K. A., Sapirstein, A., Billet, S., Allchorne, A., Poole, S., Bonventre, J. V., and Woolf, C. J. (2001) *Nature* **410**(6827), 471-475

28. Cao, C., Matsumura, K., Yamagata, K., and Watanabe, Y. (1998) *Brain Res Mol Brain Res* **56**(1-2), 45-56

29. Leahy, K. M., Ornberg, R. L., Wang, Y., Zweifel, B. S., Koki, A. T., and Masferrer, J. L. (2002) *Cancer Res* **62**(3), 625-631

30. Sinicrope, F. A. (2006) *Mol Carcinog* **45**(6), 447-454

31. Yedgar, S., Cohen, Y., and Shoseyov, D. (2006) *Biochim Biophys Acta* **1761**(11), 1373-1382

32. Ghosh, M., Tucker, D. E., Burchett, S. A., and Leslie, C. C. (2006) *Prog Lipid Res* **45**(6), 487-510

33. Mounier, C. M., Ghomashchi, F., Lindsay, M. R., James, S., Singer, A. G., Parton, R. G., and Gelb, M. H. (2004) *J Biol Chem* **279**(24), 25024-25038

34. Ni, Z., Okeley, N. M., Smart, B. P., and Gelb, M. H. (2006) *J Biol Chem* **281**(24), 16245-16255

35. Leslie, C. C. (1997) *J Biol Chem* **272**(27), 16709-16712

36. Lin, L. L., Lin, A. Y., and DeWitt, D. L. (1992) *J Biol Chem* **267**(33), 23451-23454

37. Hoeck, W. G., Ramesha, C. S., Chang, D. J., Fan, N., and Heller, R. A. (1993) *Proc Natl Acad Sci U S A* **90**(10), 4475-4479

38. Maxwell, A. P., Goldberg, H. J., Tay, A. H., Li, Z. G., Arbus, G. S., and Skorecki, K. L. (1993) *Biochem J* **295 (Pt 3)**, 763-766

39. Wu, T., Levine, S. J., Lawrence, M. G., Logun, C., Angus, C. W., and Shelhamer, J. H. (1994) *J Clin Invest* **93**(2), 571-577

40. Murakami, M., Matsumoto, R., Urade, Y., Austen, K. F., and Arm, J. P. (1995) *J Biol Chem* **270**(7), 3239-3246

41. Miyakawa, T., Kojima, M., and Ui, M. (1998) *Biochem J* **329 (Pt 1)**, 107-114

42. Clapham, D. E. (1995) *Nature* **375**(6533), 634-635

43. Bootman, M. D., and Berridge, M. J. (1995) *Cell* **83**(5), 675-678

44. Reynolds, L. J., Hughes, L. L., Louis, A. I., Kramer, R. M., and Dennis, E. A. (1993) *Biochim Biophys Acta* **1167**(3), 272-280

45. Loo, R. W., Conde-Frieboes, K., Reynolds, L. J., and Dennis, E. A. (1997) *J Biol Chem* **272**(31), 19214-19219

46. Clark, J. D., Lin, L. L., Kriz, R. W., Ramesha, C. S., Sultzman, L. A., Lin, A. Y., Milona, N., and Knopf, J. L. (1991) *Cell* **65**(6), 1043-1051

47. Das, S., Rafter, J. D., Kim, K. P., Gygi, S. P., and Cho, W. (2003) *J Biol Chem* **278**(42), 41431-41442

48. Bonventre, J. V., Huang, Z., Taheri, M. R., O'Leary, E., Li, E., Moskowitz, M. A., and Sapirstein, A. (1997) *Nature* **390**(6660), 622-625

49. Uozumi, N., Kume, K., Nagase, T., Nakatani, N., Ishii, S., Tashiro, F., Komagata, Y., Maki, K., Ikuta, K., Ouchi, Y., Miyazaki, J., and Shimizu, T. (1997) *Nature* **390**(6660), 618-622

50. Hirabayashi, T., Murayama, T., and Shimizu, T. (2004) *Biol Pharm Bull* **27**(8), 1168-1173

51. Hegen, M., Sun, L., Uozumi, N., Kume, K., Goad, M. E., Nickerson-Nutter, C. L., Shimizu, T., and Clark, J. D. (2003) *J Exp Med* **197**(10), 1297-1302

52. Takaku, K., Sonoshita, M., Sasaki, N., Uozumi, N., Doi, Y., Shimizu, T., and Taketo, M. M. (2000) *J Biol Chem* **275**(44), 34013-34016

53. Hong, K. H., Bonventre, J. C., O'Leary, E., Bonventre, J. V., and Lander, E. S. (2001) *Proc Natl Acad Sci U S A* **98**(7), 3935-3939

54. Nagase, T., Uozumi, N., Ishii, S., Kita, Y., Yamamoto, H., Ohga, E., Ouchi, Y., and Shimizu, T. (2002) *Nat Med* **8**(5), 480-484

55. Nagase, T., Uozumi, N., Ishii, S., Kume, K., Izumi, T., Ouchi, Y., and Shimizu, T. (2000) *Nat Immunol* **1**(1), 42-46

56. Kalyvas, A., and David, S. (2004) *Neuron* **41**(3), 323-335

57. Oikawa, Y., Yamato, E., Tashiro, F., Yamamoto, M., Uozumi, N., Shimada, A., Shimizu, T., and Miyazaki, J. (2005) *FEBS Lett* **579**(18), 3975-3978

58. Murakami, M., Shimbara, S., Kambe, T., Kuwata, H., Winstead, M. V., Tischfield, J. A., and Kudo, I. (1998) *J Biol Chem* **273**(23), 14411-14423

59. Murakami, M., Koduri, R. S., Enomoto, A., Shimbara, S., Seki, M., Yoshihara, K., Singer, A., Valentin, E., Ghomashchi, F., Lambeau, G., Gelb, M. H., and Kudo, I. (2001) *J Biol Chem* **276**(13), 10083-10096

60. Satake, Y., Diaz, B. L., Balestrieri, B., Lam, B. K., Kanaoka, Y., Grusby, M. J., and Arm, J. P. (2004) *J Biol Chem* **279**(16), 16488-16494

61. Murakami, M., and Kudo, I. (2004) *Biol Pharm Bull* **27**(8), 1158-1164

62. Alaoui-El-Azher, M., Wu, Y., Havet, N., Israel, A., Lilienbaum, A., and Touqui, L. (2002) *Mol Pharmacol* **61**(4), 786-794

63. Nakano, T., and Arita, H. (1990) *FEBS Lett* **273**(1-2), 23-26

64. Crowl, R. M., Stoller, T. J., Conroy, R. R., and Stoner, C. R. (1991) *J Biol Chem* **266**(4), 2647-2651

65. Pfeilschifter, J., Schalkwijk, C., Briner, V. A., and van den Bosch, H. (1993) *J Clin Invest* **92**(5), 2516-2523

66. Kuwata, H., Sawada, H., Murakami, M., and Kudo, I. (1999) *Adv Exp Med Biol* **469**, 183-188

67. Pruzanski, W., Vadas, P., Stefanski, E., and Urowitz, M. B. (1985) *J Rheumatol* **12**(2), 211-216

68. Pruzanski, W., Keystone, E. C., Sternby, B., Bombardier, C., Snow, K. M., and Vadas, P. (1988) *J Rheumatol* **15**(9), 1351-1355

69. Vadas, P. (1984) *J Lab Clin Med* **104**(6), 873-881

70. Green, J. A., Smith, G. M., Buchta, R., Lee, R., Ho, K. Y., Rajkovic, I. A., and Scott, K. F. (1991) *Inflammation* **15**(5), 355-367

71. Vadas, P., and Pruzanski, W. (1993) *Circ Shock* **39**(2), 160-167

72. Bidgood, M. J., Jamal, O. S., Cunningham, A. M., Brooks, P. M., and Scott, K. F. (2000) *J Immunol* **165**(5), 2790-2797

73. Gijon, M. A., Spencer, D. M., Siddiqi, A. R., Bonventre, J. V., and Leslie, C. C. (2000) *J Biol Chem* **275**(26), 20146-20156

74. Balsinde, J., Balboa, M. A., and Dennis, E. A. (1998) *Proc Natl Acad Sci U S A* **95**(14), 7951-7956

75. Reddy, S. T., and Herschman, H. R. (1997) *J Biol Chem* **272**(6), 3231-3237

76. Murakami, M., Kambe, T., Shimbara, S., and Kudo, I. (1999) *J Biol Chem* **274**(5), 3103-3115

77. Reddy, S. T., and Herschman, H. R. (1994) *J Biol Chem* **269**(22), 15473-15480

78. Murakami, M., Kuwata, H., Amakasu, Y., Shimbara, S., Nakatani, Y., Atsumi, G., and Kudo, I. (1997) *J Biol Chem* **272**(32), 19891-19897

79. Roshak, A., Sathe, G., and Marshall, L. A. (1994) *J Biol Chem* **269**(42), 25999-26005

80. Langenbach, R., Morham, S. G., Tiano, H. F., Loftin, C. D., Ghanayem, B. I., Chulada, P. C., Mahler, J. F., Lee, C. A., Goulding, E. H., Kluckman, K. D., Kim, H. S., and Smithies, O. (1995) *Cell* **83**(3), 483-492

81. Kobayashi, T., and Narumiya, S. (2002) *Prostaglandins Other Lipid Mediat* **68-69**, 557-573

82. Naraba, H., Murakami, M., Matsumoto, H., Shimbara, S., Ueno, A., Kudo, I., and Oh-ishi, S. (1998) *J Immunol* **160**(6), 2974-2982

83. Moncada, S., and Vane, J. R. (1979) *Fed Proc* **38**(1), 66-71

84. Liou, J. Y., Shyue, S. K., Tsai, M. J., Chung, C. L., Chu, K. Y., and Wu, K. K. (2000) *J Biol Chem* **275**(20), 15314-15320

85. Bustos, M., Coffman, T. M., Saadi, S., and Platt, J. L. (1997) *J Clin Invest* **100**(5), 1150-1158

86. Okahara, K., Sun, B., and Kambayashi, J. (1998) *Arterioscler Thromb Vasc Biol* **18**(12), 1922-1926

87. Caughey, G. E., Cleland, L. G., Penglis, P. S., Gamble, J. R., and James, M. J. (2001) *J Immunol* **167**(5), 2831-2838

88. Solomon, S. D., McMurray, J. J., Pfeffer, M. A., Wittes, J., Fowler, R., Finn, P., Anderson, W. F., Zauber, A., Hawk, E., and Bertagnolli, M. (2005) *N Engl J Med* **352**(11), 1071-1080

89. Bresalier, R. S., Sandler, R. S., Quan, H., Bolognese, J. A., Oxenius, B., Horgan, K., Lines, C., Riddell, R., Morton, D., Lanas, A., Konstam, M. A., and Baron, J. A. (2005) *N Engl J Med* **352**(11), 1092-1102

90. DeWitt, D. L., Day, J. S., Sonnenburg, W. K., and Smith, W. L. (1983) *J Clin Invest* **72**(6), 1882-1888

91. Schildknecht, S., Bachschmid, M., Baumann, A., and Ullrich, V. (2004) *FASEB J* **18**(6), 757-759

92. Brock, T. G., McNish, R. W., and Peters-Golden, M. (1999) *J Biol Chem* **274**(17), 11660-11666

93. Urade, Y., and Hayaishi, O. (1999) *Biochim Biophys Acta* **1436**(3), 606-615

94. Eguchi, N., Minami, T., Shirafuji, N., Kanaoka, Y., Tanaka, T., Nagata, A., Yoshida, N., Urade, Y., Ito, S., and Hayaishi, O. (1999) *Proc Natl Acad Sci U S A* **96**(2), 726-730

95. Heavey, D. J., Ernst, P. B., Stevens, R. L., Befus, A. D., Bienenstock, J., and Austen, K. F. (1988) *J Immunol* **140**(6), 1953-1957

96. Diaz, B. L., Satake, Y., Kikawada, E., Balestrieri, B., and Arm, J. P. (2006) *Biochim Biophys Acta* **1761**(12), 1489-1497

97. Kabashima, K., and Narumiya, S. (2003) *Prostaglandins Leukot Essent Fatty Acids* **69**(2-3), 187-194

98. Lehmann, J. M., Moore, L. B., Smith-Oliver, T. A., Wilkison, W. O., Willson, T. M., and Kliewer, S. A. (1995) *J Biol Chem* **270**(22), 12953-12956

99. Forman, B. M., Tontonoz, P., Chen, J., Brun, R. P., Spiegelman, B. M., and Evans, R. M. (1995) *Cell* **83**(5), 803-812

100. Scher, J. U., and Pillinger, M. H. (2005) *Clin Immunol* **114**(2), 100-109

101. Ide, T., Egan, K., Bell-Parikh, L. C., and FitzGerald, G. A. (2003) *Thromb Res* **110**(5-6), 311-315

102. Chinetti, G., Griglio, S., Antonucci, M., Torra, I. P., Delerive, P., Majd, Z., Fruchart, J. C., Chapman, J., Najib, J., and Staels, B. (1998) *J Biol Chem* **273**(40), 25573-25580

103. Azuma, Y., Shinohara, M., Wang, P. L., and Ohura, K. (2001) *Biochem Biophys Res Commun* **283**(2), 344-346

104. Urade, Y., and Eguchi, N. (2002) *Prostaglandins Other Lipid Mediat* **68-69**, 375-382

105. Grill, M., Peskar, B. A., Schuligoi, R., and Amann, R. (2006) *Neuropharmacology* **50**(2), 165-173

106. Murakami, M., Matsumoto, R., Austen, K. F., and Arm, J. P. (1994) *J Biol Chem* **269**(35), 22269-22275

107. Harada, Y., Hatanaka, K., Kawamura, M., Saito, M., Ogino, M., Majima, M., Ohno, T., Ogino, K., Yamamoto, K., Taketani, Y., Yamamoto, S., and Katori, M. (1996) *Prostaglandins* **51**(1), 19-33

108. Li, S., Wang, Y., Matsumura, K., Ballou, L. R., Morham, S. G., and Blatteis, C. M. (1999) *Brain Res* **825**(1-2), 86-94

109. Ueno, N., Takegoshi, Y., Kamei, D., Kudo, I., and Murakami, M. (2005) *Biochem Biophys Res Commun* **338**(1), 70-76

110. Tanioka, T., Nakatani, Y., Semmyo, N., Murakami, M., and Kudo, I. (2000) *J Biol Chem* **275**(42), 32775-32782

111. Murakami, M., and Kudo, I. (2004) *Prog Lipid Res* **43**(1), 3-35

112. Kamei, D., Yamakawa, K., Takegoshi, Y., Mikami-Nakanishi, M., Nakatani, Y., Oh-Ishi, S., Yasui, H., Azuma, Y., Hirasawa, N., Ohuchi, K., Kawaguchi, H., Ishikawa, Y., Ishii, T., Uematsu, S., Akira, S., Murakami, M., and Kudo, I. (2004) *J Biol Chem* **279**(32), 33684-33695

113. Myers, L. K., Kang, A. H., Postlethwaite, A. E., Rosloniec, E. F., Morham, S. G., Shlopov, B. V., Goorha, S., and Ballou, L. R. (2000) *Arthritis Rheum* **43**(12), 2687-2693

114. Trebino, C. E., Stock, J. L., Gibbons, C. P., Naiman, B. M., Wachtmann, T. S., Umland, J. P., Pandher, K., Lapointe, J. M., Saha, S., Roach, M. L., Carter, D., Thomas, N. A., Durtschi, B. A., McNeish, J. D., Hambor, J. E., Jakobsson, P. J., Carty, T. J., Perez, J. R., and Audoly, L. P. (2003) *Proc Natl Acad Sci U S A* **100**(15), 9044-9049

115. Engblom, D., Saha, S., Engstrom, L., Westman, M., Audoly, L. P., Jakobsson, P. J., and Blomqvist, A. (2003) *Nat Neurosci* **6**(11), 1137-1138

116. Wang, L. H., Hajibeigi, A., Xu, X. M., Loose-Mitchell, D., and Wu, K. K. (1993) *Biochem Biophys Res Commun* **190**(2), 406-411

117. Xu, X. M., Tang, J. L., Chen, X., Wang, L. H., and Wu, K. K. (1997) *J Biol Chem* **272**(11), 6943-6950

118. Duquette, M., and Laneuville, O. (2002) *J Biol Chem* **277**(47), 44631-44637

119. DeLong, C. J., and Smith, W. L. (2005) *Biochem Biophys Res Commun* **338**(1), 53-61

120. Topper, J. N., Cai, J., Falb, D., and Gimbrone, M. A., Jr. (1996) *Proc Natl Acad Sci U S A* **93**(19), 10417-10422

121. Xie, W. L., Chipman, J. G., Robertson, D. L., Erikson, R. L., and Simmons, D. L. (1991) *Proc Natl Acad Sci U S A* **88**(7), 2692-2696

122. Kujubu, D. A., Reddy, S. T., Fletcher, B. S., and Herschman, H. R. (1993) *J Biol Chem* **268**(8), 5425-5430

123. Fletcher, B. S., Kujubu, D. A., Perrin, D. M., and Herschman, H. R. (1992) *J Biol Chem* **267**(7), 4338-4344

124. Herschman, H. R., Fletcher, B. S., and Kujubu, D. A. (1993) *J Lipid Mediat* **6**(1-3), 89-99

125. Asano, K., Lilly, C. M., and Drazen, J. M. (1996) *Am J Physiol* **271**(1 Pt 1), L126-131

126. Kaufmann, W. E., Worley, P. F., Taylor, C. V., Bremer, M., and Isakson, P. C. (1997) *Brain Dev* **19**(1), 25-34

127. Harris, R. C., and Breyer, M. D. (2001) *Am J Physiol Renal Physiol* **281**(1), F1-11

128. Bagga, D., Wang, L., Farias-Eisner, R., Glaspy, J. A., and Reddy, S. T. (2003) *Proc Natl Acad Sci U S A* **100**(4), 1751-1756

129. Chen, C. Y., and Shyu, A. B. (1994) *Mol Cell Biol* **14**(12), 8471-8482

130. Kang, Y. J., Wingerd, B. A., Arakawa, T., and Smith, W. L. (2006) *J Immunol* **177**(11), 8111-8122

131. Kang, Y. J., Mbonye, U. R., Delong, C. J., Wada, M., and Smith, W. L. (2007) *Prog Lipid Res*

132. Hwang, D., Jang, B. C., Yu, G., and Boudreau, M. (1997) *Biochem Pharmacol* **54**(1), 87-96

133. Mestre, J. R., Mackrell, P. J., Rivadeneira, D. E., Stapleton, P. P., Tanabe, T., and Daly, J. M. (2001) *J Biol Chem* **276**(6), 3977-3982

134. Scheinman, R. I., Cogswell, P. C., Lofquist, A. K., and Baldwin, A. S., Jr. (1995) *Science* **270**(5234), 283-286

135. Auphan, N., DiDonato, J. A., Rosette, C., Helmberg, A., and Karin, M. (1995) *Science* **270**(5234), 286-290

136. Farrajota, K., Cheng, S., Martel-Pelletier, J., Afif, H., Pelletier, J. P., Li, X., Ranger, P., and Fahmi, H. (2005) *Arthritis Rheum* **52**(1), 94-104

137. Kapoor, M., Kojima, F., Qian, M., Yang, L., and Crofford, L. J. (2006) *J Biol Chem*

138. Subbaramaiah, K., Lin, D. T., Hart, J. C., and Dannenberg, A. J. (2001) *J Biol Chem* **276**(15), 12440-12448

139. Chen, C. Y., and Shyu, A. B. (1995) *Trends Biochem Sci* **20**(11), 465-470

140. Chen, C. Y., Gherzi, R., Ong, S. E., Chan, E. L., Raijmakers, R., Pruijn, G. J., Stoecklin, G., Moroni, C., Mann, M., and Karin, M. (2001) *Cell* **107**(4), 451-464

141. Mukherjee, D., Gao, M., O'Connor, J. P., Raijmakers, R., Pruijn, G., Lutz, C. S., and Wilusz, J. (2002) *EMBO J* **21**(1-2), 165-174

142. Stoecklin, G., Mayo, T., and Anderson, P. (2006) *EMBO Rep* **7**(1), 72-77

143. Lasa, M., Mahtani, K. R., Finch, A., Brewer, G., Saklatvala, J., and Clark, A. R. (2000) *Mol Cell Biol* **20**(12), 4265-4274

144. Lasa, M., Brook, M., Saklatvala, J., and Clark, A. R. (2001) *Mol Cell Biol* **21**(3), 771-780

145. Dixon, D. A., Tolley, N. D., King, P. H., Nabors, L. B., McIntyre, T. M., Zimmerman, G. A., and Prescott, S. M. (2001) *J Clin Invest* **108**(11), 1657-1665

146. Murmu, N., Jung, J., Mukhopadhyay, D., Houchen, C. W., Riehl, T. E., Stenson, W. F., Morrison, A. R., Arumugam, T., Dieckgraefe, B. K., and Anant, S. (2004) *Proc Natl Acad Sci U S A* **101**(38), 13873-13878

147. Mukhopadhyay, D., Houchen, C. W., Kennedy, S., Dieckgraefe, B. K., and Anant, S. (2003) *Mol Cell* **11**(1), 113-126

148. Rockwell, P., Yuan, H., Magnusson, R., and Figueiredo-Pereira, M. E. (2000) *Arch Biochem Biophys* **374**(2), 325-333

149. Figueiredo-Pereira, M. E., Li, Z., Jansen, M., and Rockwell, P. (2002) *J Biol Chem* **277**(28), 25283-25289

150. Xiao, G., Chen, W., and Kulmacz, R. J. (1998) *J Biol Chem* **273**(12), 6801-6811

151. Otto, J. C., DeWitt, D. L., and Smith, W. L. (1993) *J Biol Chem* **268**(24), 18234-18242

152. Garavito, R. M., Malkowski, M. G., and DeWitt, D. L. (2002) *Prostaglandins Other Lipid Mediat* **68-69**, 129-152

153. Malkowski, M. G., Ginell, S. L., Smith, W. L., and Garavito, R. M. (2000) *Science* **289**(5486), 1933-1937

154. Rieke, C. J., Mulichak, A. M., Garavito, R. M., and Smith, W. L. (1999) *J Biol Chem* **274**(24), 17109-17114

155. Kulmacz, R. J., and Wang, L. H. (1995) *J Biol Chem* **270**(41), 24019-24023

156. Smith, W. L., and Song, I. (2002) *Prostaglandins Other Lipid Mediat* **68-69**, 115-128

157. Kiefer, J. R., Pawlitz, J. L., Moreland, K. T., Stegeman, R. A., Hood, W. F., Gierse, J. K., Stevens, A. M., Goodwin, D. C., Rowlinson, S. W., Marnett, L. J., Stallings, W. C., and Kurumbail, R. G. (2000) *Nature* **405**(6782), 97-101

158. Dietz, R., Nastainczyk, W., and Ruf, H. H. (1988) *Eur J Biochem* **171**(1-2), 321-328

159. Lu, G., Tsai, A. L., Van Wart, H. E., and Kulmacz, R. J. (1999) *J Biol Chem* **274**(23), 16162-16167

160. Landino, L. M., Crews, B. C., Gierse, J. K., Hauser, S. D., and Marnett, L. J. (1997) *J Biol Chem* **272**(34), 21565-21574

161. Laneuville, O., Breuer, D. K., Xu, N., Huang, Z. H., Gage, D. A., Watson, J. T., Lagarde, M., DeWitt, D. L., and Smith, W. L. (1995) *J Biol Chem* **270**(33), 19330-19336

162. Mevkh, A. T., Miroshnikov, K. A., Igumnova, N. D., and Varfolomeev, S. D. (1993) *FEBS Lett* **321**(2-3), 205-208

163. Mevkh, A. T., Miroshnikov, K. A., Igumnova, N. D., and Varfolomeev, S. D. (1993) *Biokhimiia* **58**(10), 1573-1579

164. Meusser, B., Hirsch, C., Jarosch, E., and Sommer, T. (2005) *Nat Cell Biol* **7**(8), 766-772

165. McCracken, A. A., and Brodsky, J. L. (2003) *Bioessays* **25**(9), 868-877

166. Spiro, R. G. (2004) *Cell Mol Life Sci* **61**(9), 1025-1041

167. Stoka, V., Turk, B., and Turk, V. (2005) *IUBMB Life* **57**(4-5), 347-353

168. Rubinsztein, D. C. (2006) *Nature* **443**(7113), 780-786

169. Ciechanover, A. (2005) *Cell Death Differ* **12**(9), 1178-1190

170. Finn, P. F., and Dice, J. F. (2006) *Nutrition* **22**(7-8), 830-844

171. Zwickl, P., Voges, D., and Baumeister, W. (1999) *Philos Trans R Soc Lond B Biol Sci* **354**(1389), 1501-1511

172. Peters, J. M., Cejka, Z., Harris, J. R., Kleinschmidt, J. A., and Baumeister, W. (1993) *J Mol Biol* **234**(4), 932-937

173. Adams, J. (2003) *Cancer Treat Rev* **29 Suppl 1**, 3-9

174. Wang, J., and Maldonado, M. A. (2006) *Cell Mol Immunol* **3**(4), 255-261

175. Miller, J., and Gordon, C. (2005) *FEBS Lett* **579**(15), 3224-3230

176. Yao, T., and Cohen, R. E. (2002) *Nature* **419**(6905), 403-407

177. Braun, B. C., Glickman, M., Kraft, R., Dahlmann, B., Kloetzel, P. M., Finley, D., and Schmidt, M. (1999) *Nat Cell Biol* **1**(4), 221-226

178. Coffino, P. (2001) *Nat Rev Mol Cell Biol* **2**(3), 188-194

179. Newman, R. M., Mobascher, A., Mangold, U., Koike, C., Diah, S., Schmidt, M., Finley, D., and Zetter, B. R. (2004) *J Biol Chem* **279**(40), 41504-41511

180. Zhang, M., Pickart, C. M., and Coffino, P. (2003) *EMBO J* **22**(7), 1488-1496

181. Kahana, C., Asher, G., and Shaul, Y. (2005) *Cell Cycle* **4**(11), 1461-1464

182. Hampton, R. Y. (2002) *Curr Opin Cell Biol* **14**(4), 476-482

183. McCracken, A. A., and Brodsky, J. L. (2005) *Curr Top Microbiol Immunol* **300**, 17-40

184. Pety de Thozee, C., and Ghislain, M. (2006) *ScientificWorldJournal* **6**, 967-983

185. Hirsch, C., Jarosch, E., Sommer, T., and Wolf, D. H. (2004) *Biochim Biophys Acta* **1695**(1-3), 215-223

186. Trombetta, E. S., and Parodi, A. J. (2003) *Annu Rev Cell Dev Biol* **19**, 649-676

187. Guo, W., Shea, J. E., and Berry, R. S. (2005) *Ann N Y Acad Sci* **1066**, 34-53

188. Carvalho, P., Goder, V., and Rapoport, T. A. (2006) *Cell* **126**(2), 361-373

189. Ismail, N., and Ng, D. T. (2006) *Cell* **126**(2), 237-239

190. Ahner, A., and Brodsky, J. L. (2004) *Trends Cell Biol* **14**(9), 474-478

191. Mueller, B., Lilley, B. N., and Ploegh, H. L. (2006) *J Cell Biol* **175**(2), 261-270

192. Nishikawa, S. I., Fewell, S. W., Kato, Y., Brodsky, J. L., and Endo, T. (2001) *J Cell Biol* **153**(5), 1061-1070

193. Brodsky, J. L., Werner, E. D., Dubas, M. E., Goeckeler, J. L., Kruse, K. B., and McCracken, A. A. (1999) *J Biol Chem* **274**(6), 3453-3460

194. McCracken, A. A., and Brodsky, J. L. (1996) *J Cell Biol* **132**(3), 291-298

195. Pollock, S., Kozlov, G., Pelletier, M. F., Trempe, J. F., Jansen, G., Sitnikov, D., Bergeron, J. J., Gehring, K., Ekiel, I., and Thomas, D. Y. (2004) *Embo J* **23**(5), 1020-1029

196. Caramelo, J. J., Castro, O. A., Alonso, L. G., De Prat-Gay, G., and Parodi, A. J. (2003) *Proc Natl Acad Sci U S A* **100**(1), 86-91

197. Trombetta, E. S., and Helenius, A. (2000) *J Cell Biol* **148**(6), 1123-1129

198. Jakob, C. A., Burda, P., Roth, J., and Aebi, M. (1998) *J Cell Biol* **142**(5), 1223-1233

199. Tokunaga, F., Brostrom, C., Koide, T., and Arvan, P. (2000) *J Biol Chem* **275**(52), 40757-40764

200. Hosokawa, N., Tremblay, L. O., You, Z., Herscovics, A., Wada, I., and Nagata, K. (2003) *J Biol Chem* **278**(28), 26287-26294

201. Denic, V., Quan, E. M., and Weissman, J. S. (2006) *Cell* **126**(2), 349-359

202. Kim, W., Spear, E. D., and Ng, D. T. (2005) *Mol Cell* **19**(6), 753-764

203. Gnann, A., Riordan, J. R., and Wolf, D. H. (2004) *Mol Biol Cell* **15**(9), 4125-4135

204. Oda, Y., Hosokawa, N., Wada, I., and Nagata, K. (2003) *Science* **299**(5611), 1394-1397

205. Molinari, M., Calanca, V., Galli, C., Lucca, P., and Paganetti, P. (2003) *Science* **299**(5611), 1397-1400

206. Plemper, R. K., Bohmler, S., Bordallo, J., Sommer, T., and Wolf, D. H. (1997) *Nature* **388**(6645), 891-895

207. Kabani, M., Kelley, S. S., Morrow, M. W., Montgomery, D. L., Sivendran, R., Rose, M. D., Gierasch, L. M., and Brodsky, J. L. (2003) *Mol Biol Cell* **14**(8), 3437-3448

208. Fagioli, C., Mezghrani, A., and Sitia, R. (2001) *J Biol Chem* **276**(44), 40962-40967

209. Tortorella, D., Story, C. M., Huppa, J. B., Wiertz, E. J., Jones, T. R., Bacik, I., Bennink, J. R., Yewdell, J. W., and Ploegh, H. L. (1998) *J Cell Biol* **142**(2), 365-376

210. Kalies, K. U., Allan, S., Sergeyenko, T., Kroger, H., and Romisch, K. (2005) *EMBO J* **24**(13), 2284-2293

211. Wiertz, E. J., Tortorella, D., Bogyo, M., Yu, J., Mothes, W., Jones, T. R., Rapoport, T. A., and Ploegh, H. L. (1996) *Nature* **384**(6608), 432-438

212. Pariyarath, R., Wang, H., Aitchison, J. D., Ginsberg, H. N., Welch, W. J., Johnson, A. E., and Fisher, E. A. (2001) *J Biol Chem* **276**(1), 541-550

213. Pilon, M., Schekman, R., and Romisch, K. (1997) *EMBO J* **16**(15), 4540-4548

214. Van den Berg, B., Clemons, W. M., Jr., Collinson, I., Modis, Y., Hartmann, E., Harrison, S. C., and Rapoport, T. A. (2004) *Nature* **427**(6969), 36-44

215. Clemons, W. M., Jr., Menetret, J. F., Akey, C. W., and Rapoport, T. A. (2004) *Curr Opin Struct Biol* **14**(4), 390-396

216. Wirth, A., Jung, M., Bies, C., Frien, M., Tyedmers, J., Zimmermann, R., and Wagner, R. (2003) *Mol Cell* **12**(1), 261-268

217. Hamman, B. D., Chen, J. C., Johnson, E. E., and Johnson, A. E. (1997) *Cell* **89**(4), 535-544

218. Lilley, B. N., and Ploegh, H. L. (2004) *Nature* **429**(6994), 834-840

219. Ye, Y., Shibata, Y., Yun, C., Ron, D., and Rapoport, T. A. (2004) *Nature* **429**(6994), 841-847

220. Jarosch, E., Taxis, C., Volkwein, C., Bordallo, J., Finley, D., Wolf, D. H., and Sommer, T. (2002) *Nat Cell Biol* **4**(2), 134-139

221. Jarosch, E., Geiss-Friedlander, R., Meusser, B., Walter, J., and Sommer, T. (2002) *Traffic* **3**(8), 530-536

222. Oda, Y., Okada, T., Yoshida, H., Kaufman, R. J., Nagata, K., and Mori, K. (2006) *J Cell Biol* **172**(3), 383-393

223. Pye, V. E., Beuron, F., Keetch, C. A., McKeown, C., Robinson, C. V., Meyer, H. H., Zhang, X., and Freemont, P. S. (2007) *Proc Natl Acad Sci U S A* **104**(2), 467-472

224. Chen, B., Mariano, J., Tsai, Y. C., Chan, A. H., Cohen, M., and Weissman, A. M. (2006) *Proc Natl Acad Sci U S A* **103**(2), 341-346

225. Fang, S., Ferrone, M., Yang, C., Jensen, J. P., Tiwari, S., and Weissman, A. M. (2001) *Proc Natl Acad Sci U S A* **98**(25), 14422-14427

226. Schulze, A., Standera, S., Buerger, E., Kikkert, M., van Voorden, S., Wiertz, E., Koning, F., Kloetzel, P. M., and Seeger, M. (2005) *J Mol Biol* **354**(5), 1021-1027

227. Zhong, X., Shen, Y., Ballar, P., Apostolou, A., Agami, R., and Fang, S. (2004) *J Biol Chem* **279**(44), 45676-45684

228. Schuberth, C., and Buchberger, A. (2005) *Nat Cell Biol* **7**(10), 999-1006

229. Bar-Nun, S. (2005) *Curr Top Microbiol Immunol* **300**, 95-125

230. Katiyar, S., Joshi, S., and Lennarz, W. J. (2005) *Mol Biol Cell* **16**(10), 4584-4594

231. Li, G., Zhao, G., Zhou, X., Schindelin, H., and Lennarz, W. J. (2006) *Proc Natl Acad Sci U S A* **103**(22), 8348-8353

232. Ravid, T., Doolman, R., Avner, R., Harats, D., and Roitelman, J. (2000) *J Biol Chem* **275**(46), 35840-35847

233. Murray, B. P., and Correia, M. A. (2001) *Arch Biochem Biophys* **393**(1), 106-116

234. Webster, J. M., Tiwari, S., Weissman, A. M., and Wojcikiewicz, R. J. (2003) *J Biol Chem* **278**(40), 38238-38246

235. Alzayady, K. J., Panning, M. M., Kelley, G. G., and Wojcikiewicz, R. J. (2005) *J Biol Chem* **280**(41), 34530-34537

236. Sever, N., Song, B. L., Yabe, D., Goldstein, J. L., Brown, M. S., and DeBose-Boyd, R. A. (2003) *J Biol Chem* **278**(52), 52479-52490

237. Sever, N., Yang, T., Brown, M. S., Goldstein, J. L., and DeBose-Boyd, R. A. (2003) *Mol Cell* **11**(1), 25-33

238. Song, B. L., Javitt, N. B., and DeBose-Boyd, R. A. (2005) *Cell Metab* **1**(3), 179-189

239. Song, B. L., Sever, N., and DeBose-Boyd, R. A. (2005) *Mol Cell* **19**(6), 829-840

240. Evett, G. E., Xie, W., Chipman, J. G., Robertson, D. L., and Simmons, D. L. (1993) *Arch Biochem Biophys* **306**(1), 169-177

241. Herschman, H. R. (1996) *Biochim Biophys Acta* **1299**(1), 125-140

242. Shao, J., Sheng, H., Inoue, H., Morrow, J. D., and DuBois, R. N. (2000) *J Biol Chem* **275**(43), 33951-33956

243. Tsai, B., Ye, Y., and Rapoport, T. A. (2002) *Nat Rev Mol Cell Biol* **3**(4), 246-255

244. Ellgaard, L., and Helenius, A. (2001) *Curr Opin Cell Biol* **13**(4), 431-437

245. Robertson, R. P. (1998) *Diabetes* **47**(9), 1379-1383

246. Ristimaki, A., Honkanen, N., Jankala, H., Sipponen, P., and Harkonen, M. (1997) *Cancer Res* **57**(7), 1276-1280

247. Nemeth, J. F., Hochgesang, G. P., Jr., Marnett, L. J., and Caprioli, R. M. (2001) *Biochemistry (Mosc)* **40**(10), 3109-3116

248. Fagioli, C., and Sitia, R. (2001) *J Biol Chem* **276**(16), 12885-12892

249. Hosokawa, N., Wada, I., Hasegawa, K., Yorihuzi, T., Tremblay, L. O., Herscovics, A., and Nagata, K. (2001) *EMBO Rep* **2**(5), 415-422

250. Kitzmuller, C., Caprini, A., Moore, S. E., Frenoy, J. P., Schwaiger, E., Kellermann, O., Ivessa, N. E., and Ermonval, M. (2003) *Biochem J* **376**(Pt 3), 687-696

251. Tsuda, H., Tokunaga, F., Nagamitsu, H., and Koide, T. (2006) *Thromb Res* **117**(3), 323-331

252. Yu, Y., Fan, J., Hui, Y., Rouzer, C. A., Marnett, L. J., Klein-Szanto, A. J., FitzGerald, G. A., and Funk, C. D. (2007) *J Biol Chem* **282**(2), 1498-1506

253. Cok, S. J., and Morrison, A. R. (2001) *J Biol Chem* **276**(25), 23179-23185

254. Dixon, D. A., Kaplan, C. D., McIntyre, T. M., Zimmerman, G. A., and Prescott, S. M. (2000) *J Biol Chem* **275**(16), 11750-11757

255. Kostova, Z., and Wolf, D. H. (2003) *EMBO J* **22**(10), 2309-2317

256. Spear, E. D., and Ng, D. T. (2005) *J Cell Biol* **169**(1), 73-82

257. Mbonye, U. R., Wada, M., Rieke, C. J., Tang, H. Y., Dewitt, D. L., and Smith, W. L. (2006) *J Biol Chem* **281**(47), 35770-35778

258. Sevigny, M. B., Li, C. F., Alas, M., and Hughes-Fulford, M. (2006) *FEBS Lett* **580**(28-29), 6533-6536

259. Wu, Y., Swulius, M. T., Moremen, K. W., and Sifers, R. N. (2003) *Proc Natl Acad Sci U S A* **100**(14), 8229-8234

260. Wu, Y., Termine, D. J., Swulius, M. T., Moremen, K. W., and Sifers, R. N. (2007) *J Biol Chem* **282**(7), 4841-4849

261. Cabral, C. M., Liu, Y., and Sifers, R. N. (2001) *Trends Biochem Sci* **26**(10), 619-624

262. Kelleher, D. J., Kreibich, G., and Gilmore, R. (1992) *Cell* **69**(1), 55-65

263. Nilsson, I. M., and von Heijne, G. (1993) *J Biol Chem* **268**(8), 5798-5801

264. Bolt, G., Kristensen, C., and Steenstrup, T. D. (2005) *Glycobiology* **15**(5), 541-547

265. Tanaka, N., Sato, T., Fujita, H., and Morita, I. (2004) *Arterioscler Thromb Vasc Biol* **24**(3), 607-612

266. Miyamoto, T., Ogino, N., Yamamoto, S., and Hayaishi, O. (1976) *J Biol Chem* **251**(9), 2629-2636

267. Xu, X. M., Tang, J. L., Hajibeigi, A., Loose-Mitchell, D. S., and Wu, K. K. (1996) *Am J Physiol* **270**(1 Pt 1), C259-264

268. Song, I., Ball, T. M., and Smith, W. L. (2001) *Biochem Biophys Res Commun* **289**(4), 869-875

269. Wada, M., Yokoyama, C., Hatae, T., Shimonishi, M., Nakamura, M., Imai, Y., Ullrich, V., and Tanabe, T. (2004) *J Biochem (Tokyo)* **135**(4), 455-463

270. Habenicht, A. J., Goerig, M., Grulich, J., Rothe, D., Gronwald, R., Loth, U., Schettler, G., Kommerell, B., and Ross, R. (1985) *J Clin Invest* **75**(4), 1381-1387

271. Barnett, J., Chow, J., Ives, D., Chiou, M., Mackenzie, R., Osen, E., Nguyen, B., Tsing, S., Bach, C., Freire, J., and et al. (1994) *Biochim Biophys Acta* **1209**(1), 130-139

272. Rowlinson, S. W., Crews, B. C., Lanzo, C. A., and Marnett, L. J. (1999) *J Biol Chem* **274**(33), 23305-23310

273. Riese, J., Hoff, T., Nordhoff, A., DeWitt, D. L., Resch, K., and Kaever, V. (1994) *J Leukoc Biol* **55**(4), 476-482

274. Martoglio, B., and Dobberstein, B. (1998) *Trends Cell Biol* **8**(10), 410-415

275. Sanders, S. L., and Schekman, R. (1992) *J Biol Chem* **267**(20), 13791-13794

276. Schmitz, A., and Herzog, V. (2004) *Eur J Cell Biol* **83**(10), 501-509

277. Sato, T., Nyborg, A. C., Iwata, N., Diehl, T. S., Saido, T. C., Golde, T. E., and Wolfe, M. S. (2006) *Biochemistry (Mosc)* **45**(28), 8649-8656

278. Loureiro, J., Lilley, B. N., Spooner, E., Noriega, V., Tortorella, D., and Ploegh, H. L. (2006) *Nature* **441**(7095), 894-897

279. Serwold, T., Gonzalez, F., Kim, J., Jacob, R., and Shastri, N. (2002) *Nature* **419**(6906), 480-483

280. Saric, T., Chang, S. C., Hattori, A., York, I. A., Markant, S., Rock, K. L., Tsujimoto, M., and Goldberg, A. L. (2002) *Nat Immunol* **3**(12), 1169-1176

281. York, I. A., Chang, S. C., Saric, T., Keys, J. A., Favreau, J. M., Goldberg, A. L., and Rock, K. L. (2002) *Nat Immunol* **3**(12), 1177-1184

282. Saveanu, L., Carroll, O., Lindo, V., Del Val, M., Lopez, D., Lepelletier, Y., Greer, F., Schomburg, L., Fruci, D., Niedermann, G., and van Endert, P. M. (2005) *Nat Immunol* **6**(7), 689-697

283. Heinemann, F. S., and Ozols, J. (1998) *Mol Biol Cell* **9**(12), 3445-3453

284. Heinemann, F. S., Mziaut, H., Korza, G., and Ozols, J. (2003) *Biochemistry (Mosc)* **42**(23), 6929-6937

285. Heinemann, F. S., Korza, G., and Ozols, J. (2003) *J Biol Chem* **278**(44), 42966-42975

286. Mziaut, H., Korza, G., and Ozols, J. (2000) *Proc Natl Acad Sci U S A* **97**(16), 8883-8888

287. Donoso, G., Herzog, V., and Schmitz, A. (2005) *Biochem J* **387**(Pt 3), 897-903